2003

Steady state and transient analysis of thermoelectric devices using finite element method

Gurjinder Singh

Steady State and Transient Analysis of Thermoelectric Devices using Finite Element Method

by

Gurjinder Singh

A thesis submitted in partial fulfillment of the
requirements for the degree of
Master of Science in Mechanical Engineering

Approved By:

Dr. Edward Hensel
Department Head of Mechanical Engineering

Edward Hensel
(Thesis Advisor)

Dr. Satish Kandlikar
Department of Mechanical Engineering

Satish Kandlikar

Dr. Hany Ghoneim
Department of Mechanical Engineering

Hany Ghoneim

Dr. Alan Nye
Assoc. Department Head of Mechanical Engineering

Alan Nye
(Department Representative)

Department of Mechanical Engineering
Rochester Institute of Technology
Rochester, NY 14623
July 2003

Steady State and Transient Analysis of Thermoelectric Devices using Finite Element Method

I, Gurjinder Singh, grant permission to the Wallace Memorial Library to reproduce my thesis in whole or in part. Any reproduction will not be for commercial use.

Gurjinder Singh

(Gurjinder Singh)

9/4/13

Date

Abstract

Thermoelectric devices offer noiseless and environment friendly operation, which makes them the most suitable devices of the future in their category. However, the performance of these devices is still way below its competitor thermal and electrical systems. The major factor that decides the performance of these devices is the thermoelectric material. Although the use of Silicon as a thermoelectric material greatly improved the performance of new thermoelectric devices over the metal based thermoelectric devices, it is still not close to the performance level of heat engines or refrigerators.

With a limit on the material properties, these devices must be optimized based on all known effects that occur in the thermoelectric devices. The various effects that occur in a thermoelectric device are Seebeck effect, Peltier effect, Joule effect and Thomson effect. Most of the time, the design of thermoelectric generators and sensors is based on the steady state characteristics, which include only the governing thermoelectric effect (Seebeck effect) into the mathematical model. The Joule effect, Thomson effect and Peltier effect are historically assumed to have negligible influence on its performance characteristics.

In this thesis, a complete steady state and transient model of thermoelectric generator is formed incorporating all the thermoelectric effects. The comprehensive model accounts for the internal heat generation inside the thermoelements due to the Joule effect and the Thomson effect. The Peltier effect is included as a plane heat source at the junctions that release heat in both directions. The model is formulated using finite element method, which is implemented into a computer program. The influence of different thermoelectric effects is studied under various working conditions. The use of finite element program, as a design tool for thermoelectric devices, is also demonstrated.

Acknowledgments

I would like to express my gratitude to my thesis advisor Dr. Edward Hensel, who provided me with an opportunity to work under his excellent guidance. His expert and stimulating advice encouraged me to accomplish the goals of this research work. Further, I extend my thanks to Dr. Ghoneim for his valuable advice related to finite element method and ANSYS. I would also like to thank Dr. Kandlikar and Dr. Ghoneim for their time to review my thesis work and to be in my thesis committee. I am grateful to the Mechanical Engineering Department of Rochester Institute of Technology for providing financial support that helped to continue this work without interruption.

I would never forget the company I had from my fellow students of my department. In particular, I am thankful to Amar, Ritesh and Jeff for creative discussion related to finite element analysis, ANSYS and MEMS. I am very thankful to all my friends in graduate lab who were always there to provide valuable advice.

I would like to give my special thanks to my wife Sukhjinder for her love and patience during countless hours of work on thesis. I am grateful to my parents and my sister for their love, encouragement and support.

Gurjinder Singh

Contents

List of Figures

List of Tables

Nomenclature

I	Current (Amp)
$\vec{J}$	Current density vector (Amp/m^2)
Q_J	Heat liberated or absorbed due to the Joule effect (W)
Q_P	Heat liberated or absorbed due to the Peltier effect (W)
Q_{th}	Heat liberated or absorbed due to the Thomson effect (W)
R	Resistance (Ω)
S_A	Absolute Seebeck coefficient of thermoelement 'A' (V/K)
S_{AB}	Relative Seebeck coefficient $\equiv S_A - S_B$ (V/K)
T	Temperature (°C)
Z	Figure of Merit
c_p	Specific Heat (J/KgK)
h	Convective film coefficient (W/m^{2}K)
k	Thermal Conductivity (W/mK)
q''	Heat Flux vector (W/m^2)
q_J'''	Internal heat generation per unit volume due to the Joule effect (W/m^3)
q_P''	Internal heat flux at the junction due to the Peltier effect (W/m^2)
q_{th}'''	Internal heat generation per unit volume due to the Thomson effect (W/m^3)
t	Time (sec)
ε	Emissivity
γ	Electrical Resistivity (Ωm)
π_{AB}	Peltier Coefficient (V)
ρ	Density (Kg/m^3)
σ	Thomson coefficient (V/K)
σ_{rad}	Stefan-Boltzmann Constant
ϕ	Seebeck voltage (Volt)
Δ	Difference symbol

∇	Gradient operator ($\hat{i}\frac{\partial}{\partial x}+\hat{j}\frac{\partial}{\partial y}$) where $\hat{i}$ *and* $\hat{j}$ denotes the unit vectors along x and y co-ordinates respectively
∇^2	Laplacian operator ($\nabla.\nabla=\frac{\partial^2}{\partial x^2}+\frac{\partial^2}{\partial y^2}$)

Nomenclature used in finite element model formulation

b_i	Basis function corresponding to node 'i' obtained by assembling elemental shape functions
$\{N\}^e$	Elemental shape function
N_e	Total number of elements
N_n	Total number of nodes
R	Residual over full domain
R_i	Residual at node 'i'
T(x,y)	Exact solution
$\hat{T}$ (x,y)	Approximate temperature in global co-ordinates
{T}	Global vector containing nodal temperature values
$\{T\}^e$	Elemental vector containing nodal temperature values
[β]	Beta matrix (Derivative of shave function vector)
Γ	Boundary of full domain
Γ^e	Boundary of element 'e'
Ω	Domain of full problem
Ω^e	Doamin of element 'e'

1 Background and Problem Description

The age of thermoelectricity can be imagined by the fact that the first thermoelectric effect was discovered in 1822, which was even before Ohm enunciated his famous voltage current relationship. The I^2R law of heat dissipation was discovered 17 years later and Clausius expressed the second law of thermodynamics in 1850 [Egli, 1960]. Although the thermoelectricity is a very old science, the performance of thermoelectric devices has been still at very initial stages of development as compared to the thermal and electrical systems. However, the science of thermoelectricity provides a way towards noiseless thermal and electrical systems without any moving parts. It requires development of new materials having high thermoelectric properties and optimum device design to match the performance of these devices with well-established mechanical systems. Thermoelectricity utilizes a unique way of inter-conversion of electric and thermal energy, which requires a simple system, consists of two dissimilar conductors connected at their ends.

The phenomenon of thermoelectricity and different thermoelectric effects are introduced in this chapter, which is followed by a brief introduction to the process of thermoelectric device design and performance analysis. The various fields of applications of thermoelectric devices are also reviewed.

1.1 Thermoelectricity

Thermoelectricity is a combination of two words "Thermo" and "Electricity", which means electrical energy produced from thermal energy. Generally, the definition of thermoelectricity is not restricted only to the conversion of electric energy to thermal energy; but defined in a broad sense as a phenomenon involving the inter-conversion of heat and electrical energy in a conductor. A device based on thermoelectricity consists of two dissimilar conductors connected at their ends, to form the junctions. The junctions play a very important role in the working of the device. The various reversible and irreversible effects that occur in the conductors and at the junctions are listed below [Heikes, 1961].

Reversible Effects:

Seebeck Effect

Peltier Effect

Thomson Effect

Irreversible Effects:

Joule Heating

Thermal Conduction

Electrical Conduction

The first four effects involve inter-conversion of electrical and heat energy and termed as thermoelectric effects. Whereas, the thermal and electrical conduction are pure thermal and electrical effects respectively.

1.1.1. Seebeck Effect

A German physicist Seebeck discovered the first thermoelectric effect in 1822 [Egli, 1960]. He observed that when two dissimilar conductors are connected at their ends and the junctions are maintained at different temperatures, voltage is developed across the junctions. The voltage developed in such a way was found to be a function of material property and the temperature difference between the junctions. The device that works on this principle is known as the thermocouple and the conductors used to make the thermocouple are called the thermoelements.

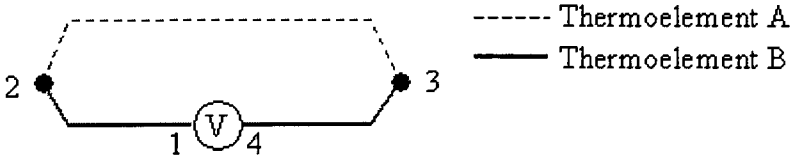

Figure 1-1 Thermocouple

Figure 1-1 shows a thermoelectric circuit made up of thermoelement 'A' and thermoelement 'B' connected to form two junctions 3 and 4. When the junctions are maintained at different temperatures, a potential difference will be developed across the

junctions, which can be measured by inserting a voltmeter in the circuit. The voltage difference (ϕ_{14}) across the voltmeter terminals is given by the following relation [Egli, 1960].

$$\phi_{14} = S_{AB}(T_2 - T_3) \qquad (1.1)$$

where S_{AB} is called the relative Seebeck coefficient and T_2 and T_3 are the temperature of junction 2 and 3 respectively. The relative Seebeck coefficient is the property of the thermoelectric circuit and it can be defined in terms of the absolute Seebeck coefficient of individual thermoelements as below.

$$S_{AB} \equiv S_A - S_B$$

where S_A and S_B are the absolute Seebeck coefficients of thermoelement A and thermoelement B respectively. S_A and S_B are found to be the functions of temperature and chemical composition of the material. In case of silicon, alteration in doping concentration changes the value of Seebeck coefficient

Equation (1.1) can be derived using the expressions for voltage developed in each segment of the circuit, shown in Figure 1-1. Let us say we are interested in the electromotive potential difference developed across the voltmeter junctions 1 and 4. The theoretical expression for the voltage developed across a segment, from point 'x' to point 'y', of thermoelement is given as follows.

$$\int_{\phi_x}^{\phi_y} d\phi = \int_{T_x}^{T_y} S \, dT \qquad (1.2)$$

where S is the absolute Seebeck coefficient of the segment. Using this expression, the net Seebeck voltage across voltmeter junctions can be derived as follows.

Voltage difference between junction 1 and 2: $\phi_{12} = \int_{T_1}^{T_2} S_B dT$

Voltage difference between junction 2 and 3: $\phi_{23} = \int_{T_2}^{T_3} S_A dT$

Voltage difference between junction 3 and 4: $\phi_{34} = \int_{T_3}^{T_4} S_B dT$

where T_1, T_2, T_3 and T_4 are the temperature of junction 1, 2, 3 and 4 respectively.

Net output Voltage: $\phi_{14} = \phi_{12} + \phi_{23} + \phi_{34}$

$$\phi_{14} = \int_{T_1}^{T_2} S_B dT + \int_{T_2}^{T_3} S_A dT + \int_{T_3}^{T_4} S_B dT$$

Assuming that the temperature of junction 1 and 4 remains constant at some reference temperature throughout the device operation. i.e. $T_1 = T_4 = T$, then we can simplify the previous expression as:

$$\phi_{14} = \int_{T}^{T_2} S_B dT + \int_{T_2}^{T_3} S_A dT + \int_{T_3}^{T} S_B dT$$

$$\phi_{14} = \int_{T_2}^{T_3} S_A dT + \left(\int_{T_3}^{T} S_B dT + \int_{T}^{T_2} S_B dT \right)$$

$$\phi_{14} = \int_{T_2}^{T_3} S_A dT + \int_{T_3}^{T_2} S_B dT = \int_{T_2}^{T_3} (S_A - S_B) dT$$

$$\phi_{14} = (S_A - S_B)(T_3 - T_2)$$

This shows that the net Seebeck voltage in the circuit is directly proportional to the relative Seebeck coefficient and the temperature difference between the junction 3 and 2. The relative Seebeck coefficient is independent of dimension and geometry of the thermoelements.

For one-dimensional case, the relationship between the temperature gradient and the voltage gradient can be derived by differentiating Equation (1.2) with respect to spatial variable 'x'.

$$\frac{d\phi}{dx} = S \frac{dT}{dx}$$

The above expression can be written in a general form as:

$$\nabla\phi = S\nabla T \qquad (1.3)$$

Equation (1.3) gives an important relationship that will be used to develop expressions for the internal heat generation due to different thermoelectric effects that occurs due to the Seebeck voltage.

1.1.2. Peltier Effect

In 1834, a French physicist Peltier discovered a thermoelectric effect that was opposite to the Seebeck effect. He observed that heat was liberated at one junction and absorbed at the other junction of Seebeck's antimony-bismuth thermocouple, when an electric current was passed through the junctions [ASTM, 1974]. The direction of heat flow between the junction and its surrounding can be reversed by reversing the direction of the current as illustrated in Figure 1-2. An interesting fact to note here is that the Peltier effect takes place whether the current is introduced externally or is induced internally by Seebeck effect [ASTM, 1974]. Therefore, only the presence of temperature difference at the junctions of a thermocouple can cause heat absorption or liberation at the junctions due to the Peltier effect. This reversible thermoelectric effect is independent of the shape and dimension of thermoelements forming the junction.

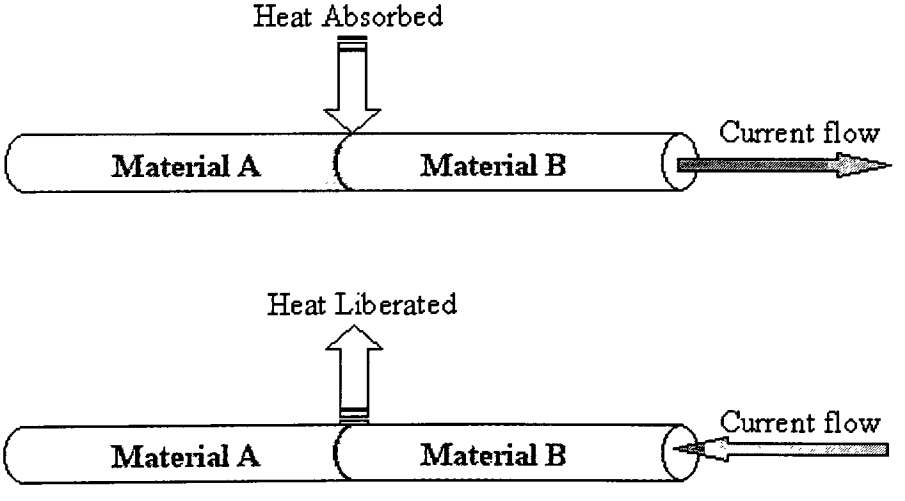

Figure 1-2 Peltier Effect

Mathematically, the magnitude of the heat absorbed or liberated at the junction due to the Peltier effect is given by the following expression [Harman, 1961].

$$Q_P = \pi_{AB} I \tag{1.4}$$

where π_{AB} is a constant of proportionality called the Peltier coefficient of the junction, made by joining the ends of thermoelement A and B. It represents the amount of heat liberated or absorbed, when a unit current passes through the junction for unit time. It has the units of voltage and is closely to the relative Seebeck coefficient by the Kelvin relation [Harman, 1961].

$$\pi_{AB} = T_{abs} (S_A - S_B) \tag{1.5}$$

where T_{abs} is the absolute temperature of the junction. S_A and S_B are the absolute Seebeck coefficients of thermoelement A and B respectively.

The Peltier effect can be seen as a plane heat source placed at the junction surface that release heat in both directions along the length of the thermoelements. The intensity of the plane heat source can be derived by dividing equation (1.4) with the cross sectional area (A) of the junction.

$$\text{Intensity of Peltier heat source } (q''_P) = \pi_{AB} \frac{I}{A} = \pi_{AB} \vec{J} \tag{1.6}$$

where J is the electric current density, which can be due to an external current source or due to the Seebeck voltage.

The mechanism behind the Peltier effect can be described by the fact that the electric current tends to drag heat energy in a thermoelectric circuit. The charge carriers carry internal energy while flowing from one end to another end of a conductor. When they pass across the junction, from one material to another having different entropy of transportation, heat must be evolved or absorbed at the junction to make up the change in the energy of the carriers.

1.1.3. Thomson Effect

In 1857, Thomson discovered that heat was either absorbed or liberated in a conductor when an electric current passes from a material at one temperature to the same material at

different temperature. In other words, the liberation or absorption of heat occurs in a conductor with both temperature and voltage gradient imposed. The direction of energy exchange between the conductor and its surroundings depends on the relative direction of net current and net heat flow in the conductor. As shown in Figure 1-3, the heat is liberated at a certain point along the length of a conductor, if the direction of flow of heat and current is same and heat is absorbed if the direction of flow of heat and current is opposite. It should be noted here that the Thomson effect takes place in a thermoelectric circuit whether the current in the circuit is externally applied or internally developed due to the Seebeck effect.

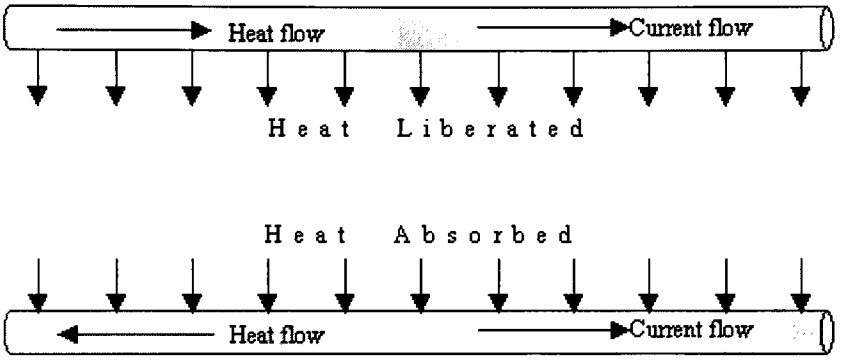

Figure 1-3 Thomson effect

Like the Peltier effect, the Thomson effect is also reversible. The Peltier effect only occurs at junctions of two dissimilar conductors, while the Thomson effect occurs throughout the volume of the homogeneous conductor.

The net heat produced (Q_{th}) in a conductor per unit length (ℓ), due to the Thomson effect, is given by the following expression.

$$\frac{Q_{th}}{\ell} = \sigma I \frac{dT}{dx} \tag{1.7}$$

where σ is the Thomson coefficient, which is also referred as the specific heat of electricity because of its analogy with the thermodynamic specific heat [ASTM, 1974]. The thermodynamic specific heat represents the amount of heat transfer per unit

temperature difference per unit mass; and the Thomson coefficient represents amount of heat absorbed per unit temperature difference per unit current.

The amount of heat generation per unit volume (q'''_{th}) due to the Thomson effect can be derived from equation (1.7). Assuming constant cross sectional area (A) of the conductor, the heat generation per unit volume is given by:

$$q'''_{th} = \frac{Q_{th}}{V} = \sigma \frac{I}{A}\frac{dT}{dx} = \sigma \vec{J}\frac{dT}{dx} \tag{1.8}$$

where V is the volume of the conductor and J is the electric current density vector. The equation (1.8) is more specific to one-dimensional cases, which can be extended for a general case using the gradient operator.

$$q'''_{th} = \sigma(\vec{J}.\vec{\nabla}T) \tag{1.9}$$

1.1.4. Joule Effect

The Joule effect is an irreversible thermoelectric effect that causes internal heating of a current carrying conductor. Unlike the Thomson effect, heat due to the Joule effect is always absorbed in a conductor irrespective of the direction of the current and the presence of temperature gradient. The magnitude of Joule heating depends on the current and the resistivity of the conductor.

The rate of the internal heat generation in a conductor due to the Joule effect is given as:

$$Q_j = I^2R \tag{1.10}$$

where I is the current passing through the conductor and R is the resistance of the conductor.

The resistance of the conductor can be replaced by an expression involving electrical resistivity (γ) of the conductor, which is an intrinsic material property.

$$R = \gamma\frac{\ell}{A}$$

where ℓ is the length and A is the cross-sectional area of the conductor.

The amount of Joule heat per unit volume (q_J''') can be obtained by dividing equation (1.10) with volume (V) of the conductor.

$$q_J''' = \frac{Q_J}{V} = \frac{I^2 R}{A\ell}$$

$$q_J''' = \gamma\left(\frac{I}{A}\right)^2$$

$$q_J''' = \gamma(\vec{J}\bullet\vec{J}) = \gamma|\vec{J}|^2 \qquad (1.11)$$

1.1.5. Thermal Conduction

Thermal heat conduction is an irreversible process and it arises due to the presence of temperature gradient in a conductor that induces a flow of heat in the direction of the negative temperature gradient. The rate of heat conducted is given by the Fourier law, which states that the rate of heat conducted across a unit surface is proportional to the temperature gradient.

$$\vec{q} = -\,k\nabla T \qquad (1.12)$$

where $\vec{q}$ is the heat flux, which is defined as the rate of heat flow per unit area and k is the thermal conductivity. The thermal conductivity may or may not be dependent upon the temperature of the material.

1.1.6. Electrical Conduction

The presence of a voltage gradient in a conductor induces a flow of charge carriers from high potential region to low potential region. The flow of charge carriers is known as electric current, which is related to the voltage gradient as given by Ohm's law.

$$\vec{J} = \frac{1}{\gamma}\nabla\phi \qquad (1.13)$$

where J is the current density, which is defined as the rate of flow of charge carriers per unit area or the current per unit area, and ϕ is the voltage distribution in the conductor.

1.2 Thermoelectric Devices

The driving phenomenon for various practical applications of thermoelectricity is either the Seebeck effect or the Peltier effect. The devices based on Seebeck effect are used to

convert thermal signals into electrical signals and devices based on Peltier effect are used to convert electrical signals into thermal signals. Whether the driving force for a device is Seebeck effect or Peltier effect, all the thermoelectric effects occurs in the device. For example, in a device based on the Seebeck effect, one might think that the only effects that are present in the circuit are the Seebeck effect, thermal conduction and electrical conduction. However, due to the presence of electrical current in the circuit, which is a result of Seebeck effect, the Joule, Peltier and Thomson effect will also come into the picture. Although the magnitude of Joule, Peltier and Thomson effect will entirely depend on the Seebeck voltage. Based on the field of applications, the thermoelectric devices may be divided into following three categories.

Thermoelectric Sensor
Thermoelectric Generators
Thermoelectric Coolers

1.2.1. Thermoelectric Sensor

The primary function of a thermoelectric sensor is to measure temperature. However, thermoelectric sensors are also employed to measure non-thermal signals such as flow velocity, radiation intensity and heat flux by first converting them into heat flow, which is then transformed into temperature difference that can be sensed using the Seebeck circuit. The unknown temperature difference between the junctions is computed from the known voltage in the circuit.

Consider a thermoelectric sensor shown in Figure 1-4 whose one junction is placed at a known reference temperature and other junction is in thermal contact with the wall. The output voltage given by the voltmeter can be related to the unknown wall temperature with the following relation.

$$\phi = (S_A - S_B)(T_1 - T_2) \tag{1.14}$$

where T_1 is the wall temperature and T_2 is the known reference temperature. The unknown wall temperature can then be determined from (1.14) as follows.

$$T_1 = \frac{\phi}{S_A - S_B} + T_2 \tag{1.15}$$

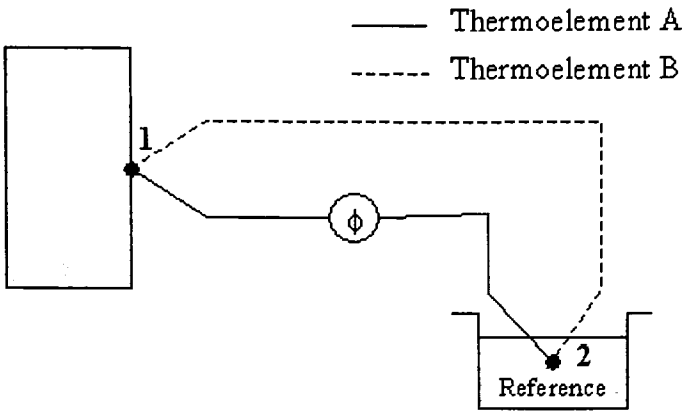

Figure 1-4 Thermoelectric Sensor measuring wall temperature

Equation (1.15) shows that the wall temperature is a linear function of Seebeck voltage assuming constant values of absolute Seebeck coefficients. However, the Seebeck coefficient is greatly influenced by temperature and the selection of thermoelectric material set is made such that the variation of relative Seebeck coefficient in the working temperature range should be constant.

Generally, the voltage developed by one thermocouple is very small (on the order of millivolts for common thermoelectric materials) and to improve the sensitivity a number of thermocouples are connected electrically in series and thermally in parallel to form a thermopile. The advantage of using thermopile is that the output voltage can be increased by a factor of n, which is the number of thermocouples used to form the thermopile.

The thermoelectric sensors are employed in the measurement of temperature, heat flux, flow rate and radiation. The simplicity, ruggedness, low cost, small size and wide temperature range of thermocouples make them the most common type of temperature sensor for industrial applications.

1.2.2. Thermoelectric Generators

The purpose of a thermoelectric generator is to supply electric power to a load connected in the circuit. The operation of a thermoelectric generator is based on the Seebeck effect.

A schematic of a thermoelectric generator is shown in Figure 1-5. It consists of two dissimilar conductors connected at their ends and two heat reservoirs at different temperatures T_H and T_c.

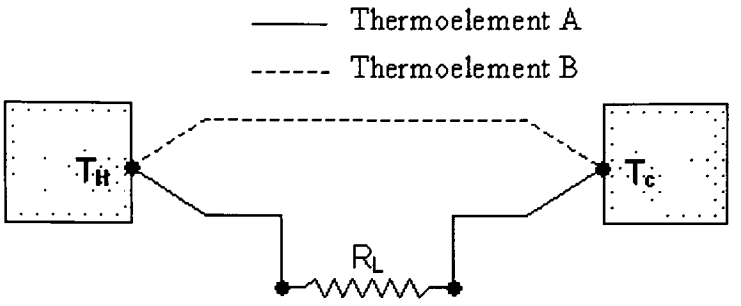

Figure 1-5 Thermoelectric generator

When the junctions of thermocouple are placed in the heat reservoirs, the voltage ϕ develops across the load resistance R_L. The voltage ϕ is a function of the temperature difference between the heat reservoirs. The magnitude of the voltage and the current in the circuit can be derived as follow:

$$\phi = S_{AB}(T_H - T_c)$$

$$I = \frac{\phi}{R_L + R} \tag{1.16}$$

Where R is the internal resistance of the Seebeck circuit.

The voltage across the load resistance can be obtained using the magnitude of the current across the load resistance.

$$\phi_L = I\,R_L = \frac{\phi}{R_L + R} R_L \tag{1.17}$$

The power output (P) from the thermoelectric generator is the product of current and voltage drop across the load resistance.

$$P = \left(\frac{\phi}{R_L + R}\right)^2 R_L \tag{1.18}$$

For the maximum efficiency, the load resistance must be equal to the internal resistance of thermoelectric circuit *i.e.* $R_L = R$. Therefore the maximum power that can be obtained from the thermoelectric generator is given as follows.

$$\text{Maximum power output} = P_{max} = \frac{\phi^2}{4R} \tag{1.19}$$

Thermoelectric generators find their application in the field of electric power generation. These are best suited for the applications that require low power, high reliability and operation at remote sites. Other sources of power under such conditions are batteries, solar cells, engine driven generators or extended landlines. Each of these has its disadvantages, which may encourage the use of thermoelectric generators. Application of thermoelectric generators in space is particularly important, where RTGs (Radioisotope Thermoelectric Generator) are used to convert radioactive heat to the electric energy. RTG's are also used at remote sites to supply continuous electric power to the data collecting systems; such applications include weather monitoring of a remote site.

1.2.3. Thermoelectric Cooler

Thermoelectric coolers are based on the Peltier effect and are employed to convert electric energy into thermal energy. When an electric current (or an external voltage), source is inserted in a thermoelectric circuit, one junction absorbs heat and other junction liberates heat. Therefore, thermoelectric coolers can be used to produce cooling or heating by supplying electric power. The thermoelectric coolers function similar to the heat pumps, as they pump heat from one junction to other on the application of current in the circuit.

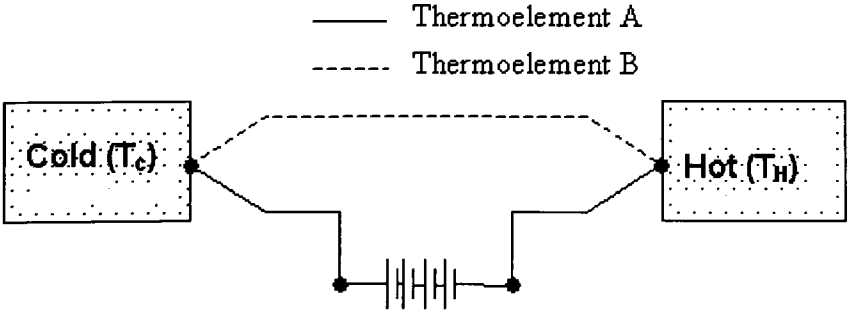

Figure 1-6 Thermoelectric Cooler

As the refrigeration effect produced by thermoelectric cooler is directly proportional to the supplied current, it is very convenient to control cooling by adjusting the current in the circuit. The development in semiconductor process technology remarkably improved the performance of thermoelectric coolers. It is comparatively difficult to obtain steady state temperature using conventional refrigeration systems because of their "on" and "off" mode of operation. Also mechanical system may be a source of noise because of their moving parts. On the other hand, thermoelectric coolers are quiet and have neither moving parts to wear out nor gases to leak away. Thermoelectric coolers have the ability to operate in conjugation with proportional control systems rather than on-off system. Thermoelectric coolers are employed for carrying medical supplies in small boxes, for storage of perishable goods in automobiles and control of temperature particularly for scientific instruments and for electronic and optoelectronic systems [Rowe, 1995].

1.3 Problem Description and Thesis Objectives

The design of thermoelectric devices, used in industrial applications, has been focused on the selection of thermoelectric material set that would provide required sensitivity, efficient operation and stability under the working environment. The parameters involved in the selection of thermoelectric materials are Seebeck coefficient, electrical resistivity and thermal conductivity. A relation involving these parameters, called figure of merit, is used to evaluate the relative advantage of different thermoelements.

$$\text{Figure of Merit (Z)} = \frac{S^2}{k\gamma}$$

The performance analysis of thermoelectric devices is mostly based on steady state response analysis that includes thermal conduction and the driving thermoelectric effect (Seebeck effect for thermoelectric generators and Peltier effect for thermoelectric coolers). The influence of Joule effect, Thomson effect and other thermoelectric effect (Peltier effect or Seebeck effect based on the device) on the performance characteristics of the device are typically considered negligible. However, the influence of such effects depends on the material properties and working conditions for the device. As the properties of thermoelectric materials are continuously improving and devices are

employed in harsh working environment, the negligible assumed effects can play an important role in the performance of next generation thermoelectric devices.

The role of thermoelectric effects in a thermoelectric device, based on the Seebeck effect, can be visualized with the following example. Consider a thermoelectric device, whose cold junctions are kept at a fixed temperature and hot junction is exposed to constant flux environment. The difference in junction temperatures causes heat to flow from hot junction to cold junction. In addition to the flow of heat, the current will also flow in the closed thermocouple circuit due to the Seebeck effect. The intensity of current depends on total circuit resistance, relative Seebeck coefficient and temperature difference across the junctions. The flow of current causes internal heat generation in the thermoelements due to the Joule effect. Also depending on the relative direction of current and heat flow, the heat will be absorbed or liberated from the thermoelements as given by Thomson effect. Heat will also be liberated at one junction and absorbed at the other junction due to the Peltier effect. The change in heat energy of thermoelements caused by Joule and Thomson effect may considerably influence the temperature distribution within the thermoelements and also at the junctions, which in turn can change the output voltage and the transient characteristics of the device. Therefore, a complete analysis of a thermoelectric device must account for all the thermoelectric effects.

The objective of this thesis is to develop a numerical analysis tool to study steady state and transient response of thermoelectric devices based on the Seebeck effect. All thermoelectric effects (Thomson effect, Joule effect and Peltier effect) will be included in the analysis. The influence of individual thermoelectric effects will be analyzed under fixed temperature, fixed flux and convective environment at the hot junction. The objective will be accomplished in the following steps:

1. Develop a mathematical model of thermoelectric device from the fundamental principles of thermoelectricity, heat transfer and electrical.
2. Implement the model (steady state and transient) using finite element method.
3. Validate the finite element model against limiting theory and numerical cases.

4. Use the validated finite element code to study the significance of Seebeck effect, Joule effect, Thomson effect and Peltier effect on the performance of thermoelectric devices under different working conditions.
5. Demonstrate the use of the model as a design tool for predicting performance characteristics of thermoelectric devices.

1.4 Steady State and Transient Model of Thermoelectric Device

The complete model of a thermoelectric Device consists of coupled thermal and electrical domains that incorporate Seebeck effect, Joule effect, Thomson effect, Peltier effect and thermal conduction into the analysis. The model can be utilized to study the influence of individual thermoelectric effect as well as the combined influence of all thermoelectric effects on the performance characteristics of the device. The steady state thermal model is based on an elliptical partial differential equation that governs temperature distribution in the thermoelectric circuit. The Seebeck effect couples thermal model to the electric model by computing voltage and current density distribution as a function of temperature and material properties of the thermoelements. The Joule, Thomson and Peltier effect couples electrical model back to the thermal model by relating surface and body heat sources in governing temperature distribution equation to the current density distribution on finite elements.

Figure 1-7 graphically describes coupled thermal and electrical model of thermoelectric device, where the Seebeck effect couples thermal model to electrical model by linking the voltage distribution to temperature distribution and Joule, Thomson and Peltier effect links the electrical model to the thermal model by internal heat generation term and internal flux boundary condition in the governing thermal model equation.

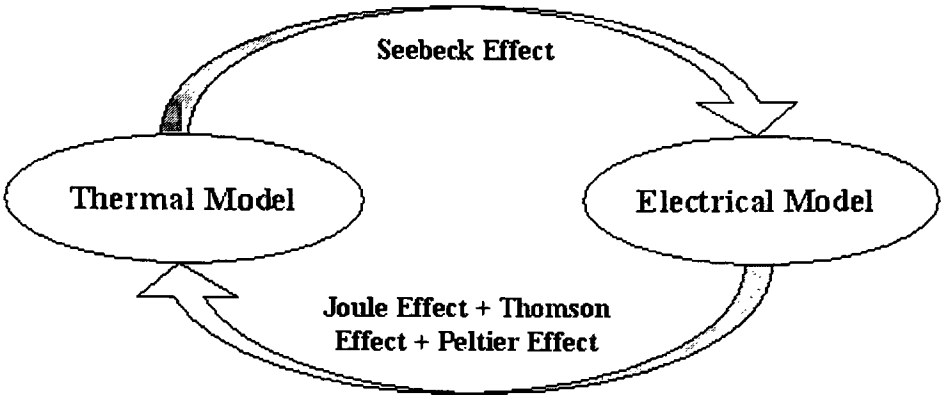

Figure 1-7 Thermal and Electrical Domains

1.4.1. Mathematical Model for Steady State Response

The steady state model of a thermoelectric device computes temperature and voltage distribution in the thermoelements as a function of spatial co-ordinates. The thermal and electrical governing equations are independent of time in the steady state finite element model, which simplifies the modeling by eliminating the heat storage term from the governing heat conduction equation.

The heat conduction equation governs temperature distribution and the Seebeck equation governs voltage distribution in the thermoelectric circuit. Both equations are coupled to each other with Joule, Thomson and Peltier effect. In this section the governing equations for temperature and voltage distribution, incorporating the coupling, are derived.
The steady state heat conduction equation in two-dimensional space is given by:

$$k\nabla^2 T = -\, q_0''' \qquad \text{subjected to } q_p'' \text{ at the junctions} \qquad (1.20)$$

where k is thermal conductivity, T is temperature as a function of space variables and q_0''' is the coupling term that includes internal heat generation per unit volume due to Joule (q_J''') and Thomson effect(q_J'''). q_p'' is the internal heat generation per unit area due to the Peltier effect.

$$q_0''' = q_J''' + q_{Th}''' \qquad (1.21)$$

The internal heat generation terms due to Joule and Thomson depend on the current flow in the circuit, which in turn depends on temperature distribution. In the following paragraphs, q'''_J, q'''_{Th} and q''_p are derived as a function of temperature.

Heat Generation due to Joule Effect

The heat generation per unit volume inside the thermoelements due to the Joule effect can be written in terms of current density ($\vec{J}$) and electrical resistivity of thermoelements (γ) as follow:

$$q'''_J = \gamma \, \vec{J} \bullet \vec{J} \tag{1.22}$$

The current density (current per unit area) can be defined in terms of electric potential (ϕ) using Ohm's law.

$$\vec{J} = \frac{1}{\gamma} \nabla\phi \tag{1.23}$$

In the case of a thermoelectric device based on Seebeck effect, the electric potential in a thermoelectric circuit is only due to the Seebeck effect and the relation between the temperature gradient and voltage gradient is given by Equation (1.3).

$$\nabla\phi = S\nabla T \tag{1.24}$$

Substituting Equation (1.24) in Equation (1.23) to obtain current density as a function of temperature gradient.

$$\vec{J} = \frac{S}{\gamma} \nabla T \tag{1.25}$$

Using Equation (1.25) in Equation (1.22) gives Joule heat per unit volume in terms of temperature.

$$q'''_J = \gamma \left(\frac{S}{\gamma}\right)^2 (\nabla T \bullet \nabla T)$$

$$q'''_J = \frac{S^2}{\gamma} (\nabla T \bullet \nabla T) \tag{1.26}$$

Equation (1.26) shows that the Joule heat generation per unit volume is directly proportional to the square of temperature gradient and the square of the Seebeck coefficient and inversely proportional to the electrical resistivity.

Heat generation due to Thomson Effect

The amount of heat absorbed or liberated per unit volume of a thermoelement due to the Thomson effect is given by Equation (1.9).

$$q'''_{th} = \sigma(\vec{J} \bullet \vec{\nabla} T)$$

In case of a thermoelectric device based on Seebeck effect, the current density depends only on the temperature distribution. Therefore the Thomson heat term can be expressed in terms of temperature gradient as follows.

$$q'''_{Th} = \frac{\sigma S}{\gamma}(\vec{\nabla} T \bullet \vec{\nabla} T) \qquad (1.27)$$

Flux Constraint at the Junction due to the Peltier Effect

The expression for the Peltier heat per unit volume, as given by Equation (1.6), can be transformed into a function of temperature gradient as a special case for the thermoelectric devices based on Seebeck effect, in which the current source is only internal.

$$q''_P = \pi_{AB} \frac{S}{\gamma} \nabla T$$

Complete Thermal Model

The steady state temperature distribution in the thermoelements including the influence of Joule effect, Thomson effect and Peltier effect can be obtained from the following non-linear partial differential equation subjected to an additional flux constraint at the junction.

$$k\nabla^2 T = -\frac{S^2}{\gamma}(\vec{\nabla} T \bullet \vec{\nabla} T) - \frac{\sigma S}{\gamma}(\vec{\nabla} T \bullet \vec{\nabla} T) \qquad (1.28)$$

$$q_P'' = \pi_{AB} \frac{S}{\gamma} \nabla T \qquad \text{(at the junctions)}$$

To simplify the expression, lets define q'''_0, a heat generation term as a function of temperature gradient and material properties.

$$k\vec{\nabla}^2 T(x,y) = q_0''' \tag{1.29}$$

where $q_0''' = -\left(\frac{S^2}{\gamma} + \frac{\sigma S}{\gamma}\right)(\vec{\nabla}T \bullet \vec{\nabla}T)$ (1.30)

The voltage distribution in the thermoelements can be obtained using Seebeck relation given below:

$$\int d\phi = \int S dT \tag{1.31}$$

1.4.2. Mathematical Model for Transient Response of Thermoelectric Devices

The Transient finite element model of a thermoelectric device is used to obtain temperature and voltage as a function of spatial and temporal variable. The transient finite element model of a thermoelectric device provides information regarding the response time of the device. It is assumed that the electrical response of thermoelectric device is comparatively much faster than the thermal response. Therefore, the same electrical governing equation is used to compute transient voltage distribution that has been used in steady state model. The elliptical partial differential equation that was used to compute temperature distribution is replaced by parabolic partial differential equation that gives temperature distribution as a function of time.

The transient thermal equations can be described as follows:

Governing Equation: $$k\vec{\nabla}^2 T(x,y,t) = q_0''' + \rho c_p \frac{\partial T}{\partial t} \tag{1.32}$$

$$q_P'' = \pi_{AB} \frac{S}{\gamma} \nabla T \qquad \text{(At the Junctions)}$$

where t denotes time, ρ is density and c_p is the specific heat.

The governing electrical equation used for transient analysis to obtain the voltage (ϕ) distribution is given as follows:

Governing Equation: $$\int d\phi = \int S dT \tag{1.33}$$

1.5 Different Methods of Analyzing Thermoelectric Device

Analyzing complete thermoelectric device model involves solving non-linear partial differential equation subjected to boundary conditions, nonlinear junction constraint and initial condition. Different techniques those are available to solve the partial differential equations are listed below, which have their own advantages and disadvantages.

Analytical Methods
Numerical Methods

Analytical methods are restricted to problems involving simple geometries, linear material properties and boundary conditions. A complete coupled thermoelectric device model involves nonlinear internal heat generation terms and nonlinear constraint at the junctions, which make it very difficult to obtain the solution using analytical methods. Numerical methods provide a very powerful tool for solving non-linear partial differential equations in multi-dimensions involving irregular geometries. Unlike analytical methods, that yield exact solution to the governing equation, the numerical methods yield approximate solution at discrete points over the domain. The most widely used numerical methods are finite element method, finite difference method and boundary element method.

With the advent of modern computer technology, it becomes possible to provide fast and easy way to analyze complex analysis problems using numerical methods. Numerical methods transform the partial differential equation into a set of linear equations that can be easily solved with the use of computers. Many software based on numerical methods are commercially available to analyze a vast category of single and coupled domain problems. However no available commercial software can be used directly to solve complete thermoelectric device model. ANSYS, for example, has an option to analyze thermal problems coupled with Joule heating. However it requires additional user subroutines to include the influence of Seebeck, Peltier and Thomson effect.

For the analysis of this particular problem of thermoelectric device, two different approaches were considered. First, using a commercially available simulation software package with additional user subroutines. Another approach was to develop a finite element code using MATLAB to solve complete coupled thermoelectric device model. The MATLAB program provides more control over the finite element method, thus making easy to customize program according to the requirements.

2 Literature Review

2.1 Introduction

During 1950's, silicon emerged as a promising material for thermoelectric modules due to its high thermoelectric power [Geballe, 1955]. Besides its much larger Seebeck coefficient than any metal, it provides option to adjust thermoelectric properties just by altering the concentration of impurities. However, early attempt to implement silicon into practical thermoelectric devices lacked definitive success primarily because the large number of couples required to generate a meaningful output made the device excessively large. The introduction of micro-fabrication technology enabled the use of silicon to fabricate thermoelectric modules. The use of silicon as a thermoelectric material results in higher sensitivity and productivity, which makes it a promising material for the next generation thermoelectric modules.

The use of micro-fabrication technology to develop MEMS based thermoelectric devices has promising practical advantages. Micro thermoelectric sensors can operate effectively with minimum disturbance to its surroundings [Oh, 2000]. Also, thermoelectric sensors don't require any external current for their operation that makes these devices more favorable over bolometer detectors [Chang, 1998]. The cost of thermoelectric material is the biggest component in the module cost. In a thermoelectric device, only 1% of the material, a thin layer near the junctions, participates in the energy conversion [Aantychuk, 1996]. Therefore, reduction in the size of thermoelectric devices with the use of micro-miniaturization technology will result in lower cost. The batch fabrication of complete thermoelectric system with integrated electronics on a single chip can increase device sensitivity, reliability, stability and compactness [Aantychuk, 1996]. Micro thermoelectric generators also present promising practical use as a tiny electric power source, called microbatteries. Micro thermoelectric coolers are the potential candidates to replace larger mechanical heat sinks on electronic chips by providing on the chip cooling [Yao, 2001].

The applications of thermoelectric devices in various fields of industry and science raise the importance of optimum design and analysis. Although the materials for the thermoelements play a significant role in the performance of the thermoelectric devices, the development of mathematical models based on all known thermoelectric effects can be used to optimize design variables for enhanced performance characteristics. It has been shown that the Silicon based thermoelectric devices offers higher Seebeck coefficient and sensitivity than metal based thermoelectric devices [Muanghlua, 2000].

The literature is filled with the steady state response analysis of thermoelectric coolers and thermoelectric generators. However, the analysis includes only the driving thermoelectric effect (Seebeck in case of Thermoelectric generators and Peltier in case of thermoelectric coolers) along with the heat conduction and rest of the thermoelectric effects are considered negligible. The steady state response of these devices is based on simplified analytical solution of governing equation that considers thermocouple as a one-dimensional beam. The transient analysis of thermoelectric devices has been reported with application specific methods. Two different methods are listed in literature for fluid immersed and solid embedded thermocouple [Rabin,1999].

2.2 Literature on Steady State Response Analysis

Generally, the steady state response of thermoelectric modules involves the calculations of output voltage based on the Seebeck relation and further evaluating the efficiency of the device using output voltage and assumed fixed temperature at the junctions. The interaction of thermoelectric device with the environment is not considered in such analyses. The only points of interest on a thermocouple are considered to be the junctions and by assuming fixed temperature boundary condition and neglecting Joule, Thomson and Peltier effect from the analysis, there is no need to evaluate the temperature distribution is the thermoelements.

A thermoelectric model of a thermoelement carrying current is presented in [Heikes, 1961]. The temperature distribution is governed by parabolic partial differential equation in one dimension, which includes the internal heat generation due to the Joule effect.

$$k\frac{d^2T}{dx^2}+J^2\gamma=0 \tag{2.1}$$

$$T(0) = T_h$$

$$T(L) = T_c$$

where k is the thermal conductivity, T is the temperature as a function of space co-ordinate x, J is the current density, L is the length of thermoelement and γ is the electrical resistivity. The second term in Equation (2.1) represents the internal heat generation per unit volume due to the Joule effect. All material properties are assumed to be independent of temperature including the Seebeck coefficient of the thermoelement. The internal heat generation due to the Thomson effect is zero as the Thomson coefficient depends on the derivative of Seebeck coefficient with respect to the temperature. Therefore Equation (2.1) includes all the thermoelectric effects that occur along the length of a thermoelement. The governing equation (2.1) is solved using fixed temperature boundary conditions to obtain following temperature function.

$$T = [T_h-(x/L)(T_h-T_c)]+(\frac{J^2\rho}{2k})x(L-x) \tag{2.2}$$

The heat energy entering the hot junction of a thermoelement of cross-sectional area A and carrying a current I is computed using Equation (2.2) as follow.

$$-Ak\left.\frac{\partial T}{\partial x}\right|_{x=L}=k\frac{A}{L}(T_h-T_c)+\frac{1}{2}I^2R \tag{2.3}$$

Similarly, the rate at which heat is leaving the cold end is given by following expression.

$$-Ak\left.\frac{\partial T}{\partial x}\right|_{x=0}=k\frac{A}{L}(T_h-T_c)-\frac{1}{2}I^2R \tag{2.4}$$

Equation (2.3) and (2.4) show that exactly one-half of the Joule heat generated in the bar goes to each end of the thermoelement. It is to be noted here that the solution given by Equation (2.2) is based on the assumption that the current is independent of temperature.

The performance of a thermoelectric generator was studied using finite element analysis in [Lau, 1997]. The author included the internal heat generation in the thermoelements due to the Joule effect and on the junctions due to the Peltier effect. Two different techniques were used to include temperature dependent material properties. First, averaging technique, which uses average of material properties in the working temperature range. Second, the finite element technique, which implicitly determine temperature dependent properties based on the temperature distribution. The results of finite element analysis were compared with the results obtained using averaging techniques and the use of finite element analysis was recommended when critical device optimization is required.

The steady state model of a thermoelectric heat pump or Peltier cooler is reported in [Arenas, 2000] that includes thermal conduction, Joule effect and Peltier effect in the analysis. Authors used the commercial software, ANSYS, to solve the resulting mathematical model by combining with an additional user sub-routine. Finite element modeling of Peltier heat at the separation boundary is discussed in the reference.

A different approach is reported in [Milanović, 2000] to solve a thermoelectric device model, which includes Peltier effect and Thomson effect in the analysis. The analogy between thermal and electrical is used to transform complete thermal-electric model into pure electrical domain and then an electrical simulation tool, such as SPICE, is used to perform thermal simulation. The resultant model shows close agreement with the experimental observations.

The steady state characteristics of a thermoelectric generator are predicted in [Toriyama, 2001] and [Yajima, 2001] that account for the interaction of thermoelectric generator with the radiation environment. However, only the Seebeck effect and Fourier effect are included in the analysis. The thermoelectric device studied in the reference is a self-standing polysilicon-metal thermopile used as a micro power generator. The self-standing structure, as shown in Figure 2-1, isolate the thermoelements from the silicon substrate,

thus causing the flow of heat from hot to cold junction only through the thermoelements and not through the silicon substrate.

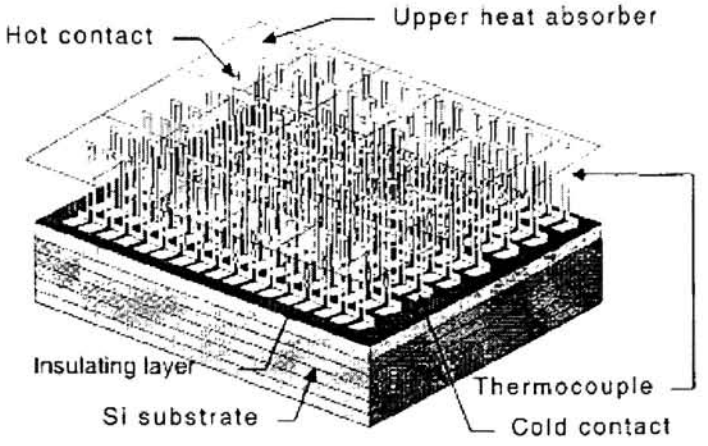

Figure 2-1 Self-standing thermopile structure *[Toriyama, 2001]*

The energy balance of a self-standing thermocouple, subjected to radiation heat source is shown in Figure 2-2. The heat absorber area absorbs thermal energy emitted by the black body source at temperature 307K. Some portion of the heat energy is emitted back from the hot junction and rest is transmitted to the cold junction through the thermoelements. The temperature difference between hot and cold junction ($T_1 - T_0$) is obtained using Equation (2.5).

$$T_1 - T_0 = \frac{\varepsilon \sigma_{rad} T_b^4 FA}{G_{th} + G_{rad}} \tag{2.5}$$

where T_b is the temperature of source black body, ε is the emissivity of heat absorber, σ_{rad} is the Stefan-Boltzmann constant, F is the form factor, A is the heat absorber area, G_{th} is the thermal conductance of thermoelectric legs and G_{rad} is the thermal conductance due to the radiation.

The output voltage (ϕ) can be computed using Seebeck relation and temperature difference as obtained from Equation (2.5).

$$\phi = N(S_1 - S_2)(T_1 - T_2) \tag{2.6}$$

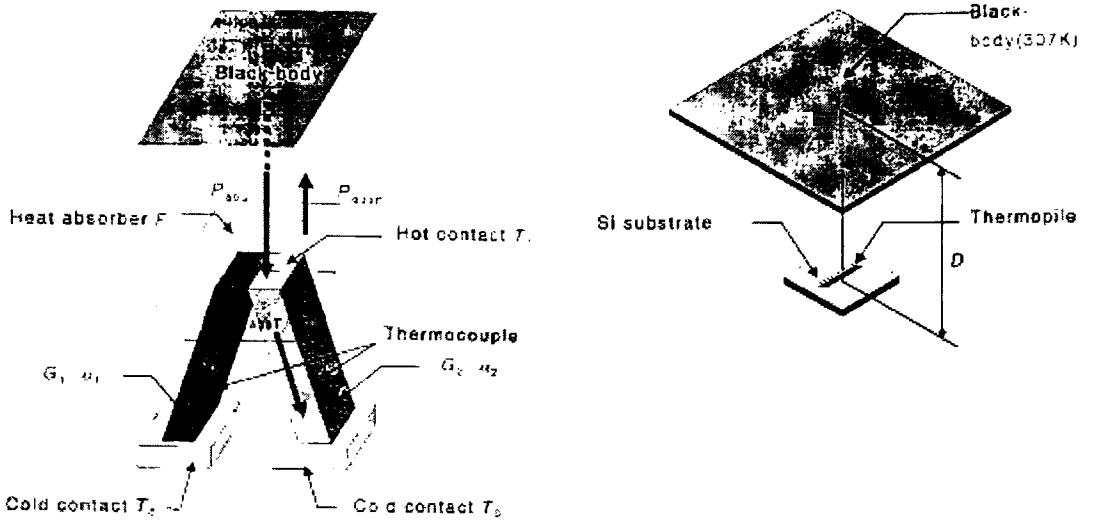

(a) (b)

Figure 2-2 (a) Energy balance of single thermocouple

(b) Experimental configuration *[Toriyama, 2001]*

The output power from the thermoelectric generator is the maximum when the load resistance is equal to the internal resistance (R) of the generator. Therefore, the maximum power (P_{out}) is given by following relation.

$$P_{out} = \frac{\phi^2}{4R} \tag{2.7}$$

2.3 Literature on Transient Response Analysis

A detailed discussion on the transient response of thermoelectric devices is presented in [Gray, 1960]. The derivation of mathematical model includes all the thermoelectric effects in the analysis. The model is developed considering an energy balance of each thermoelement and junction separately and then combining the individual energy balance relations in the overall energy balance equation.

The transient response of a thermoelectric couple was analyzed in [Lau, 1996] using finite element method. The analysis incorporated Joule effect and Peltier effect alongwith

pure thermal and electrical conduction. Temperature dependent material properties were also included in the analysis.

Two different cases of transient analysis of thermocouples are presented in [Rabin, 1999]. A different approach is used to assess transient response of fluid immersed thermocouples that assumes thermocouple as a lumped heat capacitance system based on certain conditions. The other approach is used for solid embedded thermocouples, in which the heat transfer is governed solely by conduction and complete partial differential equations are solved using analytical or numerical methods.

Consider a junction of thermocouple, which is subjected to sudden immersion in hot fluid. The sudden immersion is modeled as a step change in the temperature of the hot junction. The system can be treated as a lumped heat capacitance system if the resistance to the heat conduction within the junction is negligible as compared to the resistance to convective heat transfer. The ratio of resistance to conduction and resistance to convection heat transfer is defined as a dimensionless number, called Biot number (Bi).

$$\mathrm{Bi} = \frac{hV}{kA} \tag{2.8}$$

where h is the convective heat transfer coefficient, V is the volume of the junction immersed in the fluid, k is the thermal conductivity and A is the surface area of the junction. Bi<0.1 means a low thermal resistance to conduction heat transfer and therefore the lumped heat capacitance system can be used to assess transient response of the fluid immersed thermocouple as given in Equation (2.9).

$$\frac{T - T_\infty}{T_0 - T_\infty} = e^{\left(-\frac{hA}{c_p V} t\right)} \tag{2.9}$$

where T is the temperature of the junction, T_0 is the initial temperature, T_∞ is the temperature of the surrounding, c_p is the specific heat and t is the time. The time constant of such system is given by:

$$\tau = \frac{hA}{c_p V} \tag{2.10}$$

When the value of Biot number is greater than 0.1, we must include a transient model of the junction itself. The transient response analysis of solid embedded thermocouples is modeled using parabolic partial differential governing equation. This is comparatively much complicated than the lumped capacitance system analysis. Most common method to solve such systems is the numerical methods, which can analyze complex geometries and temperature dependent material properties.

There literature that includes all thermoelectric effects in the analysis are from 1960's and those were limited only to the theoretical modeling. The analysis of practical devices (metal based thermoelectric devices) had been limited to pure thermal conduction, electrical conduction and use of Seebeck or Peltier effect to relate thermal and electrical domains. The influence of Joule and Thomson effect was assumed to be negligibly small for metal-based thermoelectric devices. Most of the research in the field of thermoelectricity has been focused on the development of thermoelectric materials having improved figure of merit. As the semiconductor materials with high values of Seebeck coefficients have emerged and the temperature gradient in the micro-devices have been getting extremely large, the dependence of Thomson effect and Joule effect on the Seebeck coefficient and the temperature gradient forced researchers to rethink about the significance of these effects.

3 Finite Element Model Development

3.1 Finite Element Background

The finite element method is a numerical technique used to obtain an approximate solution of the partial differential equations that governs many physical and engineering problems. The finite element method originated in mid 1950's when the use of finite difference method to model complex geometries frustrated engineers and scientists [Pepper, 1992]. Initially, the applications were restricted to structural problems, but soon the versatility of this method led to the application of this method in heat conduction and fluid dynamic problems.

The finite element method requires that the geometry of the domain to be divided into finite number of smaller regions, called elements. The vertices of the elements are known as nodes and the complete geometry consisting of elements and nodes is called a mesh. The dependent variables (temperature, displacement, velocity, etc) are then approximated on the node points of each element and interpolation functions are used to approximate the dependent variable within each element. The interpolation functions can be linear or higher order polynomials that depend on the geometric location of the nodes. The governing equations are then integrated over each element using approximated unknown variables and assembled together to obtain a set of simultaneous equations, which can be solved using linear algebra methods to obtain unknown variables at each node [Pepper, 1992].

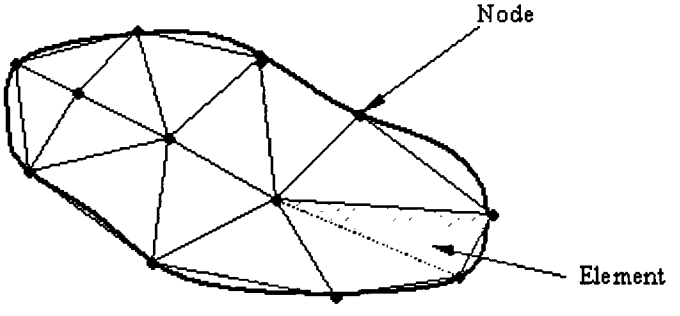

Figure 3-1 Meshed geometry

In this chapter, steady state and transient finite element models of thermoelectric device are formulated and their computer implementation is discussed.

3.2 Assumptions in Finite Element Model

1. Heat and current flow only in one plane. (Two dimensional)
2. Material properties are homogeneous and isotropic.
3. Convection and radiation heat transfer from the thermoelement lateral surface to the surroundings are negligible. (this doesn't preclude convection or radiation boundary condition on the junctions)
4. The electrical response of the sensor is assumed very fast, which eliminates the need of transient electrical model.
5. Conductor dimensions are large compared with the electronic mean free path; correspondingly the thermal and electrical conductivities show no "size dependence" [MacDonald, 1962].
6. The traditional governing heat transfer equation is valid at the dimensional scale of the device to be analyzed.
7. Thermal conductivity, electrical conductivity and heat capacity of the thermoelements are independent of temperature. However, the temperature dependence of thermoelectric properties (Seebeck coefficient, Thomson coefficient and Peltier coefficient) is included in the finite element analysis.

3.3 Steady State Model of Thermoelectric Device

The steady state finite element model of a thermoelectric device computes the temperature and voltage distribution in the thermoelements as a function of spatial co-ordinates. The thermal and electrical governing equations are independent of time in the steady state finite element model, which simplifies the modeling by eliminating the heat storage term from the governing heat transfer equation.

3.3.1. Governing Steady state Equations

The heat conduction equation governs temperature distribution and the Seebeck equation governs voltage distribution in the thermoelectric circuit based on Seebeck effect. Both

equations are coupled to each other with Joule, Thomson and Peltier effect. The coupled thermo-electrical model is transformed into thermal domain using the coupling relations, which results in a thermal model involving non-linear internal heat generation terms and nonlinear constraints at the junctions.

The steady state heat conduction equation was derived in section (1.4.1) and is given by Equation (1.28):

$$k\nabla^2 T = -\frac{\sigma S}{\gamma}(\vec{\nabla}T.\vec{\nabla}T) - \frac{S^2}{\gamma}(\nabla T.\nabla T) \qquad (3.1)$$

$$q_P'' = \pi_{AB}\frac{S}{\gamma}\nabla T \qquad \text{(flux at the junctions)}$$

The first term in Equation (3.1) represents net heat conduction, the second and third terms account for the internal heat generation per unit volume due to the Thomson effect and the Joule effect respectively. The temperature dependence of second and third term makes Equation (3.1) nonlinear. This equation is valid only for thermoelectric devices based on the Seebeck effect in which the only source of current is the Seebeck-voltage.

In the absence of external current source, the voltage distribution in a thermoelectric circuit can be related to the temperature distribution by Equation (1.31).

$$\int d\phi = \int S dT \qquad (3.2)$$

3.3.2. Finite element model for Temperature Distribution

The steady state model of a thermoelectric device is based on the non-linear partial differential Equation (3.1) that governs heat transfer in the device. All thermoelectric effects are incorporated in the analysis by introducing a temperature dependent internal heat generation term in the governing heat conduction equation and heat flux constraint at the junctions.

Consider a domain Ω shown in Figure 3-2. Γ_1 and Γ_2 are the outer boundaries of the domain Ω, which are subjected to boundary conditions.

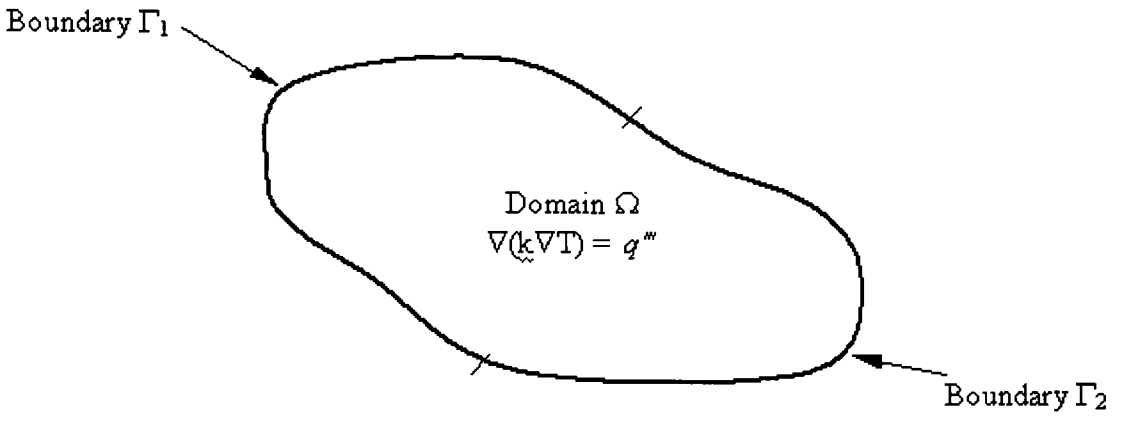

Figure 3-2 Domain with two boundaries

Let us say we are interested in finding the temperature distribution in the domain. The mathematical model of this problem can be described using following equations:

$$\vec{\nabla}(k\vec{\nabla}T(x,y)) = q_0''' \qquad (3.3)$$

$$q_P'' = \pi_{AB}\frac{S}{\gamma}\nabla T \qquad \text{(at the junctions)}$$

$$T(x,y) = T_1(x,y) \qquad \text{on boundary } \Gamma_1 \qquad (3.4)$$

$$k\vec{\nabla}(T(x,y)) = q''(x,y) \qquad \text{on boundary } \Gamma_2 \qquad (3.5)$$

Where q_0''' is the overall internal heat generation per unit volume inside domain Ω and T_1 is the known temperature distribution on boundary Γ_1 and q is the known heat flux on boundary Γ_2. The q_0''' includes the internal heat generation due to the Joule and Thomson effect and is a function of temperature.

$$q_0''' = -\frac{\sigma S}{\gamma}(\vec{\nabla}T.\vec{\nabla}T) - \frac{S^2}{\gamma}(\nabla T.\nabla T) \qquad (3.6)$$

Two methods are often used to formulate the finite element solution of steady state heat conduction problems. One is method of weighted residuals and other is Rayleigh Ritz

method. Other methods such as Galerkin's method, least square method, collocation and constant weights are subsets of the method of weighted residuals.

Regardless of the type of finite element formulation, the first step is to define a mesh consisting of a finite number of non-overlapping subdomains that cover the whole domain. These subdomains are called "elements" and the vertices of these elements are called "nodes". The temperature in the domain can be approximated in terms of the temperatures at the nodes as described by following relation. Figure 3-3 shows a meshed model of domain Ω with three node triangular elements.

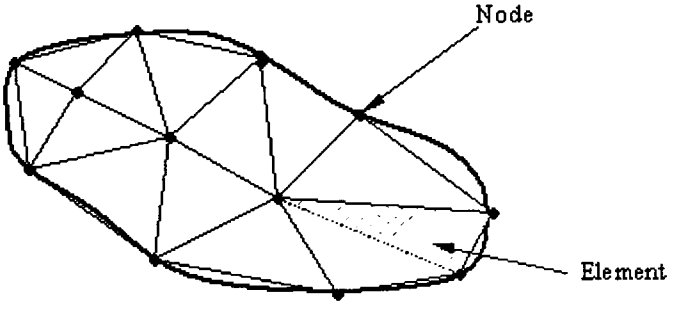

Figure 3-3 Domain Ω meshed by triangular elements

The next step, after dividing the whole domain into sub domains, is to approximate unknown dependent variable, temperature, as a function of known variables (interpolation function) that depend on the location of nodes.

$$\hat{T}(x,y) \approx \mathrm{T}\,(\mathrm{x,y}) \equiv \sum_{i=1}^{N_n} T_i b_i(x,y) \tag{3.7}$$

where $\hat{T}(x,y)$ is the exact solution of Equation (3.3) and T is the piecewise approximation of the solution. T_i is the temperature of i^{th} node and b_i is the globally defined interpolation function, known as a basis function and N_n is the total number of nodes in the mesh.

As T is an approximation, the governing Equation (3.3) may not be completely satisfied by substituting approximate temperature function. The error introduced by this approximation is termed as residual and is defined as follows:

$$R(T,x,y) \equiv k\vec{\nabla}^2 T - q_0''' \neq 0 \tag{3.8}$$

It is to be noted that the residual will be zero when using exact solution T in the governing equation.

$$R(\hat{T}(x,y)) \equiv k\vec{\nabla}^2 \hat{T} - q_0''' = 0 \tag{3.9}$$

The idea of the weighted residual method is to multiply the residual R(T,x,y) by a weighting function W(x,y) and then force the integral over the domain (Ω) to vanish. i.e.

$$\iint_{\Omega} W(x,y)R(T,x,y)d\Omega = 0 \tag{3.10}$$

In Galerkin's method, the weighting function is set equal to the interpolation function

$$W(x,y) = b_i(x,y) \tag{3.11}$$

Using basis function as a weighting function in Equation (3.10) results in the residuals at each node.

$$R_i \equiv \iint_{\Omega} b_i(x,y)\left(k\nabla^2 T(x,y) - q_0'''\right)d\Omega = 0 \qquad \text{for all i} = 1,2,\ldots,N_n \tag{3.12}$$

The Equation (3.12) is the weighted integral form of the governing partial differential equation. The N_n number of independent linear equations can be obtained by selecting N_n independent basis functions. The above integral equation can also be written as a sum of integrals over each element as shown below.

$$R_i^e \equiv \sum_{i=1}^{N_e} \iint_{\Omega^e} \psi_i(x,y)\left(k\nabla^2 T^e - q_0'''\right)d\Omega^e = 0 \qquad \text{for all i} = 1,2,\ldots,N_e \tag{3.13}$$

where N_e is the total number of elements in the domain Ω, Ψ_i is the shape function corresponding to element 'i', T^e is the elemental temperature vector of nodal values and Ω^e is the area of the element.

Equation (3.13) requires that the approximation function b_i be such that T is differentiable two times as specified in the governing equation and also satisfy the boundary condition. To reduce this requirement, the Equation (3.13) is simplified using integration by parts to distribute double integration of approximate function over the weighted function. The resulting equation is called weak formulation of the weighted integral form.

$$\iint_{\Omega^e} \psi\ (x,y)\left(k\nabla^2 T^e - q_0'''\right)d\Omega^e = k\left(\iint_{\Omega^e}\nabla\psi\nabla T^e d\Omega^e - \int_{\Gamma^e}\psi\nabla T^e d\Gamma^e\right) - \iint_{\Omega^e}\psi q_0'''\ d\Omega^e$$

$$k\left(\iint_{\Omega^e}\nabla\psi\nabla T^e d\Omega^e - \int_{\Gamma^e}\psi\nabla T^e d\Gamma^e\right) - \iint_{\Omega^e}\psi q_0''' d\Omega^e = 0 \qquad (3.14)$$

The above equation shows the weak formulation defined over one element, which can be used to evaluate weak formulation for any element and then all elemental contributions are assembled in Equation (3.13) to obtain weak formulation over the whole domain. The weak formulation has two advantages [Reddy, 1993]:

(1) The continuity requirement on the approximation function is weakened that often results in a symmetric set of algebraic equations in the coefficients.

(2) The natural boundary conditions are now contained in the weak form. Therefore, the approximate solution is only required to satisfy essential boundary condition.

The temperature distribution over an element 'e' can be approximated using shape function and nodal temperature values.

$$T^e = \sum_{i=1}^{n} T_i\psi_i(x,y) = \{\psi\}^T\{T\}^e \qquad (3.15)$$

Also $\nabla T^e = \nabla(\{\psi\}^T\{T\}^e)$

$$\nabla T^e = \nabla(\{\psi\}^T)\ \{T\}^e$$

$$\nabla T^e = [\beta]^T\ \{T\}^e \qquad (3.16)$$

where n is the number of nodes in element 'e'. T_i is the temperature of node 'i' contained in element 'e' and ψ_i is the elemental shape function.

$$\{\psi\} = \begin{Bmatrix}\psi_1\\ \psi_2\\ |\\ \psi_n\end{Bmatrix}; \qquad [\beta] = \nabla\{\psi\} = \begin{bmatrix}\frac{\partial\psi_1}{\partial x} & \frac{\partial\psi_1}{\partial y}\\ \frac{\partial\psi_2}{\partial x} & \frac{\partial\psi_2}{\partial y}\\ | & |\\ \frac{\partial\psi_n}{\partial x} & \frac{\partial\psi_n}{\partial y}\end{bmatrix} \qquad (3.17)$$

Substituting Equation (3.15) and (3.16) in Equation (3.14) gives weak form of partial differential equation in terms of nodal temperature values.

$$\left(k \iiint_{\Omega^e} [\beta][\beta]^T d\Omega^e \right) \{T\}^e - \int_{\Gamma^e} \{\psi\}(k\nabla T^e) d\Gamma^e - \iiint_{\Omega^e} \{\psi\} q_0''' d\Omega^e = 0 \tag{3.18}$$

Now lets define elemental equations as follows:

Elemental stiffness matrix: $$[K]^e = \left(k \iiint_{\Omega^e} [\beta][\beta]^T d\Omega^e \right) \tag{3.19}$$

Elemental force matrix: $$\{F\}^e = \iiint_{\Omega^e} \{\psi\} q_0''' d\Omega^e + \int_{\Gamma^e} \{\psi\}(k\nabla T^e) d\Gamma^e \tag{3.20}$$

Using equation (3.19) and (3.20) in equation (3.18) results in following equation.

$$[K]^e\{T\}^e = \{F\} \tag{3.21}$$

The stiffness matrix can be evaluated using shape functions. The second term in the force matrix can be calculated using given natural boundary condition. It can be shown that the second integral term on an element edge cancels out during assembling, if the edge is shared by other element. Therefore, that term will only contribute when the edge of the element lies on the surface of the domain Ω.

The flux at the junction due to the Peltier effect is applied as the contributions to the force matrix {F}. Let us consider a segment near the junction as shown in Figure 3-4. e^A, e^B, e^C and e^D are the elements those have common nodes at the junction. The element e^A and e^D don't share any edge with the junction surface; thus they will not contribute in the global force matrix.

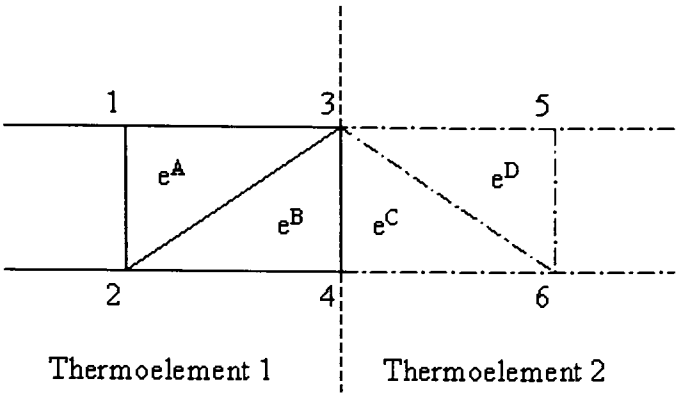

Figure 3-4 Peltier effect at the junction

The element e^B shares edge "43" and element e^C shares edge "3-4" with the junction. Generally, when the element edge lies inside the domain, the flux term on the element edge (second term in equation (3.20)) cancels with the flux term of another element that shares that edge. The idea here is that the net flux across the element edge is zero in case of no internal heat flux source. Now consider elements in Figure 3-4; the Peltier effects can be imagined as a plane heat flux source located at the junction boundary "3-4". Therefore the net flux across the edge "3-4" must include the intensity of Peltier heat source, which can be done in the following way.

For element e^B $$\{F\}^e = \int_{4-3} \{\psi\}\left(\frac{S}{\gamma}(T_{abs}S)|\nabla T^e|\right)d\Gamma^e$$

For element e^C $$\{F\}^e = \int_{3-4} \{\psi\}\left(\frac{S}{\gamma}(T_{abs}S)|\nabla T^e|\right)d\Gamma^e$$

where T_{abs} is the absolute mean temperature of the element. S is the absolute Seebeck coefficient of the element and $|\nabla T^e|$ is the magnitude of the flux vector. These contributions are then added into the global force matrix to include the influence of the Peltier effect.

The internal heat generation q_0''' is a function of temperature gradient, which requires following methodology for the solution.

1). Make an initial guess $\{T\}_{old}$ for dependent variable $\{T\}$ based on engineering judgment. Most of the time an average of the constant temperature boundary condition serves as a good initial guess for steady state analysis.

$\Rightarrow \quad \{T\}_{old} = \text{Average } (T_1(x,y))$

2). Compute the temperature dependent internal heat generation term (q_0''') in the force matrix $\{F\}$ using $\{T\}_{old}$ and solve $[K]\{T\}_{new} = \{F\}$ for new temperature distribution $\{T\}_{new}$.

3). Check convergence by comparing old and new temperature distribution as follow:

$$\varepsilon = \frac{\|T_{new} - T_{old}\|_{max}}{\|T_{new}\|_{max}}$$

$\|T_{new} - T_{old}\|_{max}$ Computes the maximum difference between old and new temperature distribution. $\|T_{new}\|_{max}$ is the maximum value of new temperature.

4). Set an allowable limit for ε i.e. $\varepsilon_{allowable}$.

If $\varepsilon > \varepsilon_{allowable}$

5). Set $T_{old} \equiv T_{new}$ and return to step 2.

If $\varepsilon < \varepsilon_{allowable}$

T_{new} is the approximate finite element solution to the governing non-linear heat transfer equation.

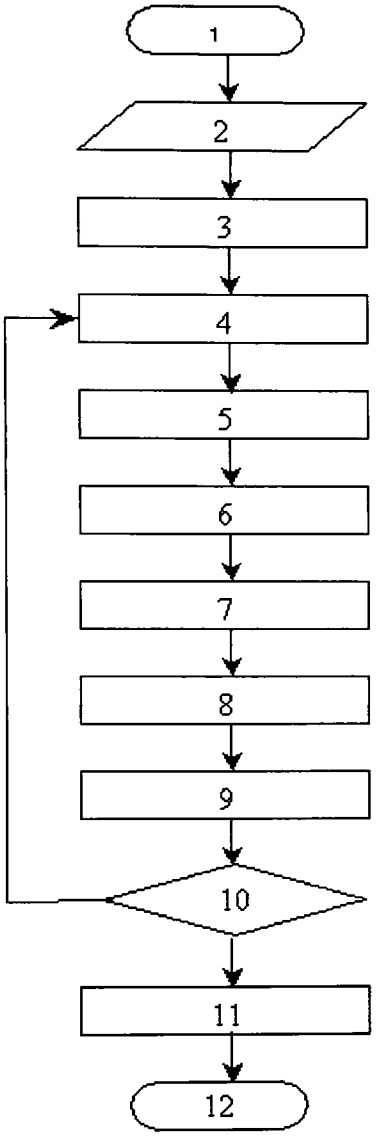

1. Start main program

2. Input mesh data, boundary condition data and program options

3. Initialize finite element matrices and new temperature vector (T) and old temperature vector T_old

4. Compute internal heat generation terms (Qgen) due to the Joule and Thomson effect based on T_old.

5. Generate global finite element matrices K_Global and F_Global based on Qgen and mesh information

6. Add flux contributions to the junction nodes due to the Peltier effect

7. Apply boundary conditions

8. Solve linear finite element equations using Gauss Elimination method to obtain new temperature vector T

9. Assign T_old = T

10. Check for convergence

11. Compute voltage distribution based on steady state temperature

12. End of the program

Figure 3-5 Flow chart of steady state finite element program

3.3.3. Finite element model for Voltage Distribution

The temperature gradient in thermoelements induces a voltage gradient due to the Seebeck effect, which is governed by equation (3.2). The relation between voltage gradient and temperature gradient can be obtained by differentiating equation (3.2) with respect to spatial position.

$$\nabla\phi = S\nabla T \tag{3.22}$$

The solution of equation (3.22) can be approached using finite element method. Let us approximate the voltage distribution as a function of voltage at nodes.

$$\hat{\phi}(x,y) \approx \phi(x,y) = \sum_{i=1}^{N_n} \phi_i b_i(x,y) \tag{3.23}$$

Where $\hat{\phi}(x,y)$ is the exact solution for the voltage distribution, $\phi(x,y)$ is the finite element piecewise approximation of the solution, N_n is the total number of nodes in domain Ω, ϕ_i is the voltage at i^{th} node and b_i is the basis function.

As this is an approximation, the governing equation will not be completely satisfied. The error introduced by this approximation is termed as residual and defined as follows:

$$R(\phi,x,y) \equiv \nabla\phi - A \neq 0 \qquad \text{where } A = S\nabla T \tag{3.24}$$

Whereas, the residual is zero for the exact solution $\hat{\phi}(x,y)$.

$$R(\hat{\phi},x,y) \equiv \nabla\hat{\phi} - A = 0$$

The idea of weighted residual method is to multiply the residual $R(\phi,x,y)$ by a weighting function and then force the integral to vanish. i.e.

$$\iint_{\Omega} W_i(x,y) R(\phi,x,y) d\Omega = 0 \tag{3.25}$$

Note that the Equation (3.25) is the nodal equation defined over full domain Ω. W_i is the weighing function corresponding to node 'i'.

Substituting Equation (3.24) in Equation (3.25) gives:

$$\iint_{\Omega} W_i(x,y)(\nabla\phi - A)\, d\Omega = 0 \tag{3.26}$$

Equation (3.26) can be written in terms of sum of integrals over element domains Ω^e as shown below.

$$\sum_{i=1}^{N_e} \iint_{\Omega^e} W_i^e (\nabla\phi - A)\, d\Omega^e = 0 \tag{3.27}$$

where W_i^e is the corresponding elemental weighing function, Ω^e is the element domain, and N_e is the total number of elements in the full domain Ω. Also, the elemental voltage vector of nodal values can be defined as follow:

$$\phi^e = \{\psi\}^T\{\phi\}^e \tag{3.28}$$

$$\nabla\phi^e = [\beta]^T\{\phi\}^e \tag{3.29}$$

where ϕ^e is the approximation function for voltage distribution over element 'e' and $\{\phi\}^e$ is the elemental voltage vector of nodal values.

In this method, weighting function is set equal to the beta function, which is the gradient of the elemental shape function.

$$W(x,y) \equiv [\beta] \tag{3.30}$$

Substituting equation (3.29) & (3.30) in equation (3.27) gives:

$$\sum_{i=1}^{N_e} \left(\left(\iint_{\Omega^e} [\beta][\beta]^T d\Omega^e \right) \{\phi\}^e - \left(\iint_{\Omega^e} [\beta] A d\Omega^e \right) \right) = 0 \tag{3.31}$$

The equation (3.31) can also be written as follow:

$$\sum_{i=1}^{N_e} \left([K]^e \{\phi\}^e - \{F\}^e \right) = 0$$

where $[K]^e = \iint_{\Omega^e} [\beta][\beta]^T d\Omega^e$ (3.32)

$$\{F\}^e = \iint_{\Omega^e} [\beta] A d\Omega^e \tag{3.33}$$

This system of linear equations given by equation (3.31) can be easily solved for the voltage distribution by constraining with one boundary condition.

3.4 Transient Finite Element Model

The transient finite element model of a thermoelectric device is used to obtain temperature and voltage as a function of spatial as well as temporal variables. The transient finite element model provides information regarding the response time of the device. It is assumed that the electrical response of thermoelectric device is comparatively very faster than thermal response. Therefore, the same electrical governing equation is used to compute transient voltage distribution that was used in the steady state

model. The elliptical partial differential equation that was used to compute temperature distribution is replaced by a parabolic partial differential equation that gives temperature distribution as a function of time.

The transient thermal equations for the region shown in Figure 3-2 can be described as follow:

Governing Equation: $\vec{\nabla}(k\vec{\nabla}T)(x,y,t) = q_0''' + \rho c_p \frac{\partial T}{\partial t}$ (3.34)

Boundary Condition: $T(x,y,t) = T_1(x,y,t)$ on boundary Γ_1

Boundary Condition: $k\vec{\nabla}(T(x,y,t)) = q(x,y,t)$ on boundary Γ_2

Initial Condition: $T(x,y,0) = T_0(x,y)$

Where t denotes time, ρ is the density and c_p is the specific heat.

The governing electrical equation used to obtain the voltage distribution (ϕ) is given as follow:

Governing Equation: $\int d\phi = \int S dT$ (3.35)

Boundary Condition: $\phi(x,y,t) = \phi_1(x,y,t)$ on boundary Γ_1

Since we assume that the electrical response is infinitely fast compared to the thermal response, we use the temperature solution $\{T\}^s$ at any time step 's' to compute steady state voltage solution $\{\phi\}^s$ at that time step. Therefore, the same electrical model is used to compute voltage distribution that is used in steady state analysis (section 3.3.3).

3.4.1. Finite element Model for Transient Temperature Distribution

The finite element model for transient temperature distribution is obtained using Galerkin's method of weighted residual. The residual of governing parabolic partial differential equation is first multiplied by weighing function (basis function) and integrated of the full domain to obtain integral weighted residual form of the governing equation. The resulting equation is then reduced to its the weak form to weaken the continuity requirement for the approximation function.

The piecewise approximation (T) of temperature as a function of space co-ordinates and time is defined as follows:

$$\hat{T}(x,y,t) \approx \mathrm{T}\,(\mathrm{x,y,t}) \equiv \sum_{i=1}^{N_n} T_i(t) b_i(x,y) \tag{3.36}$$

$\hat{T}$ is the exact solution, which is approximated using position dependent basis function and time dependent nodal temperature values.

The residual is given as follows:

$$\mathrm{R(T,x,y,t)} \equiv k\vec{\nabla}^2 T(x,y,t) - q_0''' - \rho c_p \frac{\partial T}{\partial t} \neq 0 \tag{3.37}$$

The weighted residual integral form (R_i) of the governing equation can be obtained by integrating the product of residual and the weighing function over the domain.

$$\mathrm{R_i} \equiv \iint_{\Omega} W_i(x,y) R(T,x,y,t) d\Omega = 0 \tag{3.38}$$

For Galerkin's method of weighted residual, the weighing function is the basis function.

$$\mathrm{R_i} \equiv \iint_{\Omega} b_i(x,y) R(T,x,y,t) d\Omega = 0 \tag{3.39}$$

Note that the Equation (3.39) is based on the nodal parameters over the problem domain. It can be transformed into the summation of integral defined over element domain (Ω^e) to obtain weighted residual integral over elements.

$$\mathrm{R_i} = \sum_{i=1}^{N_e} \iint_{\Omega^e} \{\psi\}_i(x,y) R(T^e,x,y,t) d\Omega^e = 0 \tag{3.40}$$

Let us concentrate on the contribution of element 'e' to R_i.

$$\mathrm{R^e} = \iint_{\Omega^e} \{\psi\}\,(x,y) R(T^e,x,y,t) d\Omega^e = 0 \tag{3.41}$$

The weak form of Equation (3.41) can be obtained by integrating by parts.

$$\left(\rho c_p \iint_{\Omega^e} \{\psi\} \frac{\partial T^e}{\partial t} d\Omega^e \right) - \left((k \iint_{\Omega^e} [\beta][\beta]^T d\Omega^e)\{T\}^e - \int_{\Gamma^e} \{\psi\}(k\nabla T) d\Gamma^e \right) + \left(\iint_{\Omega^e} \{\psi\} q_0''' d\Omega^e \right) = 0 \tag{3.42}$$

The Equation (3.42) shows the weak formulation of governing partial differential equation at one instant of time. It can be simplified by defining elemental matrices as shown below:

$$[\mathrm{C}]^e\{\dot{T}\}^e - [\mathrm{K}]^e\{\mathrm{T}\}^e + \{\mathrm{F}\}^e = 0 \tag{3.43}$$

Capacitance matrix: $[C]^e = \rho c_p \iint_{\Omega^e} \{\psi\}\{\psi\}^T d\Omega^e$ (3.44)

Stiffness matrix: $[K]^e = k \iint_{\Omega^e} [\beta][\beta]^T d\Omega^e$ (3.45)

Force matrix: $\{F\}^e = \iint_{\Omega^e} \{\psi\} q_0''' d\Omega^e + \int_{\Gamma^e} \{\psi\}(k\nabla T) d\Gamma^e$ (3.46)

To compute temperature as a function of time, the finite difference method in time is applied. The most commonly used method is the α family approximation [Reddy, 1993]. In this method a weighted average of the time derivative of a dependent variable, temperature, is approximated at two consecutive time steps (s & s+1) as shown below.

$$\{\dot{T}\} = \alpha\{T\}^{s+1} + (1-\alpha)\{T\}^s \approx \frac{\{T\}^{s+1} - \{T\}^s}{\Delta t} \quad (3.47)$$

And $\{F\}^* = \alpha\{F\}^{s+1} + (1-\alpha)\{F\}^s$ (3.48)

where α can vary from 0 to 1.

Different numerical schemes that can be obtained by varying the value of α are listed in Table 3-1:

Table 3-1 Numerical schemes for transient finite element analysis

α	Numerical Scheme
0	The forward difference method (Conditionally stable)
$\frac{1}{2}$	The crank-Nicolson scheme (Stable)
$\frac{2}{3}$	The Galerkin's scheme (Stable)
1	The backward difference scheme (Stable)

Substituting equation & in equation gives following equation:

$$\left(\frac{1}{\Delta t}[C]^e + \alpha[K]^e\right)\{T\}^{S+1} = \left(\frac{1}{\Delta t}[C]^e + (1-\alpha)[K]^e\right)\{T\}^S + (1+\alpha)\{F\}^S + \alpha\{F\}^{S+1} \quad (3.49)$$

Equation can be written in simple form as given below.

$$[M]\{\phi\}^{s+1} = \{d\}^{s+1} \quad (3.50)$$

where $[M] = \frac{1}{\Delta t}[C]^e + \alpha[K]^e$ (3.51)

$$\{d\}^{s+1} = \left(\frac{1}{\Delta t}[C]^e + (1-\alpha)[K]^e\right)\{T\}^S + (1+\alpha)\{F\}^S + \alpha\{F\}^{S+1} \quad (3.52)$$

Equation gives a set of linear equations, which can be solved after constraining the model with boundary conditions and initial conditions.

4 Analytical Verification of Finite Element Model

Before applying the finite element model to the actual thermoelectric device problem, its validity is checked against known analytical solutions and in some cases against numerical solutions obtained from ANSYS. The program is checked for a various boundary conditions on single material region and on composite material regions. The validation process is divided into following sections:

1) Problem involving temperature boundary conditions
2) Problem involving composite material and flux boundary condition
3) Problem involving internal heat generation
4) Problem involving internal heat flux source
5) Coupled problem with temperature dependent internal Joule heating (Non-linear)

The first four problems involved pure conduction and validate linear finite element program. The fifth problem involves internal heat generation due to the Joule effect and which is incorporated in the governing equation as a nonlinear term. The fifth problem is used to validate the program for nonlinear problems.

4.1 Problem involving temperature boundary conditions

Consider a rod with temperature conditions at the ends as shown in Figure 4-1. For simplicity it is assumed that that rod has uniform cross section and made up of isotropic material and heat flows only along the length of the rod.

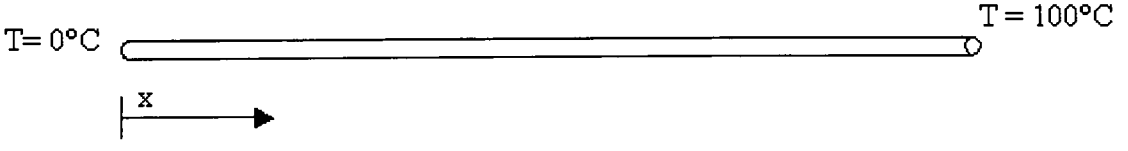

Figure 4-1 Test problem to validate temperature boundary condition

4.1.1. Steady State Analysis:

The governing equation for steady state temperature distribution (T(x)) is the Laplace equation.

$$k\frac{d^2T(x)}{dx^2} = 0 \tag{4.1}$$

Subjected to following boundary conditions.

$$T(0) = 0°C \quad \& \quad T(L) = 100°C \tag{4.2}$$

where L is the length of the rod.

An analytical solution of Equation (4.1) subjected to boundary conditions in Equation (4.2) can be found using separation of variable metho.

$$T(x) = 0 + (100-0)*(x/L) \tag{4.3}$$

The plot of temperature, given by Equation (4.3), is a straight line as shown in Figure 4-3. The MATLAB program is developed for a two-dimensional geometry. To solve this problem using the MATLAB finite element program, the rod is considered as a rectangular region, which is based on the assumption that no heat flows along the radial direction in the rod. ANSYS is used to generate mesh consisting of 3-node triangular elements and data about node co-ordinates, element type, element material, connection nodes for each element and boundary condition is supplied to the program in text files. The program uses this data to evaluate temperature distribution in the rod using finite element method.

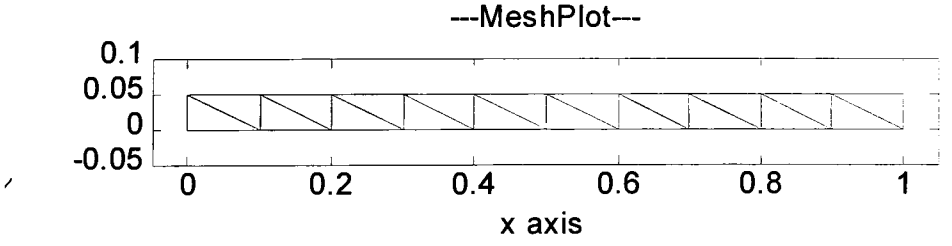

Figure 4-2 Finite element mesh

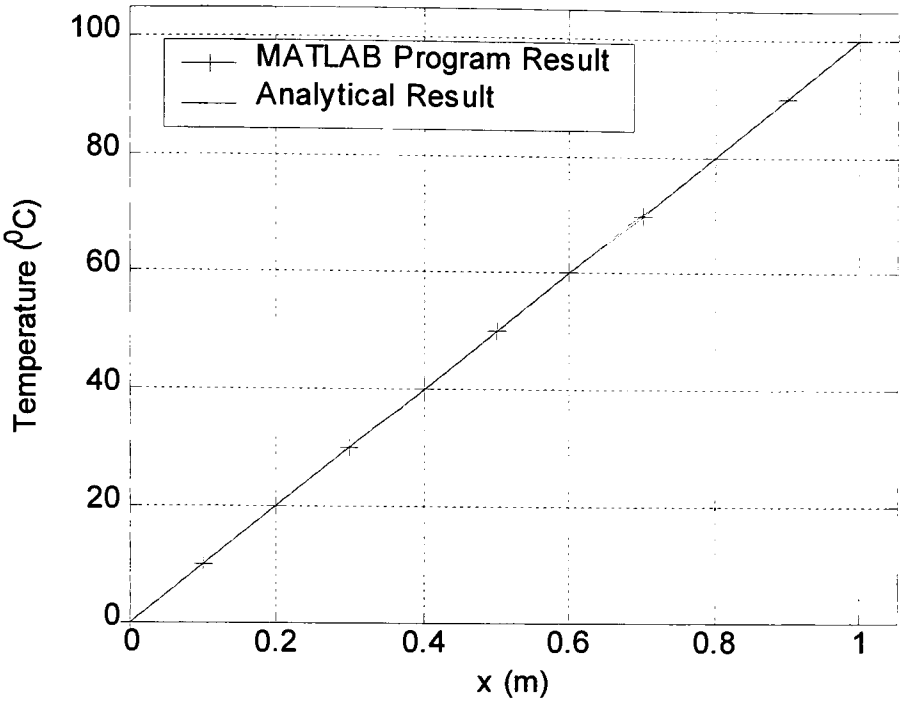

Figure 4-3 Comparison of steady state results

The MATLAB program result is compared with the temperature distribution obtained using analytical solution in Figure 4-3. The difference between analytical and finite element result at x=0.5m is 3.83e-013, which is very small. This simple test case, while not a sufficient proof of accuracy, serves as the first step in the sequence leading to code validation.

4.2 Problem Involving Composite Material and Flux Boundary Condition

In this section, the MATLAB program is checked for flux boundary condition applied on a composite material section. The geometry of the domain is taken different from simple square or rectangle, as shown in , to extend the validity of the program to any section.

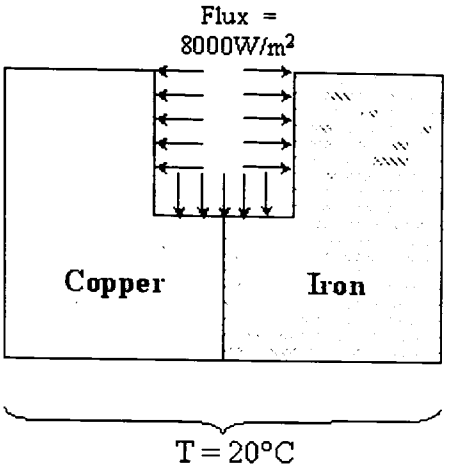

Figure 4-4 Test problem involving flux boundary condition

4.2.1. Steady state Analysis

The steady state temperature distribution in the test problem domain is governed by following partial differential equation.

$$\nabla(k\nabla T(x,y)) = 0 \qquad (4.4)$$

The boundary conditions are shown in Figure 4-4. The thermal conductivity 'k' in Equation (4.4) is a function of position because the domain consists of two different materials.

The geometry is meshed using three node triangular elements with element length of 0.005m as shown in Figure 4-5. The material properties of copper and iron are given in Table 4-1

Table 4-1 Material properties of Copper and Iron

Property (Units)	Copper	Iron
Thermal Conductivity 'k' (W/m°C)	411.6	80.3
Density 'ρ' (Kg/m^3)	8920	7870
Specific heat 'c_p' (J/Kg m)	386.4	447

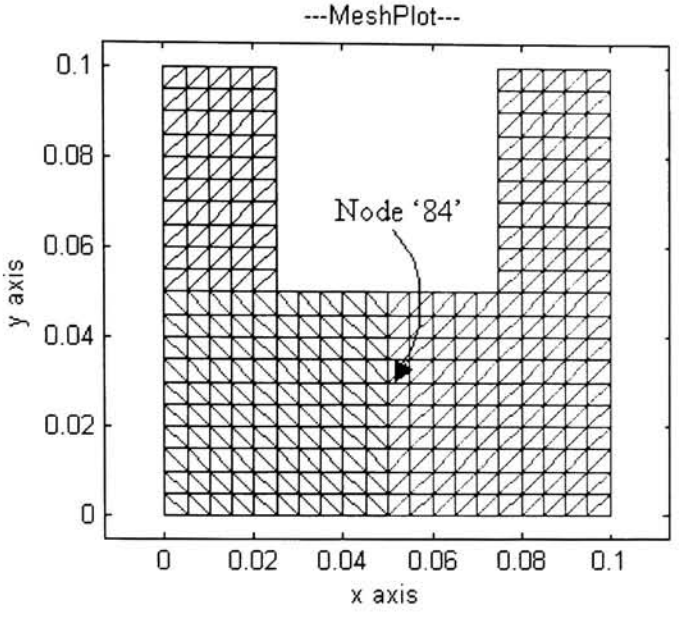

Figure 4-5 Finite element mesh with element length=0.005m

The steady state temperature distribution obtained using MATLAB program is shown in Figure 4-6.

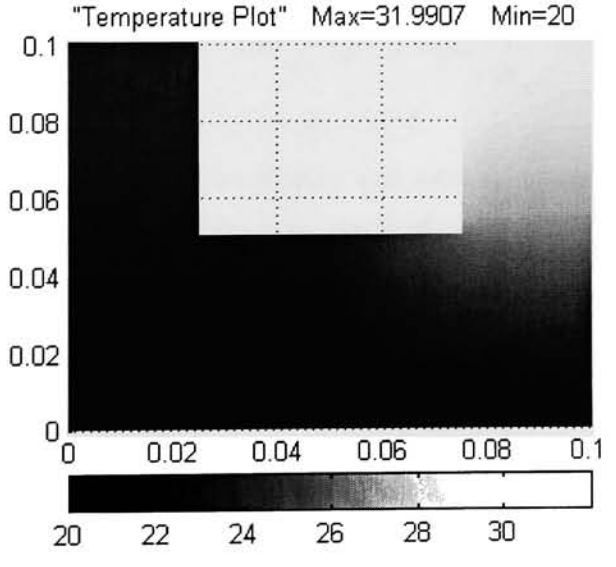

Figure 4-6 Steady state temperature distribution

The MATLAB program results are compared with ANSYS results by computing the difference in steady state temperature distributions obtained in both cases. The results obtained from ANSYS were precise up to eighth significant digits after the decimal point. Therefore, the MATLAB results were also converted into the same precision format and subtracted from ANSYS result. The error in the steady state results, with the same mesh density, is found to be zero up to eight significant digits after the decimal point.

The zero error throughout the domain confirms that the steady state temperature distribution, obtained from the MATLAB program, exactly matches with the results obtained from ANSYS. Therefore, the MATLAB program can be accurately used for analyzing steady state heat transfer problems involving heat flux boundary conditions or composite materials.

4.2.2. Transient Analysis

The test problem shown in Figure 4-4 is analyzed for transient temperature response using transient MATLAB program and ANSYS. The results are compared to check the accuracy of MATLAB program. The transient model of the problem can be described by following equations.

Governing Equation: $$\nabla(k\nabla T(x,y,t)) = \rho c_p \frac{\partial T}{\partial t} \quad (4.5)$$

Initial Condition: $T(x,y,0) = 20°C$

The finite element mesh, boundary conditions and material properties used for transient analysis are shown in Figure 4-4, Figure 4-5 and Table 4-1.

The time step (Δt) used in MATLAB program is based on Fourier number.

$$\Delta t = F_o \frac{\rho c_p (\Delta x)^2}{k}$$

Where F_o, ρ, c_p, k and Δx are Fourier number, density, specific heat, thermal conductivity, and element length respectively. The element length is 0.005m for current problem and Fourier number range from 1 to100. To obtain more precise results, Fourier number is chosen to be 1.

Based on Copper Material properties: $\Delta t = 0.2093$ sec

Based on Iron Material properties: $\Delta t = 1.099$ sec

The time step of 0.3sec is used in the transient analysis.

A variable time step is used in ANSYS, which can vary from 0.2 sec to 0.3sec. The transient temperature data at node'84' is used to compare MATLAB program and ANSYS results. The node '84' is located on the common boundary shared by copper and iron region as shown in Figure 4-5.

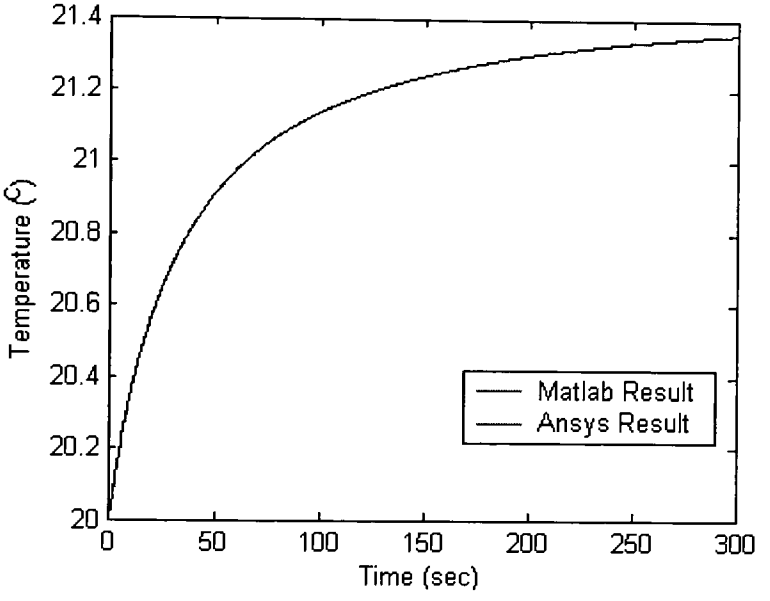

Figure 4-7 Transient temperature response at node '84'

The MATLAB program and ANSYS results are plotted in Figure 4-7, which shows that the transient response closely matches in both cases. The transient data used for comparison is precise up to four digits after the decimal point. Therefore, the difference of 0.0014°C at t = 50sec validate the MATLAB program transient result.

4.3 Problem involving internal heat generation

The Matlab finite element program will be used to analyze the response of thermoelectric devices, which involves internal heat generation due to Joule, Thomson and Peltier heat. Therefore, it is essential to check the validity of program under internal heat generation condition. A test problem is selected that involves a constant heat generation within the

domain as shown in Figure 4-8. The boundary of domain is maintained at a constant temperature, which acts as a heat sink.

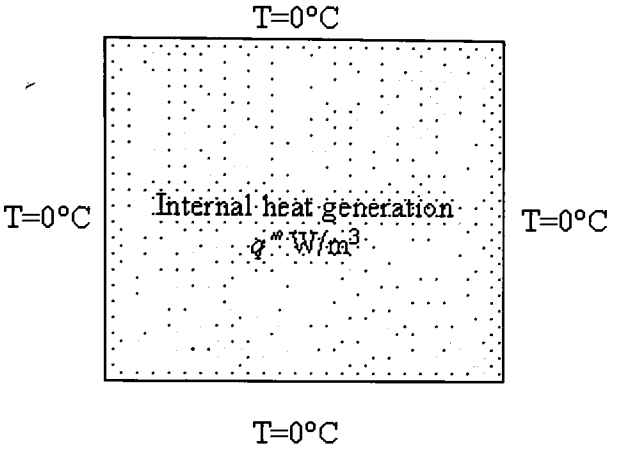

Figure 4-8 Description of test problem involving internal heat generation

In the following sections, the test problem is analyzed for steady state and transient temperature response using MATLAB program and ANSYS. The MATLAB program results are compared with ANSYS results to check their validity.

4.3.1. Steady State Analysis

The steady state model of the test problem can be described using following set of equations. Consider a boundary value problem in two dimensions described by the following equations.

Governing equation: $$k\left(\frac{\partial T^2}{\partial x^2} + \frac{\partial T^2}{\partial y^2}\right) = -q''' \quad 0<x<a,\ 0<y<b \qquad (4.6)$$

Boundary Conditions: $$T(x,0) = 0, \quad T(x,b) = 0$$

$$T(0,y) = 0, \quad T(a,y) = 0$$

The domain of the test problem is meshed using three-node triangular element as shown in Figure 4-9. The values of different variables and material properties are given in Table 4-2.

Table 4-2 Material properties and geometric data for the test problem

Property (Units)	Copper
Thermal Conductivity 'k' (W/m°C)	411.6
Density 'ρ' (Kg/m^3)	8920
Specific heat 'c_p' (J/Kg m)	386.4
Internal heat generation 'q'''' (W/m^3)	8000
Length 'a' (m)	0.1
Width 'b' (m)	0.1

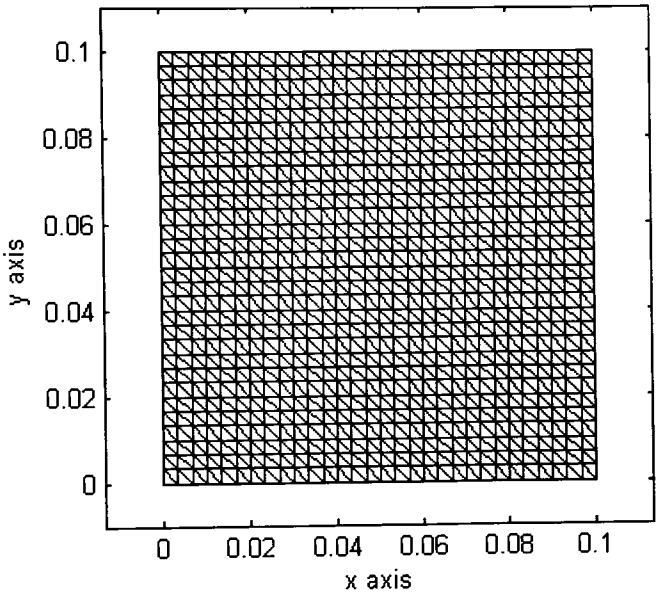

Figure 4-9 Finite element mesh (961 nodes and 1800 elements)

The steady state temperature distribution as obtained using MATLAB program is shown in Figure 4-10. The maximum temperature (0.014°C) is at the center of the domain, which was expected as the center point is at a maximum distance from the heat sinks.

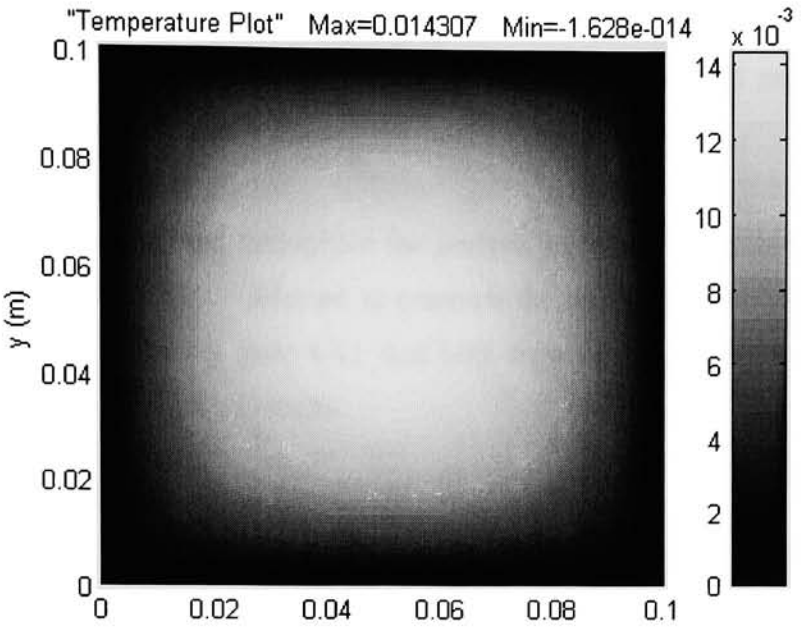

Figure 4-10 Steady state temperature distribution using MATLAB program

The temperature distribution obtained with ANSYS is used to compare steady state MATLAB program result. ANSYS results are computed precisely up to eight digits after the decimal point and compared with the MATLAB program results that have the same precision.

The difference between the MATLAB finite element program results and ANSYS results is zero up to eight significant digits. Therefore, the steady state MATLAB program is valid for problems involving internal heat generation.

4.3.2. Transient Analysis

The transient temperature response of the test problem shown in Figure 4-8 can be modeled using following equations.

Governing Equation: $$\nabla(k\nabla T(x,y,t)) = -q''' + \rho c_p \frac{\partial T}{\partial t} \qquad (4.7)$$

Boundary Conditions: $T(x,0,t) = 0, \quad T(x,b,t) = 0$

$T(0,y,t) = 0, \quad T(a,y,t) = 0$

Initial Condition: $T(x,y,0) = 0°C$

The time-step for the transient analysis is calculated using material properties given in Table 4-2 and element size of 0.003m.

$\Delta t = 0.08$ sec

A constant time step is used throughout the analysis in MATLAB program and ANSYS. The mid-point node '541' is selected to compare the results of ANSYS and MATLAB program. It is clear from Figure 4-11 that both transient curves superimpose on each other, showing close match of results.

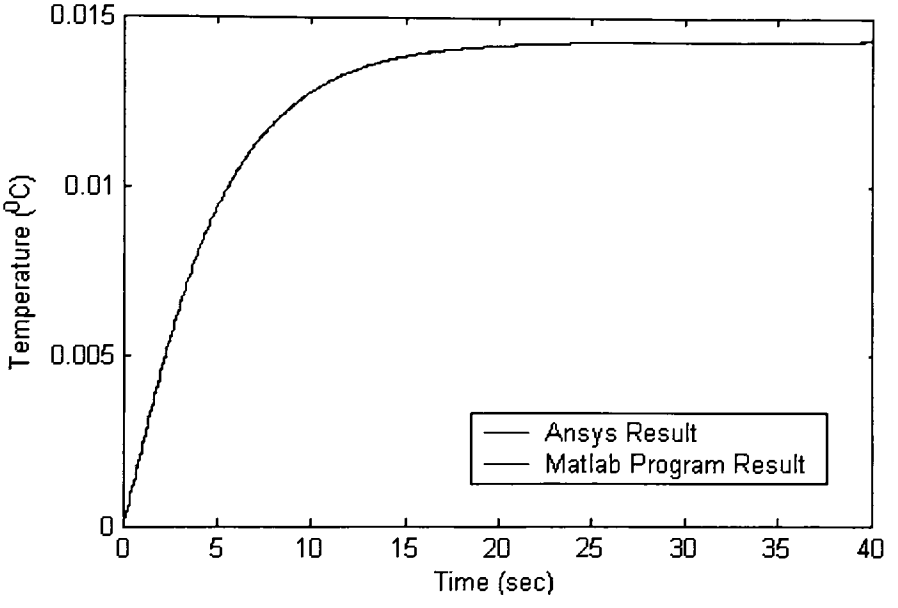

Figure 4-11 Transient temperature response

The Figure 4-12 shows the error in transient MATLAB program when compared with ANSYS results. The error is of the order of 10^{-5}, which is three orders smaller than the temperature value.

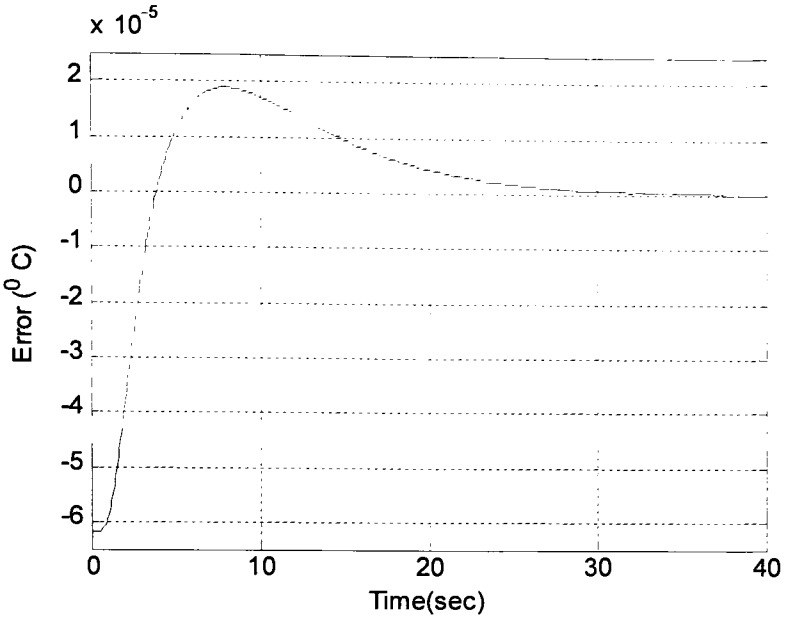

Figure 4-12 Error in transient temperature response

As time approaches settling time, the error approaches zero. The maximum error in the MATLAB program result comes during very initial time steps, which can be accounted to the available precision and the difference in time integration scheme.

4.4 Transient Analysis Involving Plane Source Of Internal Heat Generation

The internal heat generation due to the Joule effect and Thomson effect occur throughout the volume of the thermoelements, whereas the internal heat generation due to the Peltier effect comes through a plane heat source located at the junction. This is a special case of internal heat generation in which a plane, completely contained inside the domain transmits heat per unit area (flux) on both sides. The MATLAB program is tested for such a case in this section.

Consider a slab of length L is initially at zero temperature. A plane surface heat source of strength $g_s(t)$ W/m^2 is situated at x=b as shown in the figure. For time t>0, the heat source release heat from both sides of the surface while ends of the slab are kept at 0°C.

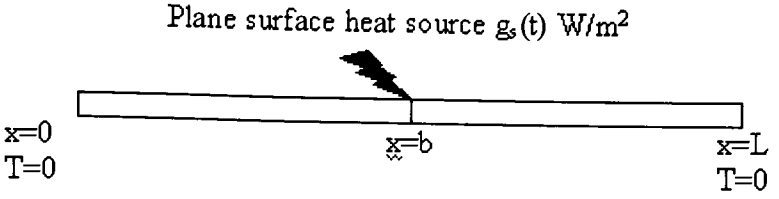

Figure 4-13 Transient test problem involving internal heat generation

In this problem the heat source is a plane surface. To relate this surface heat source (W/m^2) to the volume heat source (W/m^3), it is multiplied by Dirac delta function as

$$g(x,t) = g_s(s,t) \,.\, \delta(x-b) \tag{4.8}$$

Where $\delta(x-b)$ is zero everywhere except at $x = b$.

Governing equation can then be written as

$$\frac{\partial T^2}{\partial x^2} = \frac{1}{\alpha}\frac{\partial T}{\partial t} - \frac{1}{k} g_s(s,t) \,.\, \delta(x-b) \qquad 0<x<a,\ t>0 \tag{4.9}$$

$$T(0,t) = 0, \qquad T(L,t) = 0, \qquad T(x,t) = 0 \tag{4.10}$$

The problem is solved analytically using method of integral transform in [*Özisik*, 1968] and the solution is given by:

$$T(x,t) = \frac{2g_s}{Lk}\sum_{m=1}^{\infty}\frac{1-e^{-\alpha\beta_m t}}{\beta_m^{\,2}}.\sin(\beta_m b).\sin(\beta_m x) \tag{4.11}$$

where $\beta_m = \dfrac{m\pi}{L}$

The analytical solution for temperature distribution and transient temperature rise at the mid point of the slab is computed by implementing equation (4.11) into a computer program. Different parameters used in the transient analysis are listed in Table 4-3.

Table 4-3 Data for transient analysis

Property (Units)	Copper
Thermal Conductivity (W/m°C)	411.6
Density (Kg/m^3)	8920
Specific heat c_p (J/Kg m)	386.4

Length (m)	0.1
b	0.05
$g_s(t)$ (W/m^2)	5

The MATLAB results are compared with analytical result in Figure 4-14. These plots show close agreement between program solution and analytical solution.

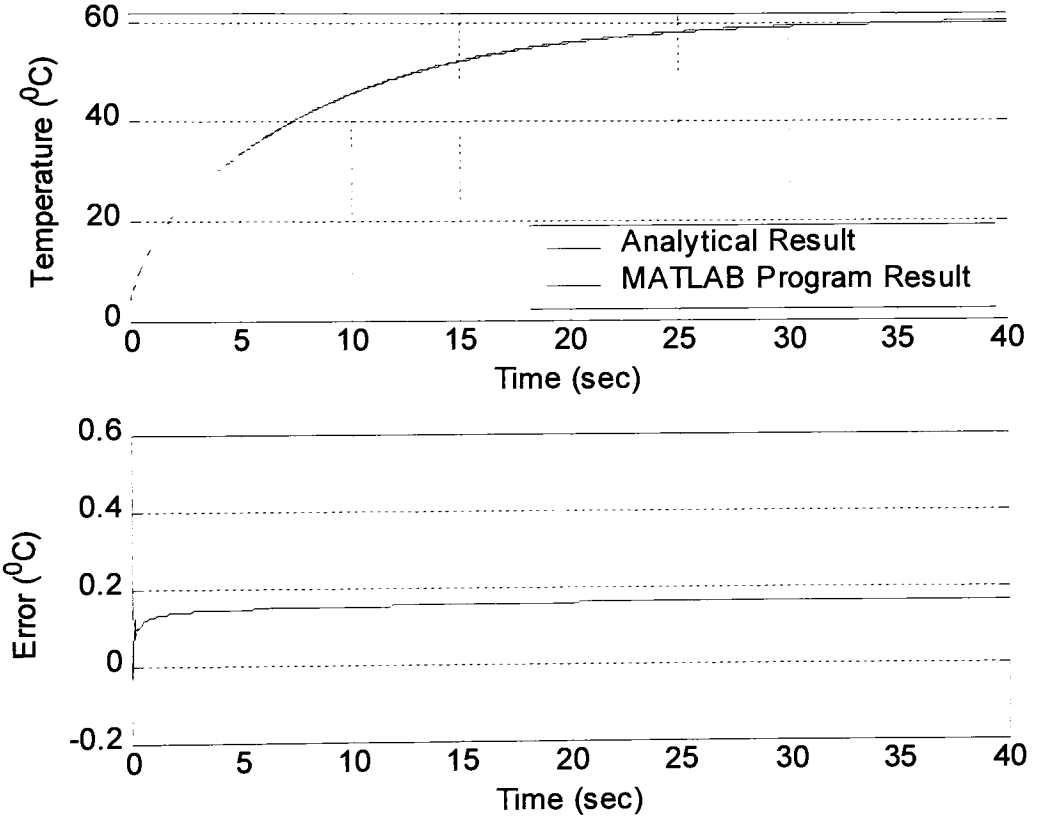

Figure 4-14 (A) Transient temperature response at mid point (node 32) (B) Error in MATLAB program (Analytical Result – MATLAB Program Result)

4.5 Coupled problem with internal Joule heating

The coupling between electrical and thermal domain in a thermoelectric device introduces non-linearity in the governing equation. The algorithm used in finite element

method to solve non-linear problems should be validated against analytical solution of the non-linear problem. A simple thermoelectric problem that includes the influence of Joule effect is selected for comparison.

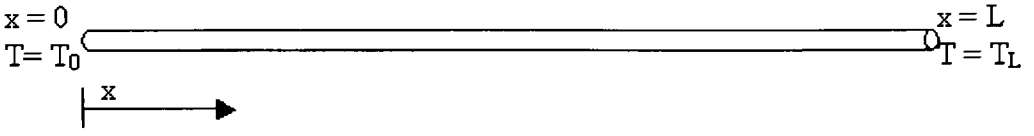

Figure 4-15 single thermoelement with Joule heating

Consider a thermoelement whose ends are kept at different temperature. The flow of current due to the Seebeck voltage causes internal heat generation due to the Joule effect. The temperature distribution in the thermoelement is governed by Poisson's equation.

$$k\nabla^2 T = -q_J'''$$

Here q_J''' is the Joule heat per unit volume in the thermoelements and it depends on the current density in the thermoelement. The internal heat generation term can be written in terms of temperature gradient to obtain non-linear governing equation.

$$k\nabla^2 T = -\frac{S^2}{\gamma}(\nabla T)^2$$

Analytical Solution

Let $\theta = \frac{dT}{dx}$

$$\frac{d\theta}{dx} = -\frac{S^2}{k\gamma}(\theta)^2$$

$$\int \frac{1}{\theta^2} d\theta = \int N dx \qquad \text{Where } N = -\frac{S^2}{k\gamma}$$

$$\theta = \frac{-1}{Nx + C_1} \qquad C_1 \text{ is a constant}$$

$$\Rightarrow \quad \frac{dT}{dx} = \frac{-1}{Nx + C_1}$$

Integrating above equation with respect to x gives following result

$$T = \frac{-1}{N}\ell n\left(\left(x+\frac{C_1}{N}\right)C_2\right) \qquad C_1 \text{ \& } C_2 \text{ are constants}$$

Apply boundary conditions:

$T(0) = 0$

$C_1C_2 = N$

$T(L) = T_L$

$$T_L = \frac{-1}{N}\ell n\left(\left(LC_2+1\right)\right)$$

$$LC_2 + 1 = e^{-NT_L}$$

$$C_2 = \frac{e^{-NT_L}-1}{L}$$

Thus $C_1 = N/C_2$

$$T(x) = \frac{-1}{N}\ell n\left(xC_2+1\right)$$

$$T(x) = \frac{-1}{N}\ell n\left(\left(\frac{x}{L}\right)\left(e^{-NT_L}-1\right)+1\right) \qquad \text{where } N = -\frac{S^2}{k\gamma}$$

Test data:

$S = 300\mu V/°C$

$K = 21.15$ W/mK

$\gamma = 49e\text{-}8\Omega m$

$L = 1m$

$T_L = 100°C$

This data is used to compare analytical results given by the expression derived in this section and the finite element solution as obtained using MATLAB program. The plot in Figure 4-16 compares MATLAB program results with analytical results. The dots in a straight line represent steady state temperature without Joule effect. The solid parabolic curve line represents steady state temperature distribution with the inclusion of Joule effect in the analysis. The dots on top of parabolic curve show close agreement between analytical and MATLAB program results.

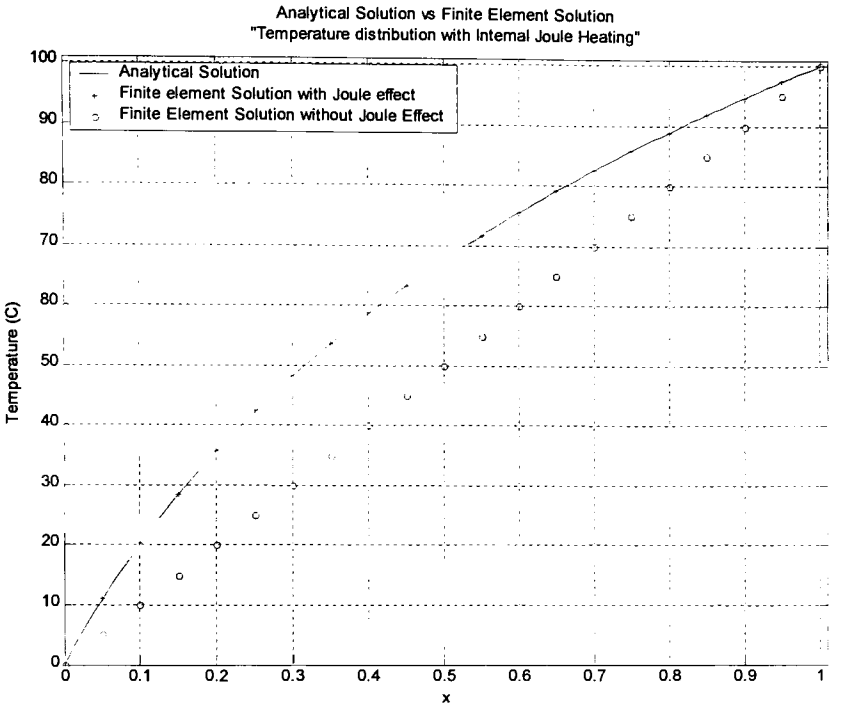

Figure 4-16 Steady state temperature distribution with and without Joule heating

5 Steady state and Transient Analysis of Micro Thermoelectric Generator

5.1 Introduction

Rapid development in the field of micro-machining technology opened a new era for mechanical devices. The size of mechanical devices is getting smaller with MEMS and NEMS-technologies. The success of MEMS based pressure sensor, flow sensor, accelerometer and thermal sensors motivates engineers and researchers to explore the world of miniature devices and transform traditional complex mechanical devices into cost effective and efficient micro devices. Much of the attention has been devoted to the development in the field of process technology and material science. The design and analysis of miniature devices is still relied on the prototype testing.

Comprehensive design and analysis tools are required to completely model the response of miniature devices. Various assumptions, which were made to simplify the analysis of macro devices, need to be validated and revised for micro devices. In this chapter, a thermoelectric device is modeled including all known thermoelectric effects in the analysis. The influence of these effects under various operating conditions and at different length scales is being studied.

5.2 Description of Micro Thermoelectric Device

A micro power generator listed in reference [Toriyama, 2001] is taken as a test-geometry to study the influence of Joule and Thomson effect. It utilizes self-standing structure of polysilicon-gold thermocouples that is said to have better performance because the thermoelements are isolated from the silicon substrate and heat transfer from heat absorber to the silicon substrate is only through thermoelements. The analytical model used in the [Toriyama, 2001] to predict the output voltage does not include Joule heating and Thomson effect in the analysis. In this chapter the results obtained using the

complete model of thermocouple will be compared with the results obtained from ideal thermocouple model (including only Seebeck effect).

The Figure 5-1 shows the schematic of micro power generator consisting of a number of thermocouples connected in series on silicon substrate. The heat absorber area is proposed in the reference to transfer thermal energy from heat source to the hot junctions of the thermocouple more effectively. The cold contact of the thermocouple is attached to the silicon substrate that acts as a heat sink. When the heat absorber is exposed to a heat source, the heat starts flowing from hot to cold contact through the thermoelements. The dissipation of heat at the sink causes temperature difference between hot and cold contact, thus producing output voltage as given by Seebeck relation.

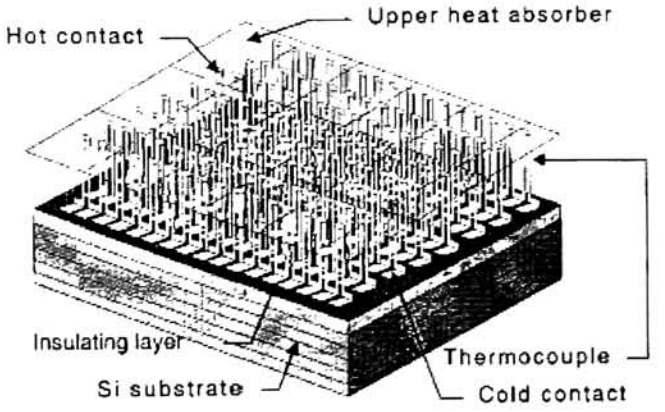

Figure 5-1 Micro power generator [Toriyama, 2001]

The thermopile used in micro power generator was fabricated by micro-machining technology in the form of layers. As shown in Figure 5-2, the bottom layer is of polysilicon, and then a layer on Au/Cr is deposited on top of polysilicon layer. One of the thermoelement is made up of a single material (Polysilicon) and other thermoelement is a composite that is made up of polysilicon, chromium and gold layer.

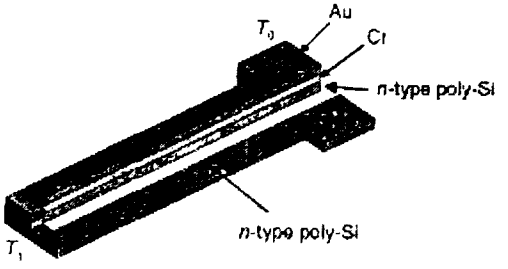

Figure 5-2 Thin layer model of micro thermocouple [Toriyama, 2001]

The dimensions of thermocouple as given in the reference [Toriyama, 2001] are shown in Figure 5-3. The same dimensions will be used in the following steady state and transient finite element analysis.

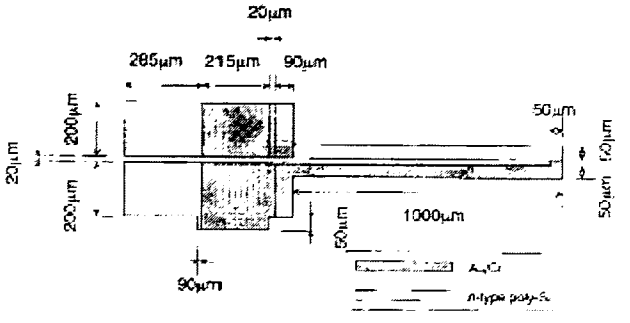

Figure 5-3 Dimensions of micro thermocouple [Toriyama, 2001]

The bulk mass on left hand side of the micro thermocouple shown in Figure 5-3 stays in contact with silicon substrate, which acts as an infinite heat sink. It is assumed that the temperature of the n-type poly-Si regions at the left side will stay constant and thus can be removed from the geometry by applying fix temperature boundary condition on AuCr interface (x=285μm). Based on this assumption, the geometry that is considered for steady state and transient analysis is shown below.

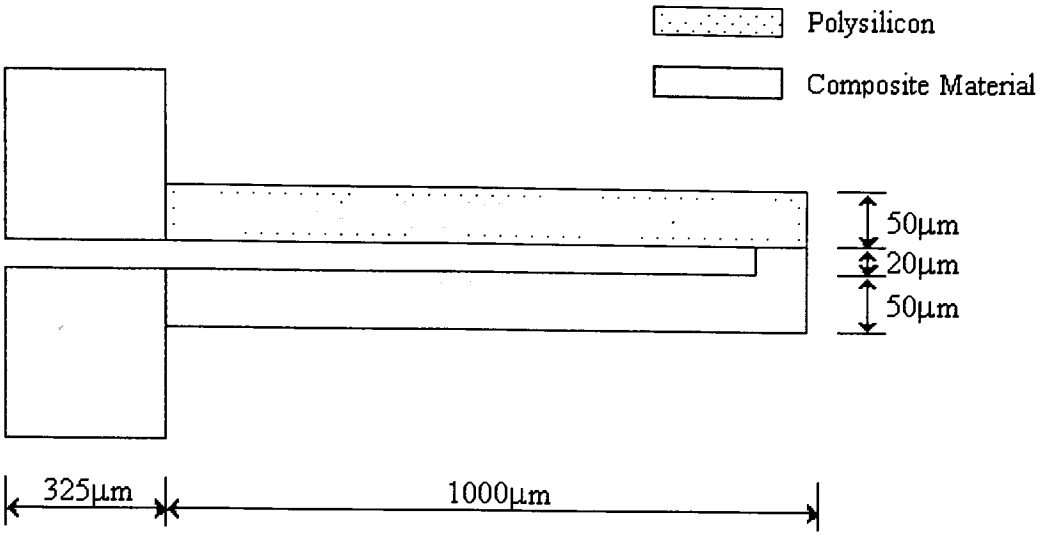

Figure 5-4 Thermocouple geometry used in analysis

The material properties of all materials are listed in Table 5-1.

Table 5-1 Material Properties

	n-type Polysilicon	Chromium	Gold
Thermal Conductivity k (W/mK) *	29.0	90.3	315.0
Density ρ(Kg/m^3)	2330	7140	19300
Specific heat (J/KgK)	710	450	128
Resistivity (Ωm) *	1.1×10^{-5}	1.31×10^{-7}	2.25×10^{-8}

5.3 Transformation from Multi-layer to Single-Layer Model

The geometry of micro thermoelectric generator consists of three materials; bottom layer of polysilicon, middle layer of chromium and top layer of gold. The different layers in the geometry require three-dimensional finite element model. However, the MATLAB finite element program is only capable of analyzing two-dimensional models. The thermocouple geometry is first transformed from multiplayer to single layer by replacing composite material regions with equivalent single material regions.

* Source: Reference [19]

The composite regions in the thermocouple can be replaced with equivalent single material regions if the physical, thermal, electrical and thermoelectric properties of both composite and its equivalent single material regions are equal. The generalized expressions for the material properties of equivalent single material are derived from the fundamental principles using a test problem shown in Figure 5-5. The figure shows a composite block, consisting of three layers of different materials, and its equivalent block made up of a single material. All the layers of composite and equivalent block have the same cross-sectional area and length.

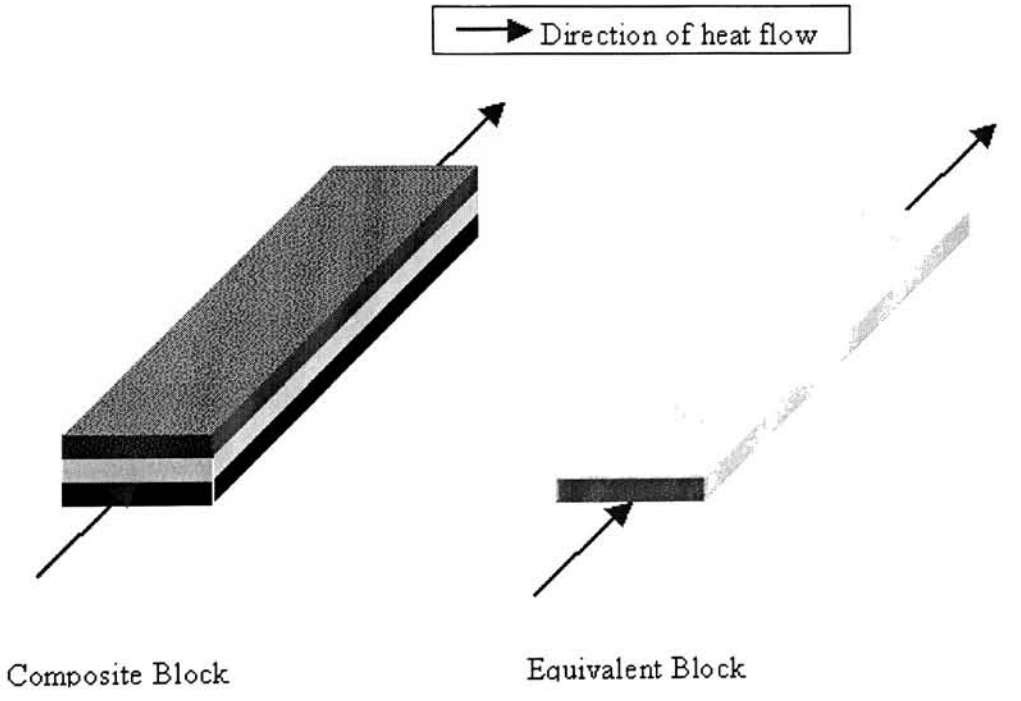

Figure 5-5 Composite block and equivalent block

Thermal conductivity

The resistance to heat flow offered by composite regions must be equal to the resistance offered by the equivalent regions. Therefore, the thermal conductivity of equivalent single material can be evaluated by equating the thermal resistance of both regions.

Thermal Resistance of Composite block $(R) = \dfrac{1}{\dfrac{k_1 A_1}{L_1} + \dfrac{k_2 A_2}{L_2} + \dfrac{k_3 A_3}{L_3}}$ (5.1)

Thermal Resistance of Equivalent block $(R_{eq}) = \dfrac{L_2}{k_{eq} A_{eq}}$ (5.2)

where k, A and L represents the thermal conductivity, cross-sectional area and length respectively. Subscript 1,2,3 and eq denote the first, second, third layer of composite block and single layer of equivalent block respectively. The relation between thermal conductivity of equivalent block and individual layers of composite block can be derived as follows.

$$R = R_{eq}$$

$$\Rightarrow \frac{k_1 A_1}{L_1} + \frac{k_2 A_2}{L_2} + \frac{k_3 A_3}{L_3} = \frac{k_{eq} A_{eq}}{L_2}$$

$$\Rightarrow k_{eq} = \left(\frac{k_1 A_1}{L_1} + \frac{k_2 A_2}{L_2} + \frac{k_3 A_3}{L_3} \right) \left(\frac{L_{eq}}{A_{eq}} \right)$$

In case, the length and cross-sectional area of all layers are equal, the equivalent thermal conductivity is the sum of the thermal conductivities of all layers of composite block.

$$\Rightarrow \quad k_{eq} = k_1 + k_2 + k_3 \tag{5.3}$$

Heat storage capacity (ρc_p):

The storage capacity of equivalent block is derived from the fact that the heat stored must be equal in both composite and its equivalent single material block. Equating the amount of thermal energy stored in each block leads to the following expression of equivalent heat storage capacity.

$$(\rho c_p)_1 \times A \times L + (\rho c_p)_2 \times A \times L + (\rho c_p)_3 \times A \times L = (\rho c_p)_{eq} \times A \times L$$

$$(\rho c_p)_{eq} = (\rho c_p)_1 + (\rho c_p)_2 + (\rho c_p)_3 \tag{5.4}$$

Electrical Resistivity:

It is assumed that the electric current flows only along the length and width and not across the layers in the composite block. Under this assumption, the three layers can be treated as three resistances in parallel. Thus the total resistance of composite Block can be expressed as follow.

$$R = \frac{1}{\frac{A}{\gamma_1 L} + \frac{A}{\gamma_2 L} + \frac{A}{\gamma_3 L}}$$

Resistance of equivalent block $R_{eq} = \frac{\gamma_{eq} L}{A}$

Equating resistance of composite block and equivalent block gives the equivalent resistivity.

$$\frac{A}{\gamma_{eq} L} = \frac{A}{\gamma_1 L} + \frac{A}{\gamma_2 L} + \frac{A}{\gamma_3 L}$$

$$\frac{1}{\gamma_{eq}} = \frac{1}{\gamma_1} + \frac{1}{\gamma_2} + \frac{1}{\gamma_3} \tag{5.5}$$

Thermoelectric properties of composite materials are assumed to be same as that of top layer *i.e.* Au layer.

5.3.1. Validation of Equivalent Single Layer Model

The relations derived for equivalent material properties are validated by comparing results from a three-dimensional model of composite block with the two-dimensional model of equivalent block. ANSYS is used to analyze and compare three-dimensional and two-dimensional models.

A composite block, shown in Figure 5-6, is analyzed for steady state and transient temperature response using three-dimensional model and equivalent two-dimensional model.

Three-dimensional model:

Governing Equation: $$k_x \frac{\partial T}{\partial x} + k_x \frac{\partial T}{\partial y} + k_x \frac{\partial T}{\partial z} = \rho c_p \frac{\partial T}{\partial t} \tag{5.6}$$

Boundary Condition: $T(x,y,0,t) = 30°C$

$q(x,y,L,t) = 1e6\ W/m^2$

Initial Condition $T(x,y,z,0) = 30°C$

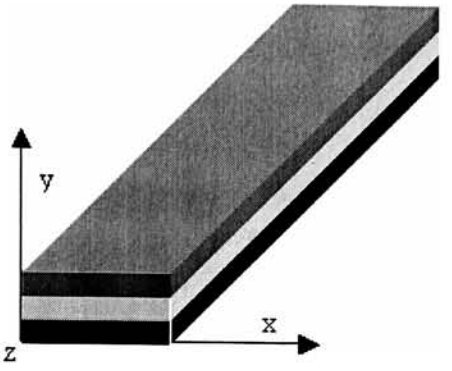

Figure 5-6 Test problem to validate equivalent material properties

where T is the temperature, x,y,z are the space co-ordinates, t is the time, k is the thermal conductivity and q is the flux. The thickness of all layers is 10μm and the width and length of the block are 50μm and 1300μm respectively.

Two-dimensional Model of Equivalent Single Material Block

The equivalent block of composite block consists of a single layer having equivalent material properties. Based on the boundary conditions on the equivalent model, the heat flow along the thickness and along the width will be zero, which provides an option to model as a one-dimensional problem. However, the problem is modeled as a two-dimensional problem to generalize the validation problem. The two dimensional model can be expressed in terms of following equations.

Governing Equation: $$k_x \frac{\partial T}{\partial x} + k_x \frac{\partial T}{\partial y} = \rho c_p \frac{\partial T}{\partial t} \quad (5.7)$$

Boundary Condition: $T(x,0,t) = 30°C$

$q(L,y,t) = 1e6\ W/m^2$

Initial Condition $T(x,y,0) = 30°C$

Figure 5-7 2D finite element model of equivalent block

The material properties of three layers of composite material and the material properties of equivalent block are given in Table 5-1 and Table 5-2.

Table 5-2 Material properties of equivalent block

Property (units)	Equivalent Material
Thermal Conductivity k (W/mK)	434.300
Heat capacity ρc_p (J/m^3K)	7.337×10^6

The three-dimensional model of the composite block is analyzed using 8-node brick element (SOLID90) and the two-dimensional is solved using 8-node quad elements (PLANE35). Different mesh densities are tested to reach at converged solution. The averages of nodal temperature values along the edge (x=0,z=0) are compared with the temperature at point (0,0) are compared. The results from three-dimensional model and two-dimensional model are given in

Table 5-3 Average of nodal temperature values along the edge (x=0,z=0) obtained using three –dimensional model

Element Length	Nodes	Elements	Average Temperature T(0,y,0)
5	75613	15600	120.568
10	11242	1950	120.576

Temperature from three-dimensional model = 120.568°C

Table 5-4 Temperature at point (x=0,y=0) obtained using two-dimensional model

Element Length	Nodes	Elements	Maximum Temperature T(0,0)
5	2871	5200	119.799
10	786	1300	119.799
15	440	696	119.799
25	159	208	119.799

Temperature from two-dimensional model = 119.799 °C

$$\text{Percentage Error} = \frac{120.568 - 119.799}{120.568} = 0.00638 = 0.638\%$$

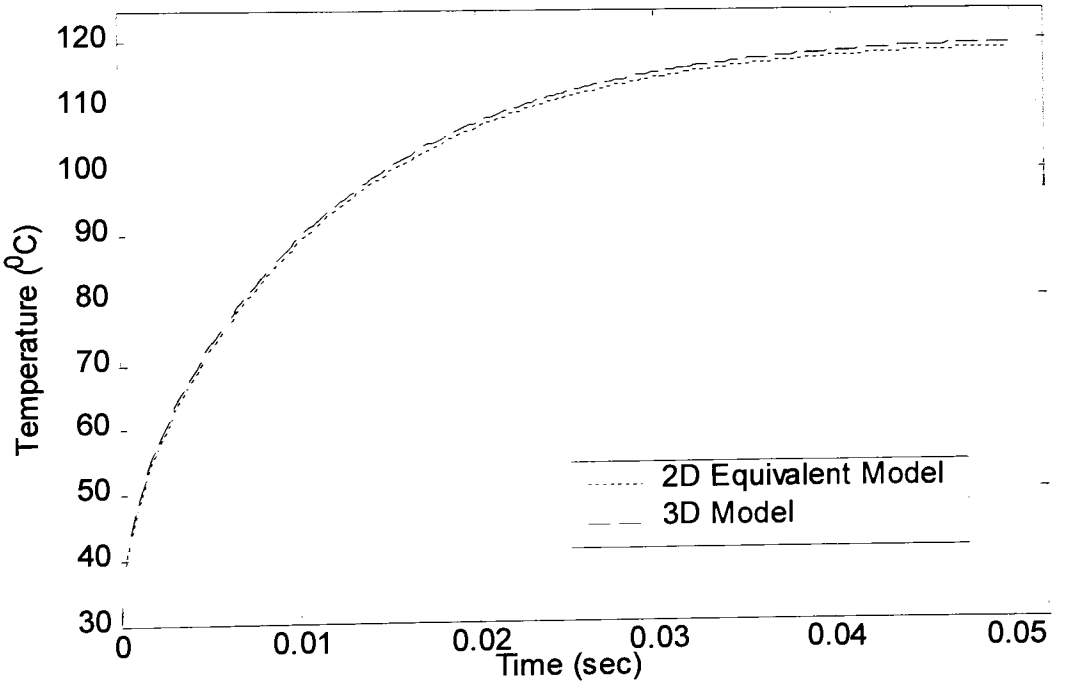

Figure 5-8 Comparison of transient response at point (L,0)

The transient analysis is performed using 800 time-steps in both two-dimensional and three-dimensional models. The results are shown in Figure 5-8, which shows an error of 0.635% at t = 0.05sec.

The transient results of equivalent two-dimensional model show reasonable agreement with the results of three-dimensional model.

5.4 Steady state Response Analysis under Constant Heat Flux Environment

The complete steady-state model of a thermoelectric device consists of coupled thermal and electrical partial differential equations in temperature and voltage as a function of space variables and subjected to known boundary conditions. The coupling relations are utilized to develop overall governing equation in a single domain. As shown in Section 1.4, an overall non-linear governing equation can be obtained in thermal domain, which includes Joule and Thomson effect as temperature dependent internal heat generation terms and Peltier effect as temperature dependent internal heat flux source. The governing partial differential equation for an ideal thermocouple, *i.e.* neglecting Joule, Peltier and Thomson effect, is linear because of the absence of temperature dependent heat generation and internal flux terms. The complete steady state model of an thermoelectric device was developed in Section 3.3.

The steady state model is analyzed using an equivalent two-dimensional model. An arbitrary thermal load is applied at the junctions such that the temperature in the system stays within the range where thermoelectric properties are well known as a function of temperature.

Figure 6-12 shows the boundary conditions used to analyze the steady state response of the thermoelectric device. Boundary 1 and 2 are attached to Silicon substrate that functions as a heat sink for the device. The temperature of the junctions that are in contact with the heat sink will remain constant, thus a constant temperature boundary condition can be applied on boundary 1 & 2. The boundary 3 and 4 are exposed to a constant power heat source. All other boundaries are assumed insulated.

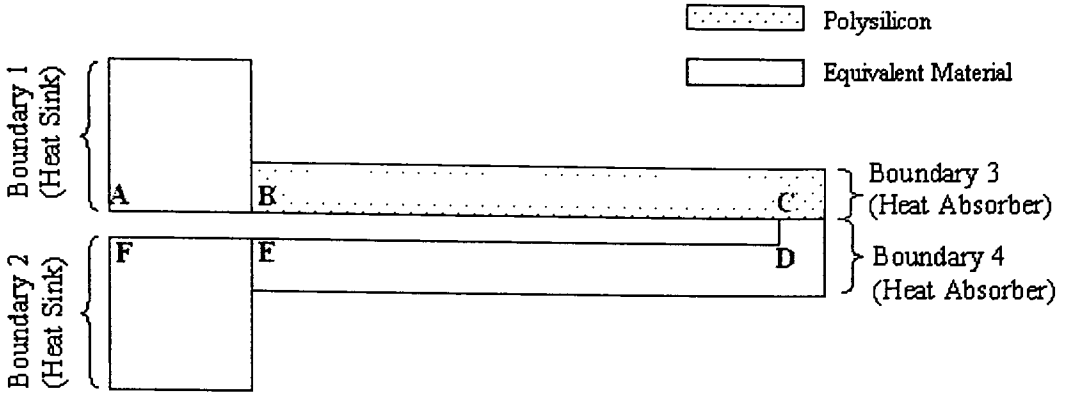

1. All boundaries unless specified are insulated.

Figure 5-9 Steady State model of micro thermoelectric device

Data used for the Analysis:

$T_1 = 30°C$	on boundary 1
$T_2 = 30°C$	on boundary 2
$q_3 = 0.2\times10^8$ W/m^2	on boundary 3
$q_4 = 0.6\times10^8$ W/m^2	on boundary 4

The flux on boundary 4 is three times the actual flux, which is modified to accommodate the three times lesser area in two-dimensional equivalent model as compared to the three-dimensional model. The mesh density with element length of 10μm, shown in Figure 5-10, is selected after testing different mesh densities. The results of mesh validation are shown in Table 5-5. The element length of 10μm gives 0.05% error assuming the solution with 5μm element length as the true solution.

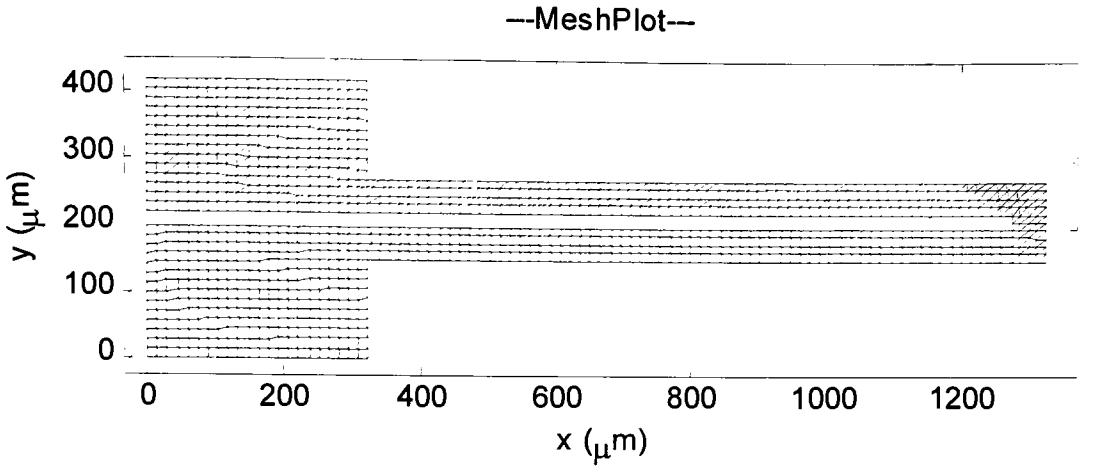

Figure 5-10 Finite element mesh with element length of 10 microns

Table 5-5 Validation of mesh density

Element Length (μm)	Number of Nodes	Number of Elements	Maximum Temperature (°C)	Time (sec)
25	492	740	690.79	2
20	840	1366	693.62	3
15	1375	2336	695.08	5
10	2634	4660	695.90	8
5	9845	18480	696.25	12

The magnitude of thermoelectric properties plays a very significant role in the analysis. The influence of all thermoelectric effects depends on the magnitude of the Seebeck coefficient and its variation with respect to temperature. Therefore, it is important to account for temperature dependence of the Seebeck coefficient, while working in a large temperature range. Two different methodologies are employed to account for temperature dependence. One is to analyze the model using temperature dependent Seebeck coefficient and other is to analyze using average Seebeck coefficient. The variation of the Seebeck coefficient and the Thomson coefficient of Silicon and Gold with temperature is shown in Figure 5-11 and Figure 5-12.

Seebeck coefficient: $S = a + bT(10)^{-2} + cT^2(10)^{-5}$

Thomson coefficient: $\sigma = -T_{abs}\frac{dS}{dT} = -T_{abs}(b(10)^{-2} + 2cT(10)^{-5})$

where T is the temperature in centigrade and T_{abs} is the absolute temperature in Kelvin. The coefficient a, b, c for silicon and gold are listed below.

For silicon [Washburn, 1929]

a = -408.2

b = -46.96

c = +351.0

For Gold [Washburn, 1929]

a = +2.9

b = +0.934

c = 0

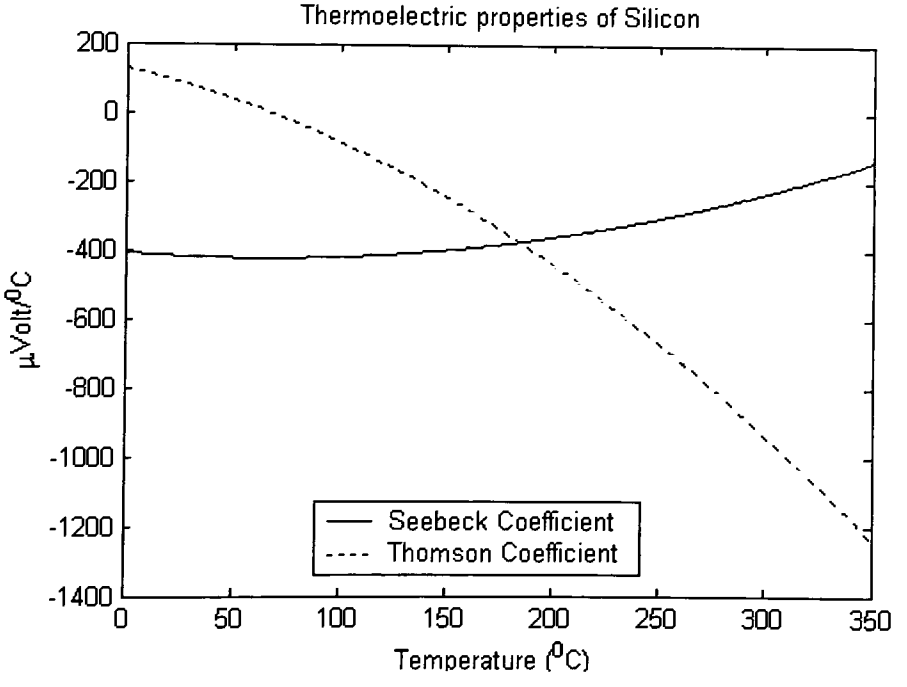

Figure 5-11 Temperature dependent thermoelectric properties of Silicon

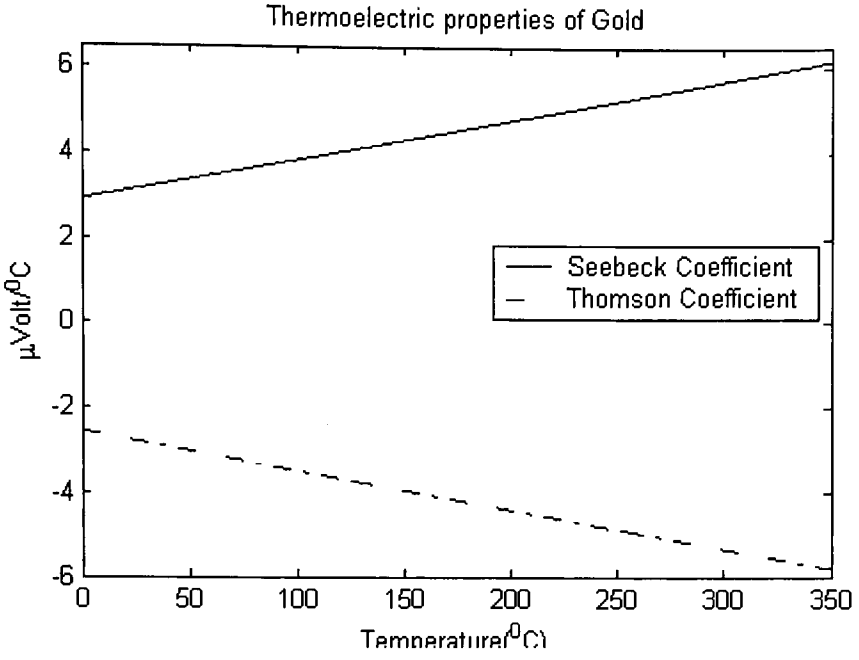

Figure 5-12 Temperature dependent thermoelectric properties of Gold (Au)

In the absence of external current in a thermoelectric circuit, the heat generation or liberation due to the Thomson heat depends on the product of Seebeck coefficient and Thomson coefficient. If the product is positive, the heat will be generated and if the product is negative, the heat will be liberated. For silicon thermoelement, the product of the Seebeck coefficient and the Thomson coefficient is negative for temperature less than 200°C and positive for temperatures greater than 200°C. The product ($S\sigma$) is negative for gold thermoelement throughout the temperature range.

The temperature distribution along the inner boundary of the thermoelectric generator is used to compare the steady state results of the analysis with and without the inclusion of different thermoelectric effects. The path "ABCDEF" is shown in Figure 5-9. The steady state temperature results along "ABCDEF" are shown in Figure 5-13. The ideal thermocouple results are obtained without the inclusion of internal heat sources due to the Joule, Thomson or Peltier effect. The temperature distribution along path "ABC", which consists of polysilicon, shows maximum change in temperature due to the inclusion of all thermoelectric effects. It is due to the large values of Seebeck coefficient and Thomson

coefficient of polysilicon. The magnitude of these properties for Gold is comparatively small, that is why the change in temperature distribution along the path "DEF" is small.

The first subplot in Figure 5-13 shows steady state temperature distribution along path "ABCDEF" and second subplot shows the difference between ideal temperature distribution and actual temperature distribution. It is clear that the maximum change in temperature due to the influence of Joule, Thomson and Peltier effect occurs near the middle of silicon thermoelement. Although the maximum change was expected to be at the junction, the high thermal conductivity of equivalent thermoelement provide easy path to the excessive heat produced at the junction.

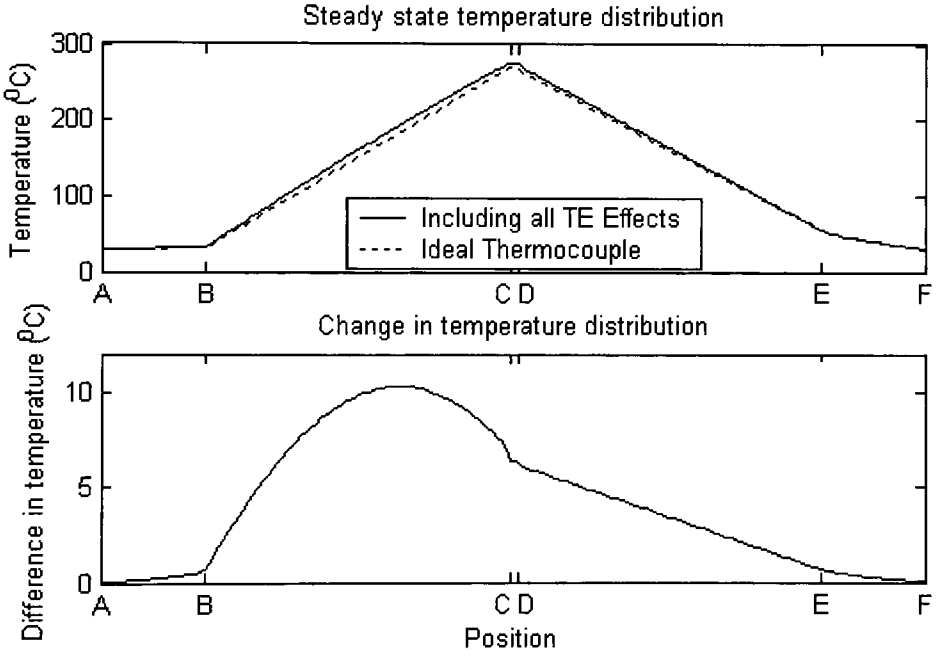

Figure 5-13 (1) Steady state temperature distribution (2) Change in temperature distribution due to the combined influence of Joule, Thomson and Peltier effect

The magnitude of output voltage also changes because of the change in junction temperatures. The steady state voltage distribution and change in the voltage distribution due to the inclusion of Joule, Thomson and Peltier effect is shown in Figure 5-14. A

maximum change in the voltage (0.0015Volt) was observed at point 'A'. It shows 1.7% increase in the output voltage with the inclusion of all thermoelectric effects.

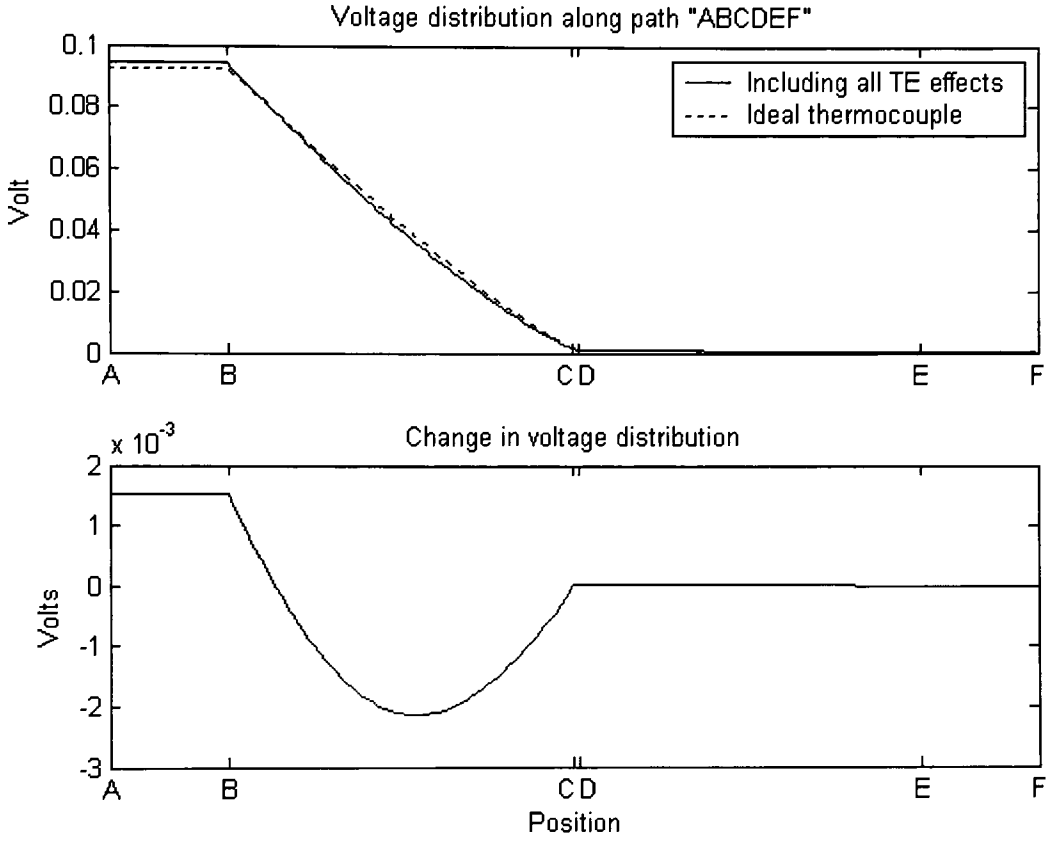

Figure 5-14 (1) Steady state voltage distribution along path "ABCDEF". (2) Difference in voltage distribution due to the Joule, Thomson and Peltier effect

The influence of individual effects is shown in Figure 5-15. The change in temperature at the hot junction (point C) is the maximum due to the Peltier effect and minimum due to the Thomson effect. The maximum change in temperature due to the Thomson effect and Joule effect occurs near the mid point of the thermoelement, and due to the Peltier effect, it occur at the junctions.

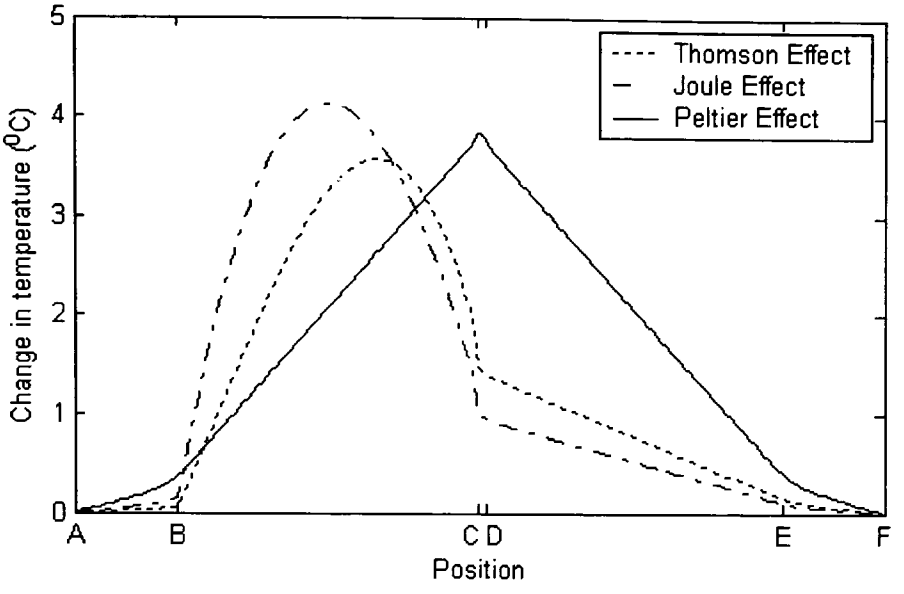

Figure 5-15 Change in temperature along the path "ABCDEF". Refer Figure 5-9 for path. Results are based on Temperature dependent thermoelectric properties

It is observed that the influence of Joule effect depends on modified figure of merit (Z_J) expressed as below.

$$Z_J = \frac{S^2}{k^2\gamma} \tag{5.8}$$

The influence of Thomson effect depends on the following parameter.

$$Z_{th} = \frac{S\sigma}{k^2\gamma} \tag{5.9}$$

The influence of Peltier effect is proportional to the following parameter.

$$Z_P = \frac{S^2}{k\gamma}$$

For an equal heat flux load, the change in temperature distribution is more in the material having greater Z_J, Z_{th} and Z_P.

The average values of thermoelectric properties, given in Table 5-6, are used to study the significance of all thermoelectric effects with respect to applied heat flux.

Table 5-6 Average thermoelectric properties of Silicon and Gold

Property (Units)	Seebeck Coefficient (μV/°C)	Thomson Coefficient (μV/°C)
Silicon	-283.245	-554.974
Gold	4.534	-4.184

The variation in the influence of all thermoelectric effects with the applied flux can be visualized in Figure 5-16. For the constant average values of thermoelectric properties, the overall influence of thermoelectric effects on the temperature distribution increases with the increase in applied heat flux. However, in case of temperature dependent thermoelectric properties, the influence of Joule, Thomson and Peltier first increases up to a certain value of flux and starts decreasing afterwards. The second case is more specific to the material properties, which shows the decrease in the influence because of the decrease in the magnitude of Seebeck coefficient at higher temperatures.

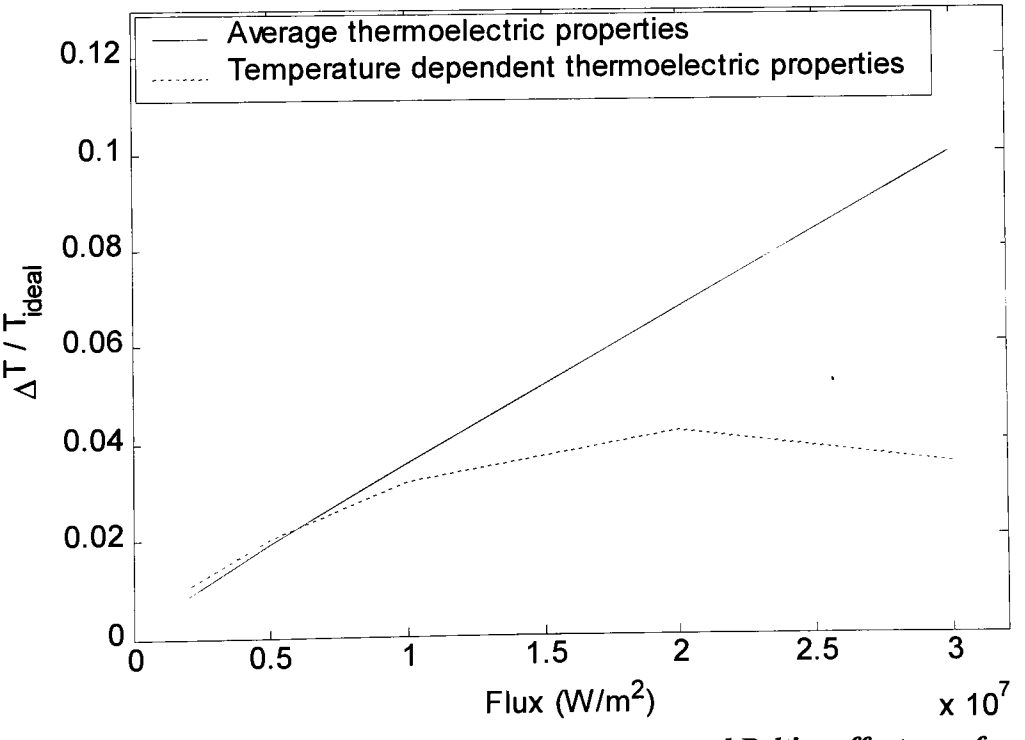

Figure 5-16 Combined influence of Joule, Thomson and Peltier effect as a function of applied heat flux

5.5 Transient Response Analysis under Constant Heat Flux Environment

Most of the engineering problems involving thermal systems have finite response time and require the solution of time dependent governing equations subjected to boundary conditions and initial condition. An initial condition specifies the temperature at the instant the new boundary conditions are applied on the system. Transient problems are also known as initial value problems. In context of thermoelectric devices, the transient solution gives temperature and voltage distribution as a function of time as well as space variables.

The transient problems are more complex because of the addition of one extra variable in the system. The geometry of the thermoelectric device is shown in Figure 5-9 and the thermal constraints at the boundaries are listed below.

Initially, at time t=0, the temperature of all the points was T_0 K. Then at the next instant of time the heat absorber area is exposed to heat source and other side remains in contact with a heat sink of temperature T_o. The governing equation is given by:

$$\nabla(k\nabla T(x,y,t)) + q''' = \rho c_p \frac{\partial T(x,y,t)}{\partial t}$$

Initial condition: $T(x,y,0) = T_o$ K

Boundary Condition: $T(x,y,t) = T_1$ K on boundary 1

$T(x,y,t) = T_2$ K on boundary 2

$q(x,y,t) = q_1$ K on boundary 3

$q(x,y,t) = q_2$ K on boundary 4

The numeric data used in the MATLAB program is given below:

$T_o = 30°C$

$T_1 = 30°C$

$T_2 = 30°C$

$q_1 = 0.3$ W/m^2

$q_2 = 3\times0.3 = 0.9$ W/m^2

Table 5-7 Material Properties

	n-type Polysilicon	Equivalent Material
Thermal Conductivity k (W/mK)	29.0	434.3
Heat capacity ρc_p (J/m^3K)	1.654×10^{6}	7.337×10^{6}
Resistivity (Ωm)	1.1×10^{-5}	0.0192×10^{-6}

A finite element mesh consisting of 1375 nodes (3-node triangular element as shown in Figure 5-10) is used to solve time dependent partial differential equation. Time step for transient finite element method is selected based on Fourier number.

Element length (Δx) = 10μm

Time step (Δt) $\cong \beta \frac{\rho c_p (\Delta x)^2}{k}$ where β is a scaling parameter. Recommended $1 \le \beta \le 100$

For n-type polysilicon: $\Delta t = \beta \times 5.704\times10^{-6}$ sec

Settling time from initial trial = 0.08 sec

Number of time steps = $0.08 / (\beta\times5.704\times10^{-6})$

$= 14024.06/\beta$

$\Rightarrow \quad 140 \le$ (time steps) ≤ 14024

For Equivalent Material: $\Delta t = \beta\times1.69\times10^{-6}$ sec

Settling time from initial trial = 0.08 sec

Number of time steps = $0.08 / (\beta\times1.69\times10^{-6})$

$= 47337.28/\beta$

$\Rightarrow \quad 473 \le$ (time steps) ≤ 47337

500 time steps are selected based on the required stability and efficiency.

Implicit time stepping technique (also known as Galerkin's technique $\theta = 2/3$) is used for solving governing differential equation.

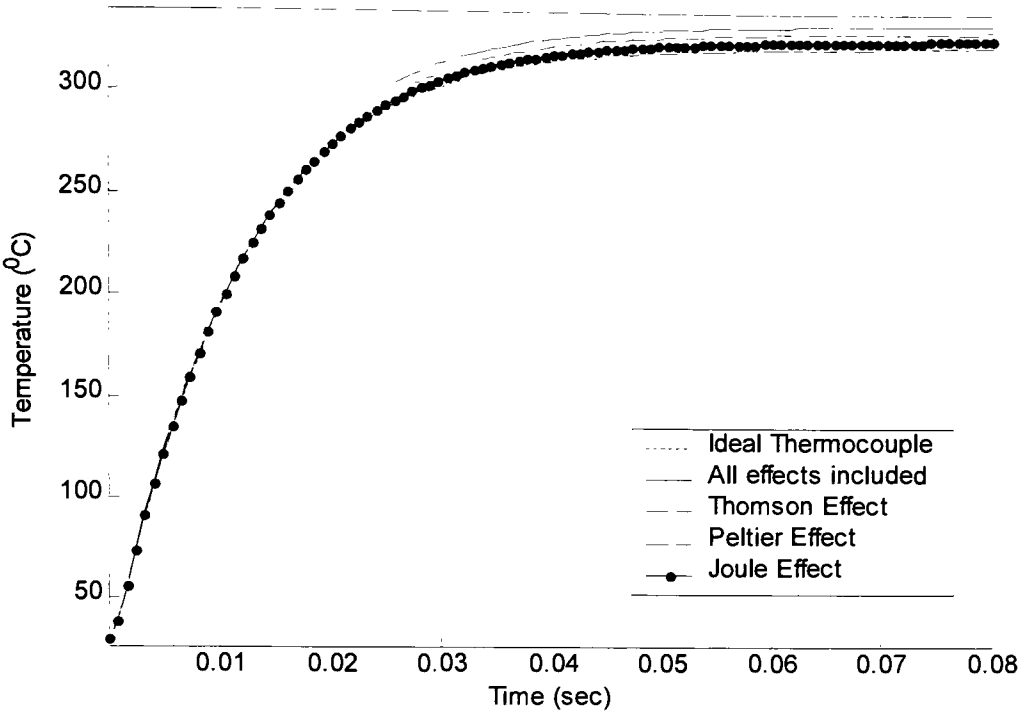

Figure 5-17 Transient temperature response of thermoelectric device at point 'C'

The plot in Figure 5-17 shows the temperature of point C (see Figure 5-9) as a function of time. The curve "Ideal thermocouple" only includes the Seebeck effect and thermal conduction into the analysis. Whereas the curve "All effects included" takes into account the internal heat generation due to the Thomson effect and Joule effect, along with the plane heat flux due to the Peltier effect at the junction. It is observed that the difference in time constant in different cases is proportional to the corresponding difference in the steady state value.

5.6 Steady state Response Analysis under Fixed Temperature Environment

The thermoelectric devices are subjected to fixed temperatures at their junction under various practical applications such as direct contact of hot junction with solid heat source. Such environment can be modeled with the MATLAB program by applying fixed temperature boundary condition at hot junction and same at the cold junction assuming

the cold junction is in direct contact with infinite heat sink. The geometry of the device is given in Figure 5-9 and the thermal constraints at the boundaries are listed below.

$T_1 = 30°C$ on boundary 1

$T_2 = 30°C$ on boundary 2

$T_3 = 350°C$ on boundary 3

$T_4 = 350°C$ on boundary 4

Figure 5-18 shows the steady state temperature distribution along path "ABCDEF" (as shown in Figure 5-9). The second subplot shows the difference in the temperature distribution when all the thermoelectric effects are included in the model. The maximum difference in temperature due to the combined effect of Joule, Thomson and Peltier effect occurs in the middle of polysilicon thermoelement. The fixed temperature constraints at the junctions act as heat sink for the excessive heat produced due to Joule effect, Thomson effect and Peltier effect. Therefore the temperature of the junction surfaces, which are in contact with the infinite heat reservoirs, will remains constant.

The influence of Joule effect and Thomson effect is very small in equivalent thermoelement as compared to polysilicon thermoelement. Although, the sign of both Seebeck coefficient and Thomson coefficient are the same, which makes Thomson effect to generate heat instead of liberating heat, but the magnitude of these coefficients is very small as compared to the Seebeck and Thomson coefficients of polysilicon.

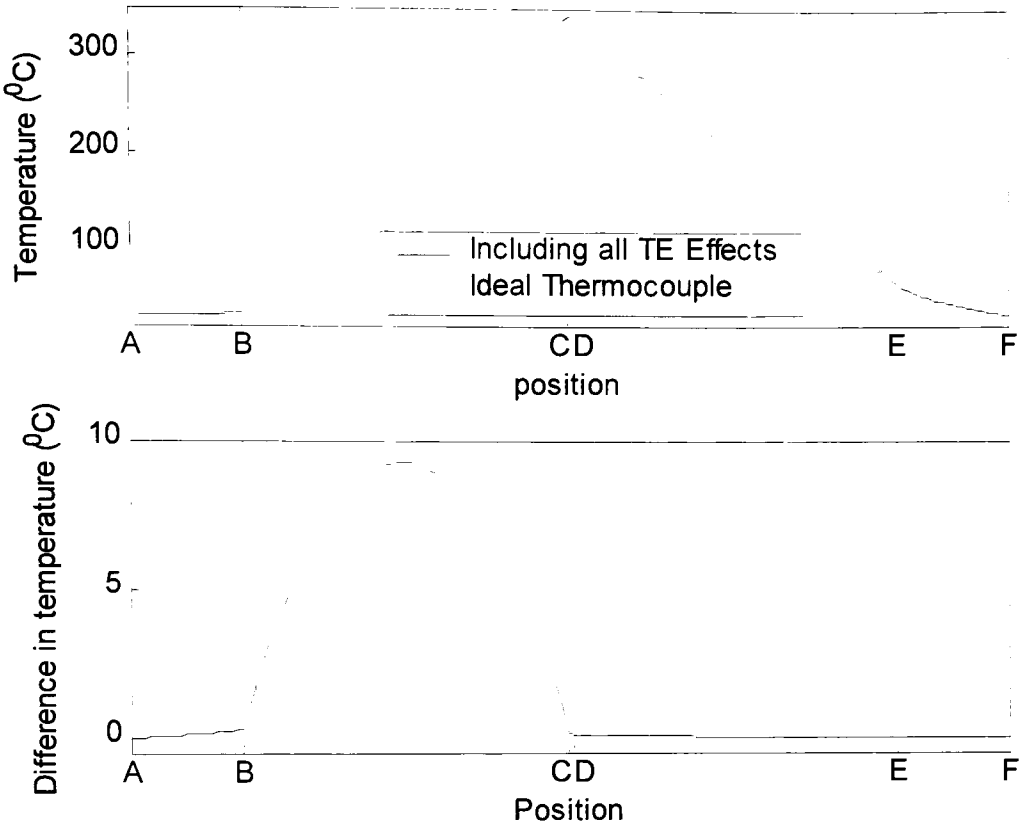

Figure 5-18 (1) Steady state temperature distribution under fixed temperature boundary conditions. (2) Difference in ideal and actual temperature distributions.

Although, the temperature of the hot junction remains fixed due to the fixed boundary condition, the temperature of the cold junction changes slightly from its ideal value due to the combined influence of all thermoelectric effects. It causes slight deviation of the actual output voltage from the ideal output voltage as shown in Figure 5-19. The actual output voltage that is obtained using complete model is less than the ideal output voltage. It can be justified with the reason that the temperature difference between the hot and cold junction is decreased due to the rise in cold junction temperature. If the cold junction is also maintained at a fixed temperature, the actual steady state output voltage will be the same as ideal steady state output voltage.

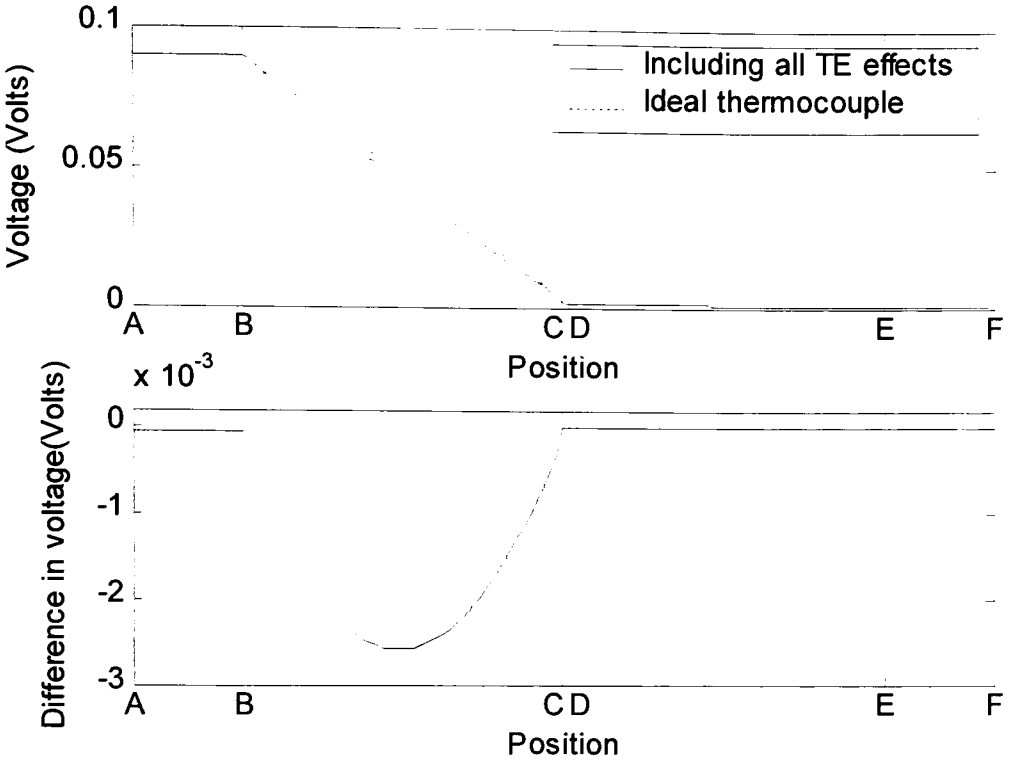

Figure 5-19 (1) Steady state voltage distribution under fixed temperature boundary conditions. (2) Difference in ideal and actual voltage distributions.

The steady state response of a thermoelectric system subjected to fixed temperature conditions at the junctions will be unaffected by the Joule effect, Thomson effect and Peltier effect.

5.7 Steady state Response Analysis under Convective Environment

The use of thermoelectric devices under convective working environment is very common. Thermal sensors are used to measure temperature of fluids and thermoelectric generators are employed in the engine exhaust to convert waste thermal energy into useful electric energy. The geometric model shown in Figure 5-9 and the thermal boundary conditions on the model are listed below.

$T_1 = 30°C$ on boundary 1

$T_2 = 30°C$ on boundary 2

$k\nabla T = h(T-350°C)$ on boundary 3

$k\nabla T = h(T-350°C)$ on boundary 4

The boundary 3 and 4 of the domain are subjected to convection heat transfer with surrounding temperature of 350°C and convective heat transfer coefficient 'h'. The domain of the thermoelectric device is meshed using three node triangular elements in ANSYS and the mesh data and boundary condition data is imported into MATLAB program to analyze the model including all thermoelectric effects.

It is observed that the Peltier effect is more significant than the Thomson effect and Joule effect under convective environment. The significance of Joule, Thomson and Peltier effect is analyzed for different values of 'h' and results are shown in Figure 5-20. A dimensionless temperature is defined to study the relative significance of a particular effect irrespective of the maximum temperature value.

$$\text{Dimensionless temperature parameter} = \frac{T - T_{ideal}}{T_{ideal}}$$

where T is the temperature of the hot junction node including thermoelectric effect in question and T_{ideal} is the ideal temperature of the hot junction node.

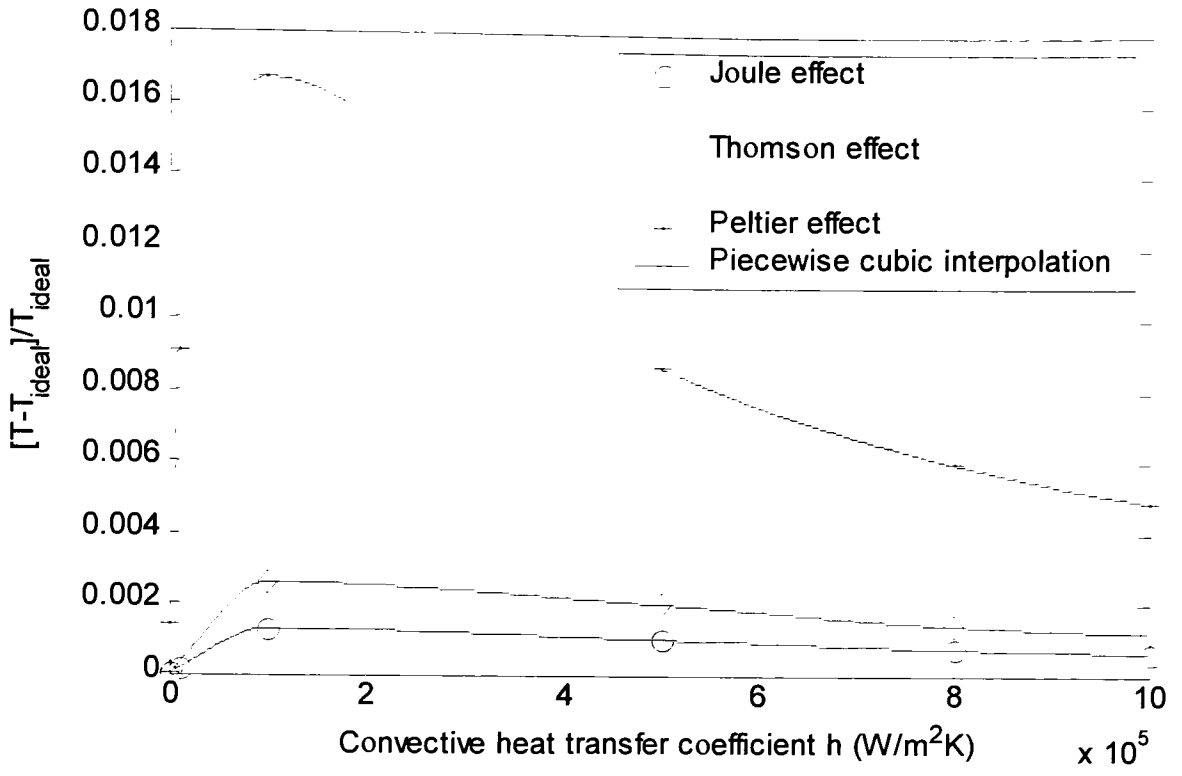

Figure 5-20 The significance of different thermoelectric effects as a function of convective heat transfer coefficient.

The influence of thermoelectric effects increases as the value of 'h' is increased to a critical value and decreases as it is increased beyond that critical value. For small values of 'h', the temperature difference between the hot and cold junction is small and thus the current in the circuit is small, which causes less influence on the steady state response of a thermoelectric device. For high values of 'h', the temperature difference between the hot and cold junction is higher and thus higher current in the circuit. However, the excessive heat that is generated due to the Joule effect, Thomson effect and Peltier effect can be transferred to the surroundings more easily for the higher values of 'h' as compared to the lower values of 'h'.

5.8 Thermoelectric Device Optimization

The Joule effect always tends to increase the temperature of the thermoelements as well as the junction. The Thomson effect may increase or decrease the temperature of the

thermoelements and the junctions depending upon the sign of Thomson coefficient relative to that of Seebeck coefficient. The Peltier effect may also increase of decrease the temperature of the junctions based on the absolute Seebeck coefficients of the materials. The performance of a thermoelectric generator can be improved by making all thermoelectric effects to cause maximum heating at the hot junction and cooling at the cold junction. This objective can be accomplished with following approaches.

(1) Select thermoelement materials, which have high Seebeck coefficients and for which the product of Seebeck coefficient and the Thomson coefficient is positive.
(2) Select material for thermoelements, which have less difference in their thermal conductivity values.

Increasing the Seebeck coefficient will increase the influence of Joule, Peltier and Thomson effect. It also directly influences output voltage characteristics. The relative sign of the Seebeck coefficient and the Thomson coefficient is important because it decides the generation or liberation of heat due to the Thomson effect. If the product is positive, heat will be generated, which will add up with the Joule effect. It the sign is negative, heat will be liberated, which counters the influence of the Joule effect. Therefore the positive product of the Seebeck effect and Thomson effect assures the positive contribution of these thermoelectric effects towards improved performance of thermoelectric generator.

Consider a single thermoelement exposed to heat flux at one end and fixed temperature boundary condition at the other end. It was observed that the maximum influence of the Joule and Thomson effect in a single conductor occurs at the end where flux boundary condition is applied. However, in the thermoelectric generator analyzed in preceding sections, the maximum difference in temperature occurs near the middle of the thermoelement. The reason for that is the difference in the thermal conductivities of thermoelements. The excessive heat that occurs at the junction due to the Joule and Thomson effect leaks through the thermoelement having higher thermal conductivity. It is observed that if the thermal conductivity of both thermoelements is set equal, the

maximum difference in the temperature due to the Joule effect and Thomson effect occurs at the junctions.

The idea presented in above paragraph is illustrated using the thermoelectric generator geometry, which is used in the preceding sections. The thermal conductivity of both thermoelements are set equal to each other and the flux applied is modified to achieve same maximum temperature as achieved with actual thermal conductivity values. The results are shown in Figure 5-21 and Figure 5-22.

Thermal conductivity of thermoelements = 29 W/mK

Modified flux value:

$q_3 = 0.794\times10^7$ W/m^2 on boundary 3

$q_4 = 0.265\times10^7$ W/m^2 on boundary 4

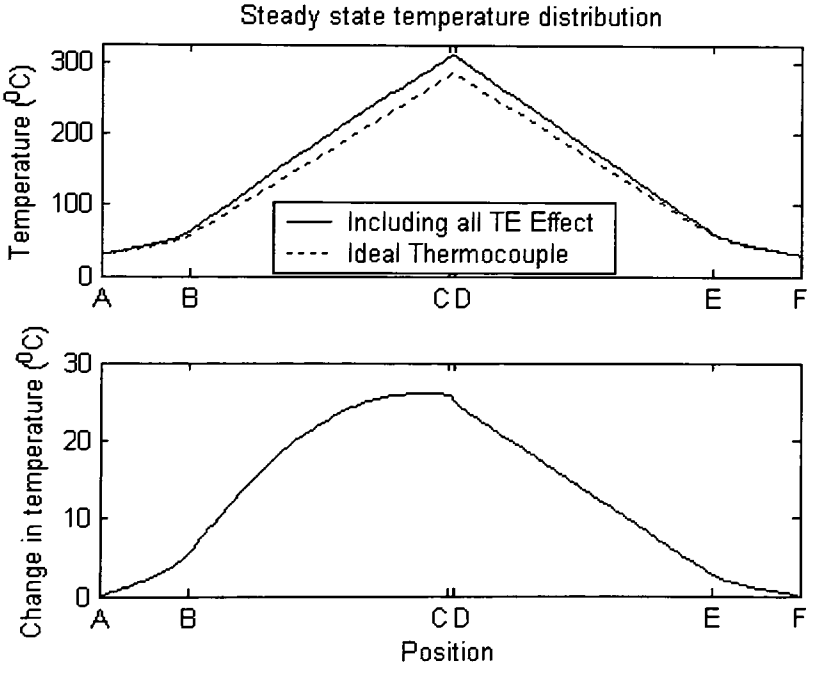

Figure 5-21 Material based optimization results. (1) Steady state temperature distribution (2) Difference in temperature due to the inclusion of all thermoelectric effects

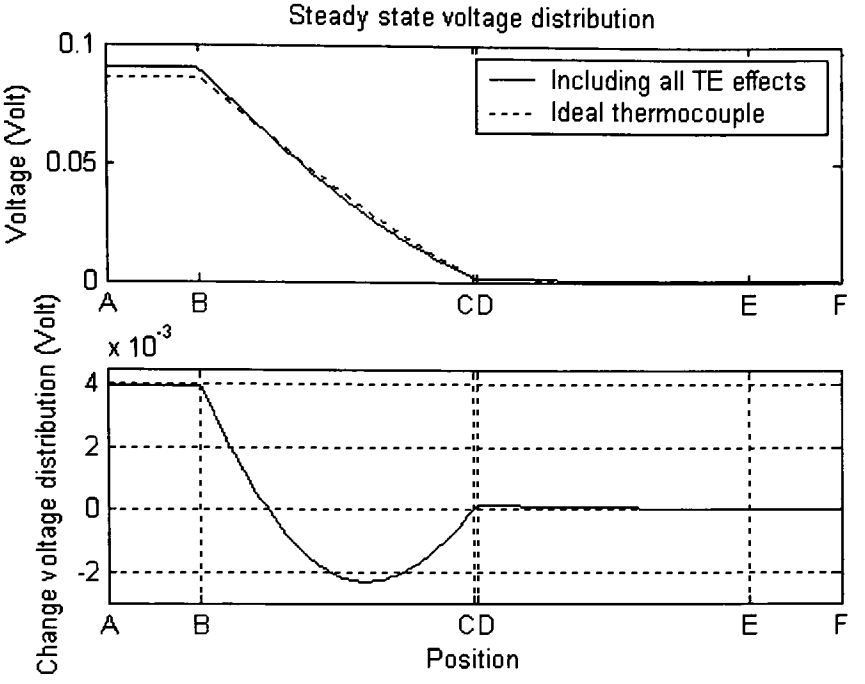

Figure 5-22 Material based optimization results. (1) steady state voltage distribution (2) Difference in temperature due to the inclusion of all thermoelectric effects

As shown in Figure 5-21, the maximum increase in temperature is occurred at the junction. The change in output voltage is 0.004 Volt, which is 2% greater than the change in case of actual conductivities, which was analyzed in Section 5.4.

6 Conclusion and Recommendations

6.1 Summary

A summary of steps taken to accomplish the objective of this thesis is listed below.

Step 1: Develop a mathematical model of thermocouple from the fundamental principles of thermoelectricity, heat transfer and electrical.

A complete steady state and transient mathematical model of a thermocouple was developed in Section 1.4, which includes Seebeck effect, Joule effect, Thomson effect and Peltier effect. The Seebeck effect couples thermal domain to electrical domain and the Joule, Thomson and Peltier effect couples the electrical domain back to the thermal domain. The complete model of thermocouple was transformed into a single domain (thermal) using the coupling relations, which results into a non-liner governing heat conduction equation subjected to linear and non-linear boundary conditions. The Thomson and Joule effects were included as a non-linear internal heat generation term and the Peltier effect was incorporated as a non-linear internal heat flux source at the junctions. The Seebeck effect was used to obtain voltage distribution from the temperature distribution in the thermoelectric circuit.

Step 2: Implement the model (steady state and transient) using finite element method.

The comprehensive model developed in Section 1.4 was implemented using finite element method. The finite element formulation of steady state and transient models was developed in Chapter 3. A computer program was developed, using MATLAB 6.5, to simulate the steady state and transient response. The program requires mesh data and boundary condition data as an input and it is capable of predicting steady state and transient response for various geometric shapes and under various working environments. The significance of material properties and thermal loads on the influence of Joule effect, Thomson effect and Peltier effect can be studied. The program can be directed to use temperature dependent or constant thermoelectric properties in the analysis. It can be used to analyze the models involving fixed temperature boundary conditions, flux

boundary conditions and convection boundary conditions. However, the program is only capable of analyzing two-dimensional models.

Step 3: Validate the finite element model against limiting theory and numerical cases.
The MATLAB program was validated in Chapter 4, where the results of the program were compared with the analytical results and commercial numerical simulation software (ANSYS) results. The program was tested for temperature boundary condition, flux boundary condition, convection boundary condition and problems involving more than one material. The capability of solving non-linear problems was validated by taking a simple one-dimensional problem involving Joule effect. The results of the MATLAB program were compared with the analytical results. The program shows good agreement with ANSYS and analytical results.

Step 4: Use the validated finite element code to study the significance of Seebeck effect, Joule effect, Thomson effect and Peltier effect on the performance of thermoelectric devices under different working conditions.
The validated finite element program was used to analyze steady state and transient response characteristics of a thermoelectric generator in chapter 5. The temperature distribution and voltage distribution for an ideal case and for cases involving Joule effect, Thomson effect and Peltier effect were predicted. The relative significance of Joule, Peltier and Thomson effect was studied under different working environment.

Step 5: Demonstrate the use of the model as a design tool for predicting performance characteristics of thermoelectric devices.
In section 5.8, the program was used to optimize the design of a thermoelectric generator based on the influence of Joule effect, Thomson effect and Peltier effect. A new criteria for material selection was developed, which incorporates the influence of Joule effect and Thomson effect on the junctions to improve the device performance.

6.2 Conclusions

The following conclusions can be made from steady state and transient analysis of thermoelectric device:

(1) The influence of Joule, Thomson and Peltier effects on the steady state and transient characteristics of a thermoelectric device greatly depends on the magnitude and the temperature dependence of absolute Seebeck coefficient. The influence of Joule and Thomson effect is proportional to the square of the temperature gradient and that of Peltier effect is proportional to the first power of the temperature gradient. At low temperatures, the temperature gradient in the thermoelements and at the junctions will be low and the influence of these effects will mainly be dependent on the material properties. In that case, the influence of the Peltier effect on the junction temperature will be greater than the other thermoelectric effects. However, at high temperatures, the temperature gradient in the thermoelements will control the influence of these effects on the temperature distribution. As the Thomson and Joule effect are proportional to the square of the temperature gradient, these will dominate the influence of Peltier effect.

(2) The steady state analysis of the thermoelectric generator shows 1.7% increase in the output voltage due to the combined influence of Joule, Thomson and Peltier effect. The thermoelectric devices, involving high thermoelectric power materials, will show even more influence of the thermoelectric effects on the performance of thermoelectric devices.

(3) The thermoelements having less difference in their thermal conductivities shows the maximum influence of Joule and Thomson effect at the hot junction. Therefore, the relative thermal conductivity should be considered as a design parameter for thermoelectric generators. It was shown in Section 5.8 that the maximum increase in temperature occurs at the junction when the thermoelements having equal thermal conductivity are used.

6.2.1. Combined Influence of Joule, Thomson and Peltier effect

The significance of Joule, Thomson and Peltier effect depends on three parameters i.e. thermal conductivity, electrical resistivity and Seebeck coefficient. The change in junction temperature due to these effects depends on the way the junctions interact with heat source and heat sink. For example, if the hot junction receives heat by convection from a source at temperature T_o, the significance of thermoelectric effects depends on convective heat transfer coefficient between the environment and the hot junction as shown in Figure 5-20. In case of constant heat flux source, such as laser, these effects alter the temperature of hot junction, which changes the output voltage from the device. In case of fixed temperature conditions on the hot and cold junctions, these effects show no change in the steady state and transient output characteristics.

From the perspective of thermal sensor

Most of the thermal sensors employed in the industry are first calibrated using experimental techniques and then used in the practical applications. The use of theoretical modeling for calibration is very rare. In case of experimental calibration, the influence of all thermoelectric effects is already included. Therefore the Joule effect, Peltier effect or Thomson effect will not produce error in the measurement if the system is used under the same working conditions in which it was calibrated. However, if the working environment is different from the calibration environment, the sensor could generate error in the reading. This can be illustrated using following example.

Consider a temperature sensor shown in Figure 6-1, employed to measure the temperature of the environment. One junction is exposed to the environment and another is placed in a reference bath. Lets say we calibrated the sensor using water as environment (convective coefficient between water and junction bead = h_1). If the temperature of the water is T_1, the temperature of the bead will be less than T_1 due to the finite value of 'h_1'. Let T_{ideal} is the temperature of the hot bead without taking into account the Joule, Thomson or Peltier effect. However, the actual temperature of the bead will be $T_{ideal} + \Delta T$, where ΔT accounts for the heating due to the Joule, Thomson and Peltier effect at the junction and its magnitude depends on the value of 'h_1' and the Seebeck coefficient of the materials.

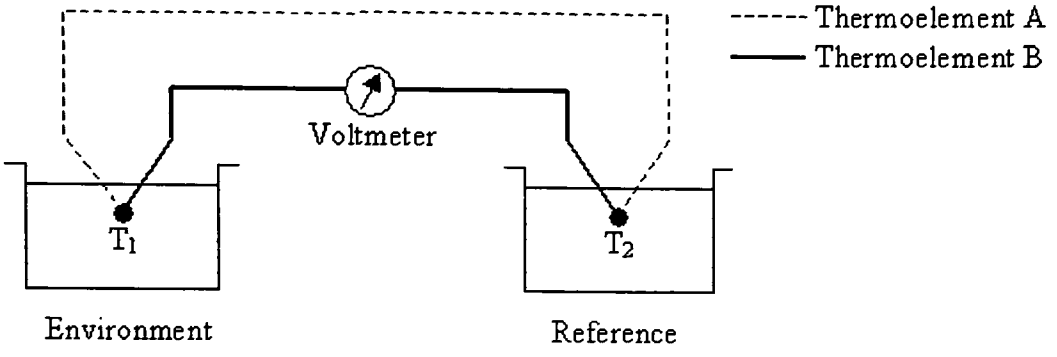

Figure 6-1 Thermal sensor

If T2 is the temperature of the reference bead, the output voltage in the experimental calibration will corresponds to a temperature difference of ($(T_{ideal} + \Delta T) - T_2$) and not to ($T_{ideal} - T_2$). The device will work without an error in the measurement as long as it is used to measure the temperature of the fluid having convective coefficient 'h_1' and within the working temperature range. When the sensor is used to measure the temperature of a fluid having different value of convective coefficient (h_2), the temperature of the junction bead will be different for the same temperature (T_1) of the fluid. This is caused by the variation in the heat produced due to the Joule, Thomson and Peltier effect (ΔT_2) at the hot junction. The thermocouple will show temperature reading corresponding to (($T_{ideal} + \Delta T_2$) – T_2), which generates error in the measurement.

The error in the sensor reading, when it is used in a working environment different from the calibration environment, can be reduced by minimizing the influence of Joule, Thomson and Peltier effect.

From the perspective of thermoelectric generator

The excess heat produced due to the Joule, Thomson and Peltier effect may increase the temperature difference between the junctions and can be used to improve the design of thermoelectric generators. But the maximum influence of the Joule effect is at the middle of the thermoelement. The geometry and materials properties can be optimized to

accumulate maximum Joule heat and Thomson heat at the hot junction and thus increasing the output voltage of micro thermoelectric generator.

6.3 Recommendations for Future Work

(1) Investigate the significance of Joule, Thomson and Seebeck effect on the performance characteristics of thermoelectric coolers. Due to the external currents in the thermoelectric cooler, the significance of Joule and Thomson effect is expected to be much higher.

(2) Extend the capability of MATLAB finite element program to three-dimensional analysis. The three-dimensional model will precisely predict the response of micro-thermoelectric devices consisting of thin film layers. The assumptions regarding thermoelectric properties of composites can then be eliminated and the voltage distribution can be computed in a three dimensional domain including all thermoelement layers in the analysis.

(3) The magnitude and temperature dependence of the Seebeck coefficient controls the influence of Joule, Thomson and Peltier effect. Therefore, it is very important to know exact thermoelectric properties of the materials involved in the analysis. Experimental studies should be conducted to find thermoelectric properties of thin film layers used in micro thermocouples.

(4) Optimize the thermoelectric device performance based on all thermoelectric effects. Besides selecting optimum materials, the shape dependence of Joule and Thomson effect should be investigated. The geometry of the device should be optimized to induce maximum influence of Joule and Thomson effect at the junctions of thermocouple.

(5) Include the temperature dependence of thermal conductivity, heat capacity and electrical resistivity in analyses involving high temperature range. The thermal

conductivity and electrical resistivity of the thermoelements affect the influence of Joule, Peltier and Thomson effect.

(6) Investigate/develop high temperature thermoelectric devices based on optimized design.

References

Anatychuk, L. I., Luste, O. J., 1996, "Physical Principles of Microminiaturization in Thermoelectricity", 15th International conference on thermoelectrics, pp. 279-287.

Arenas, A., Vázquez, J., Palacios, R., 2000, "Bidimensional Analysis of a Thermoelectric Module using Finite Element Techniques", XIX International Conference on Thermoelectrics.

ASTM., 1974, Manual on the use of Thermocouples in Temperature Measurement., pp. 4.

Chang, D. T., Asada, G. C., Kaiser, W. J., Stafsudd, O. M., "Micropower High-detectivity Infrared Sensor System", Solid State Sensor and Actuator Workshop, Hilton Head Island, South Carolina, June 7-11, 1998.

Dike, P. H., 1965, "Elementary Principles of Temperature Measurement by Thermoelectric Methods", Thermoelectric Thermometry.

Egli, P. H., 1960, Thermoelectricity. John Willey & Sons, Inc., pp 4,8.

Geballe, T. H., Hull, G. W., 1955, Seebeck effect in Silicon, Phys. Rev., pp940-947.

Gray, P. E., 1960, The Dynamic Behavior of Thermoelectric Devices, John Wiley & Sons, Inc., New York

Harman, T. C., Honig, J. M., 1967, Thermoelectric and Thermomagnetic Effects and Applications, McGraw-hill Book Company., pp. 51.

Heikes, R. R., 1961, Thermoelectricity: Science and Engineering, Interscience Publishers, Inc., pp. 1, 459.

Lau, G. P.,Buist, J. R., 1997, "Calculation of Thermoelectric Power Generation Performance using Finite Element Analysis", 16th International Cionference on Thermoelectrics.

Lau, G. P., Buist, J. R., 1996, "Temperature and Time dependent Finite-Element Model of a Thermoelectric Couple", 15th International Cionference on Thermoelectrics.

MacDonald, D. K., 1962, Thermoelectricity: an introduction to the principles, John Wiley & Sons, Inc., pp. 4.

Milanović, V., Hopcroft, M., Zincke, C., Zaghloul, M., Pister, K. S. J., 2000, "Modeling of Thermoelectric Effects in Planar Micromachined Structures Using SPICE",

International workshop on thermal investigation of IC's and systems. Budapest, Hungary.

Muanghlua, R., Cheirsirikul, S., Supadech, S., 2000, "The Study of Silicon Thermopile". IEEE. pp. III-226 – III-229.

Oh, S. H., Lee, K. C., Chun, J., Kim, M., 2000, "Micro Heat Flux Sensor using Copper Electroplating in SU-8 Microstructures", Journal of Micromechanics and Microengineering, pp221-225.

Özisik, M. N., 1968, Boundary Value Problems of Heat Conduction, International Textbook Company., pp.59-67.

Pepper, D. W., Heinrich, J. C., 1992, The finite element Method: Basic Concepts and Applications., pp. 1.

Pollock, D. D., 1991, Thermocouples Theory and Properties, CRC Press, Inc.

Powers, D. L., 1987, Boundary Value Problems, HBJ Publishers

Rabin, Y., Rittel, D., June,1999, "A model for the Time Response of Solid-Embedded Thermocouples", Experimental Mechanics, Vol. 39, No. 2.

Reddy, J. N., 1993, An Introduction to the Finite Element Method. McGraw-Hill,Inc. ISBN 0-07-051355-4, pp. 30, 228.

Rowe, D.M., 1995, CRC Handbook of Thermoelectrics., CRC Press, Inc., pp. 617-619

Sasagawa, K., Yagi, M., Saka, M., Abe, H., 1998, "Analysis of Electromigration Considering Thomson effect", ASME International Mechanical Engineering Congress and Exposition, pp 87-92.

Toriyama, T., Yajima, M., Sugiyama, S., 2001, "Thermoelectric Micro Power Generator utilizing Self-Standing Polysilicon-Meta Thermopile", IEEE publications.

Washburn, E. W., West, C. J., Dorsey, N. E., Klemenc, A., Ring, M. D., (1929), International critical tables of Numerical Data, Physics, Chemistry and Technology, Vol. VI, McGraw Hill, New York.

Yajima, M., Toriyama, T., Sugiyama,S., 2001, "Self-Standing Polysilicon-Metal Thermopile for Micro Power Generation".

Yao, D. –J., Kim, C. -J., Chen, G., 2001, "MEMS Thermoelectric Microcoolers", ICT2001, June 8-11, Beijing, China.

Yao, D. -Y., Kim, C. -J., Chen, G., 2000, "Design of Thin Film Thermoelectric Microcoolers", International mechanical engineering congress and Exhibit (ASME), Orlando,FL, November 5-10, 2000.

Appendix A

Computer Implementation of Steady state Finite Element Model

The finite element code written in MATLAB 6.5 for the steady state analysis is given below.

Main Program

```
%-------------------------------------------------------------%
%   Gurjinder Singh     'Thesis Work'                           %
%   Program:    Steady state heat transfer analysis using FEM   %
%   Requirements:     8 input files (Nodes.txt,Elements.txt,    %
%         BC1.txt,BC2.txt,BC4.txt,V_BC1.txt,Qgen.txt,Peltier.txt)
%   P.S.    Node numbers should be in order--start from 1->max  %
%-------------------------------------------------------------%
%                       :Nomenclature:                        %
%   Nodes:      "Node matrix"
%   Elements:   "Element Matrix"
%   BC1:        Boundary condition of first kind
%   BC2:        Boundary Condition of 2nd kind
%   BC3:        Convection Boundary Condition
%   BC4:        Radiation Boundary Condition
%   fQgen:  Matrix to store data from heat generation input file
%   Qgen:       Formatted heat generation matrix
%   MatProp:    Array that contains Material Properties
%   N_Elem:     Total no. of Elements
%   N_Nodes:    Total no. of nodes
%   N_BC1:      Total no. of nodes with BC1
%   N_BC2:      Total no. of elements with BC2
%   N_BC3:      Total no. of elements with BC3
%   N_Qgen:     Total no. of elements with Qgen
%   Beta:       Beta matrix of triangular element
%   Shape_Func: Shape Function vector
%   T:          field variable (Temperature)
%   phi:        Potential at nodes
```

```
%   Jacob:      Jacobian matrix for 3node(1-quad point)...
%               triangular element
%   Ke,Fe:      Elemental stiffness and force matrices
%   K_Global:   Global stiffness matrix
%   F_Global:   Global Force Matrix
%-------------------------------------------------------------------%
clear all,clc,format long e;
global ThermE_Avg
%-------------------------------------------------------------------%
Scale=1e6;                        % Used to scale material properties
DirPath = 'microT\mesh1';         % Include directory in workspace
addpath(DirPath);
InputData;   % Function that reads input files from the directory
rmpath(DirPath);                  % Remove directory from workspace
%-------------------------------------------------------------------%
ThermE_Avg=0;           %0=Temperature dependent properties
                        %1=Average thermoelectric properties
%-------------------------------------------------------------------%
T_uniform = 00;   T=T_uniform*ones(N_Nodes,1);
%-------------------------------------------------------------------%
maxIterations = 50                          % Nonlinear iterations
T__old=T;                                % Used in Convergence criteria
for NonLin=1:maxIterations, NonLin
%-------------------------------------------------------------------%
    K_Global=zeros(N_Nodes,N_Nodes);              % Initialization
    F_Global=zeros(N_Nodes,1);
%-------------------------------------------------------------------%
    Qgen = JouleHeat(T,1,1);  % Computes Joule  & Thomson heat
%-------------------------------------------------------------------%
    [K_Global,F_Global] = Matrices(Qgen);     % Create FE matrices
%-------------------------------------------------------------------%
    F_Global = Peltier(F_Global,Pel_BC,T);
%-------------------------------------------------------------------%
   [K_Global,F_Global]   =   BCondition(K_Global,F_Global);   %   Apply
Boundary Conditions
%-------------------------------------------------------------------%
    T=K_Global\F_Global;                  %Gauss Elimination Method
%-------------------------------------------------------------------%
```

```
      if NonLin==1
        T_ideal=T;
    end
%--------------------- Convergence Criteria --------------------%
    epsilon = max(abs(T-T__old))/max(T)
    if epsilon<1e-10
        display('Solution Converged');    max(T)
        break
    else
       T__old = T;
    end
    max(T)
%---------------------------------------------------------------%
end
phi = Voltage(T);
phi_ideal = Voltage(T_ideal);
```

Description

The main program contains analysis options and subroutines as described below.

Analysis option	Description
'DirPath'	The path to the directory that contains input files
'ThermE_avg'	0 = Use temperature dependent thermoelectric properties 1 = Use average thermoelectric properties
maxIterations	Maximum iterations performed to reach at steady state solution
T_uniform	Initial temperature guess

Subroutine	**Description**
InputData	# Reads input files from directory 'DirPath' into matrices.
JouleHeat(T,a,b)	# Modify internal heat generation matrix to include the influence of Joule and Thomson effect. # Input ⇒ Temperature vector from the last

	iteration; number a and number b. a = 0 or 1 ⇒ Exclude or include Joule effect b = 0 or 1 ⇒ Exclude or include Thomson effect # Output ⇒ Modified internal heat generation matrix (Qgen)
Matrices(Qgen)	# Computes elemental finite element matrices and assemble into Global finite element matrices. # Input ⇒ internal heat generation matrix. # Output ⇒ Global stiffness matrix (K_Global) and Global Force matrix (F_Global)
Peltier	# Adds contributions to F_Global # Input ⇒ F_Global, Peltier boundary condition data that contains info about elements those share common edge with the junction, temperature vector (T) to compute the magnitude of teperature dependent Peltier heat # Output ⇒ Modified F_Global
BCondition	# Apply thermal bounday conditions
Voltage	# Computes nodal voltage values based on temperature distribution # Input ⇒ Temperature Vector

"InputData" Subroutine

```
%--------------------Steady state Analysis----------------------%
%---------------------Reading Input Data------------------------%

%-----------------------------------------------------------------%
%               Ansys Input file syntax                           %
%-----------------------------------------------------------------%
% "file.txt"    "columns"    "Initial contents"
%- Nodes:       4 columns | no. | x | y | z |
%- Elements:    12 -> |no.|mat|type|NA|NA|NA|node1|2|3|4|5|6|
%- BC1:         3  -> |node|value|NA|
%- BC2:         5  -> |elem|NA|Node1|Node2|Value|
```

```
%- BC3:          5  -> |elem|NA|Node1|Node2|h|temp|
%- fQgen:        2  -> |Elem|value|
%- MatProp:      6  -> |Conduc|Sp Ht|Dens|Resisti|Seebeck|Thomson|
%-------------------------------------------------------------------%
%      Formatted syntax (After deleting unwanted columns)           %
%-------------------------------------------------------------------%
% Nodes:              |Node No.|X co-or|Y-Co-or|Z co-or|
% Elements:           |Element No.|Material|Type|node1|node2|node3|
% BC1:                |Node|Value|
% BC2:                |Element|Node1|Node2|Value|
% BC3:                |Element|Node1|Node2|h|temp|
% Qgen:               |Element|Value|
% MatProp:            |Conduc|Sp Heat|Dens|Resisti|a|b|

global Nodes Elements N_Elem N_Nodes N_V_BC1 Beta Shape_Func MatProp...
    V_BC1 Initial_Qgen BC1 BC2 BC3 BC4 N_BC1 N_BC2 N_BC3 N_BC4 N_Pel
%-------------------------------------------------------------------%
%                        Read Files                                 %
%-------------------------------------------------------------------%
    Nodes=          load('nodes.txt');
    Elements=       load('elements.txt');
    BC1 =           load('BC1.txt');
    BC2 =           load('BC2.txt');
    BC3 =           load('BC3.txt');
    BC4 =           load('BC4.txt');
    fQgen=          load('Qgen.txt');
    MatProp =       load('material.txt');
    V_BC1 =         load('V_BC1.txt');
    Pel_BC  =       load('pel_BC.txt');
%-------------------------------------------------------------------%
%           Delete unwanted columns from input data                 %
%-------------------------------------------------------------------%
    Elements(:,4:6) =       [];
    BC1(:,3)        =       [];
    BC2(:,2)        =       [];
    BC3(:,2)        =       [];
    BC4(:,2)        =       [];
%-------------------------------------------------------------------%
```

```
%                        Length of Arrays                              %
%------------------------------------------------------------------------%
      NUM1 = size(Elements);          N_Elem =    NUM1(1,1);
      NUM2 = size(Nodes);             N_Nodes =   NUM2(1,1);
      NUM3 = size(BC1);               N_BC1 =     NUM3(1,1);
      NUM4 = size(BC2);               N_BC2 =     NUM4(1,1);
      NUM5 = size(fQgen);             N_Qgen =    NUM5(1,1);
      NUM6 = size(V_BC1);             N_V_BC1 =   NUM6(1,1);
      NUM7 = size(BC3);               N_BC3 =     NUM7(1,1);
      NUM8 = size(BC4);               N_BC4 =     NUM8(1,1);
      NUM9 = size(Pel_BC);            N_Pel =     NUM9(1,1);
%------------------------------------------------------------------------%
%                         Initialization                                 %
%------------------------------------------------------------------------%
    MatProp(:,1) = Scale*MatProp(:,1);
    MatProp(:,2) = Scale^2*MatProp(:,2);
    MatProp(:,3) = Scale^-3*MatProp(:,3);
    MatProp(:,4) = Scale^-1*MatProp(:,4);
%    Nodes=1e-6*Nodes;
    Beta = [1 0;0 1;-1 -1];     Shape_Func = [1/3; 1/3; 1/3];

    Qgen = zeros(N_Elem,1);
    Initial_Qgen = zeros(N_Elem,1);
%------------------------------------------------------------------------%
%                    Compute heat generation matrix                      %
%------------------------------------------------------------------------%
if fQgen(1,1)==0              % Means no internal heat generation
    Initial_Qgen = zeros(N_Elem,1);
else
    if fQgen(1,1)==0.1   % Means uniform internal heat generation
        Initial_Qgen = ones(N_Elem,1)*fQgen(1,2);
    else      % Otherwise fill generation vector with given values
        for i=1:N_Qgen
            Initial_Qgen(fQgen(i,1),1) = fQgen(i,2);
        end
    end
end
Qgen = Initial_Qgen;
```

```
%-------------------------------------------------------------%
```

Description of input files:

There must not be alphabetic characters in the input files except "e" which is used to represent exponential. In the following input file syntaxes the text is added only for the purpose of explanation. Most of these files are imported from ANSYS (using list option) and then removing unwanted alphabetic characters from the file. For example, the BC1.txt file originally included "TEMP" word in each line and it must be removed from the file, otherwise MATLAB couldn't able to read the file.

"Nodes.txt"

Node No.	x coordinate	y coordinate	z coordinate
1	0.00000000000	0.00000000000	0.00000000000
2	0.100000000000	0.00000000000	0.00000000000

"Elements.txt"

Number	Material	NA	NA	NA	NA	Node1	Node2	Node3	NA	NA	NA
1	1	1	1	0	1	120	3	961	0	0	0
2	1	1	1	0	1	120	1	3	0	0	0
3	2	1	1	0	1	961	4	932	0	0	0
4	2	1	1	0	1	961	3	4	0	0	0

NA⇒ Not applicable

"Material.txt"

K	cp	ρ	γ	S	σ	a	b	c
67.716	447.26	7860.0	49e-8	-110e-6	98e-6	0.001	0.003	351

a,b,c are the coefficients used to compute Seebeck coefficient and Thomson coefficient

"Qgen.txt"

Element No.	Value
12	1e6

If no internal heat generation specified, change the first element to zero.

"BC1.txt"

Node No.	Value	NA
5	100	0
15	200	0

If no temperature boundary condition is specified, change the first element to zero.

"BC2.txt"

Element No.	NA	Node1	Node2	Value
5	3	12	11	1e4
15	5	11	10	1e6

If no flux boundary condition is specified, change the first element to zero.

"V_BC1.txt"

Node No.	Value
5	100
15	200

Constructed manually by selecting one end as a reference and applying fixed voltage condition.

"Pel_BC.txt"

Element No.	Node1	Node2
5	12	11
15	11	10

Constructed manually by checking elements (from the mesh plot) that has common edge with the junction.

"JouleHeat" Subroutine

```
%--------------------Steady state Analysis----------------------%
%----------- Compute Thermal Gradient, Voltage & Joule Heat ----%
%-----------------------------------------------------------------%
%-------------------- Initialization ----------------------------%
function[Qgen] =Voltage(T,var1,var2)
global Nodes Elements N_Elem N_Nodes Beta Shape_Func ...
        MatProp Initial_Qgen ThermE_Avg

QJoule=zeros(N_Elem,1);          QThomson=zeros(N_Elem,1);

for i=1:N_Elem
%------------------------- Jacobian ----------------------------%
    Jacob=[ Nodes( Elements(i,4),2 )-Nodes( Elements(i,6),2 )...
            Nodes( Elements(i,4),3 )-Nodes( Elements(i,6),3 );...
            Nodes( Elements(i,5),2 )-Nodes( Elements(i,6),2 )...
            Nodes( Elements(i,5),3 )-Nodes( Elements(i,6),3 )];

%-------------------- Thermal Gradient -------------------------%
    Flux =  inv(Jacob) * Beta' * [  T(Elements(i,4),1 );...
                                    T(Elements(i,5),1 );...
                                    T(Elements(i,6),1 )];
%------------- Compute Seebeck and Thomson coefficient  ---------%
[Seebeck,Thomson] = ThermoE_Prop(i,T,ThermE_Avg);

%--- Compute Internal heat generation due to the Joule Effect --%
    if var1==1
    QJoule(i,1) =(Seebeck^2/MatProp(Elements(i,2),4))*dot(Flux,Flux);
    end

%-- Compute Internal heat generation due to the Thomson Effect -%
    if var2==1
    QThomson(i,1)=(Seebeck*Thomson/MatProp(Elements(i,2),4))...
```

```
            *dot(Flux,Flux);
    end
end

Qgen = Initial_Qgen + QJoule + QThomson;
```

"Matrices" Subroutine

```
%--------------------Steady state Analysis----------------------%
%---------------------Forming FE matrices-----------------------%
%-----------------------------------------------------------------%
%                   Elemental & Global Matrices                   %
%-----------------------------------------------------------------%
function[K_Global,F_Global] =Matrices(Qgen)
global Nodes Elements N_Elem N_Nodes Beta Shape_Func MatProp

    Ke=zeros(3,3);              K_Global=zeros(N_Nodes,N_Nodes);
      Fe=zeros(3,1);              F_Global=zeros(N_Nodes,1);

for i=1:N_Elem
%------------------------- Jacobian ----------------------------%
    Jacob=[ Nodes( Elements(i,4),2 )-Nodes( Elements(i,6),2 )...
            Nodes( Elements(i,4),3 )-Nodes( Elements(i,6),3 );...
            Nodes( Elements(i,5),2 )-Nodes( Elements(i,6),2 )...
            Nodes( Elements(i,5),3 )-Nodes( Elements(i,6),3 )];
%------------------ Elementsl Stiffness Matrix -----------------%
    Ke =    MatProp(Elements(i,2),1) * Beta * (inv(Jacob))' *...
            inv(Jacob) * Beta' * det(Jacob) * 0.5;
%------------------ Elementsl Force Matrix ---------------------%
    Fe=     Shape_Func*det(Jacob)*Qgen(i,1)*0.5;
%------------------------- Assembly ----------------------------%
    for j=1:3
        for k=1:3
            K_Global( Elements(i,j+3),Elements(i,3+k) )=...
            K_Global( Elements(i,j+3),Elements(i,3+k) )+Ke(j,k);
        end
```

```
        F_Global( Elements(i,j+3),1 )=...
        F_Global( Elements(i,j+3),1 )+Fe(j,1);
    end

end
%-------------------------------------------------------------------%
```

"Peltier" Subroutine

```
function[F_Global] =Peltier(F_Global,Pel_BC,T)
global Nodes Elements N_Elem N_Nodes  MatProp N_Pel Beta ThermE_Avg

S_Intg = [1/sqrt(3);-1/sqrt(3)];              % Quadrature points
for i=1:N_Pel
    F2=zeros(2,1);
%------------------ Jacobian of 1D Element ---------------------%
    Jacob_1D =sqrt( (Nodes(Pel_BC(i,2),3)-Nodes(Pel_BC(i,3),3))^2+...
              (Nodes(Pel_BC(i,2),2)-Nodes(Pel_BC(i,3),2))^2 )/2;
%------- Computation of new elemental force matrix -------------%
    [Seebeck,Thomson] = ThermoE_Prop(Pel_BC(i,1),T,ThermE_Avg);

    Resistiviy = MatProp(Elements(Pel_BC(i,1),2),4);
%-------------------------------------------------------------------%
    Jacob=[       Nodes(       Elements(Pel_BC(i,1),4),2       )-Nodes(
Elements(Pel_BC(i,1),6),2 )...
            Nodes(          Elements(Pel_BC(i,1),4),3          )-Nodes(
Elements(Pel_BC(i,1),6),3 );...
            Nodes(          Elements(Pel_BC(i,1),5),2          )-Nodes(
Elements(Pel_BC(i,1),6),2 )...
            Nodes(          Elements(Pel_BC(i,1),5),3          )-Nodes(
Elements(Pel_BC(i,1),6),3 )];

%-------------------- Thermal Gradient -------------------------%
    Flux =  inv(Jacob) * Beta' * [  T(Elements(Pel_BC(i,1),4),1 );...
                                    T(Elements(Pel_BC(i,1),5),1 );...
                                    T(Elements(Pel_BC(i,1),6),1 )];
```

```
    T_avg = (T(Pel_BC(i,2))+T(Pel_BC(i,3)))/2;
    Pel_Heat                                                    =
(Seebeck)^2*(T_avg+273)*(sqrt(dot(Flux,Flux)))/Resistiviy;

    for QuadPt=1:2
        F2= F2+ [(1-S_Intg(QuadPt,1))/2;(1+S_Intg(QuadPt,1))/2]...
            *det(Jacob_1D)*Pel_Heat;
    end
%---------- Assembly of new elemental force matrix -------------%
    F_Global(Pel_BC(i,2),1)=   F_Global(Pel_BC(i,2),1)+F2(1,1);
    F_Global(Pel_BC(i,3),1)=   F_Global(Pel_BC(i,3),1)+F2(2,1);
end
```

"BCondition" Subroutine

```
 %--------------------Steady state Analysis----------------------%
%------------------Apply Boundary Conditions--------------------%
function[K_Global,F_Global] =BCondition(K_Global,F_Global)
global Nodes Elements N_Elem N_Nodes Beta Shape_Func MatProp...
  BC1 BC2 BC3 BC4 N_BC1 N_BC2 N_BC3 N_BC4

%-------------------------------------------------------------%
%                    Flux Boundary Condition                  %
%-------------------------------------------------------------%
if BC2(1,1)==0
    disp('No Flux boundary condition');
else
S_Intg = [1/sqrt(3);-1/sqrt(3)];              % Quadrature points
for i=1:N_BC2
    F2=zeros(2,1);
%------------------ Jacobian of 1D Element ---------------------%
    Jacob_1D =sqrt( (Nodes(BC2(i,2),3)-Nodes(BC2(i,3),3))^2+...
              (Nodes(BC2(i,2),2)-Nodes(BC2(i,3),2))^2 )/2;
%------- Computation of new elemental force matrix -------------%
    for QuadPt=1:2
        F2= F2+ [(1-S_Intg(QuadPt,1))/2;(1+S_Intg(QuadPt,1))/2]...
            *det(Jacob_1D)*BC2(i,4);
```

```
    end
%---------- Assembly of new elemental force matrix -------------%
    F_Global(BC2(i,2),1)=   F_Global(BC2(i,2),1)+F2(1,1);
    F_Global(BC2(i,3),1)=   F_Global(BC2(i,3),1)+F2(2,1);
end
end

%-----------------------------------------------------------------%
%               Temperature Boundary Condition                    %
%-----------------------------------------------------------------%
if BC1(1,1)==0
    disp('No Temperature boundary condition');
else
for i=1:N_BC1
       K_Global( BC1(i,1),: )=0;
       K_Global( BC1(i,1),BC1(i,1) )=1;
       F_Global( BC1(i,1),1 )=BC1(i,2);
end
end
```

"Voltage" Subroutine

```
%--------------------Steady state Analysis----------------------%
%----------- Compute Thermal Gradient, Voltage & Joule Heat ----%
%-----------------------------------------------------------------%
%-------------------- Initialization -----------------------------%
function[phi] =Voltage(T)
global Nodes Elements N_Elem N_Nodes N_V_BC1 Beta Shape_Func ...
        MatProp V_BC1 ThermE_Avg

phi=zeros(N_Nodes,1);
VKe=zeros(3,3);                 VK_Global=zeros(N_Nodes,N_Nodes);
VFe=zeros(3,1);                 VF_Global=zeros(N_Nodes,1);

for i=1:N_Elem
%------------------------ Jacobian ----------------------------%
    Jacob=[ Nodes( Elements(i,4),2 )-Nodes( Elements(i,6),2 )...
```

```
            Nodes( Elements(i,4),3 )-Nodes( Elements(i,6),3 );...
            Nodes( Elements(i,5),2 )-Nodes( Elements(i,6),2 )...
            Nodes( Elements(i,5),3 )-Nodes( Elements(i,6),3 )];

%-------------------- Thermal Gradient -------------------------%
    Flux =  inv(Jacob) * Beta' * [  T(Elements(i,4),1 );...
                                    T(Elements(i,5),1 );...
                                    T(Elements(i,6),1 )];
%-------------------- Voltage Gradient -------------------------%
    [Seebeck,Thomson] = ThermoE_Prop(i,T,ThermE_Avg);

    Vlux = Seebeck*Flux;

%---------- Compute Elemental Voltage Matrices ----------------%
    VKe =   Beta*(inv(Jacob))'*inv(Jacob)*Beta'*det(Jacob)*0.5;

    VFe =   Beta * (inv(Jacob))'*Vlux*det(Jacob)*0.5;

%---------- Assembly of Elemental Voltage matrices ------------%
    for j=1:3
        for k=1:3
            VK_Global( Elements(i,j+3),Elements(i,3+k) )=...
            VK_Global( Elements(i,j+3),Elements(i,3+k) )+VKe(j,k);
        end
        VF_Global( Elements(i,j+3),1 )=...
        VF_Global( Elements(i,j+3),1 )+VFe(j,1);
    end
end
 %------ Apply boundary condition to global voltage matrices -----%
 for i=1:N_V_BC1
     VK_Global( V_BC1(i,1),: )            = 0;
     VK_Global( V_BC1(i,1),V_BC1(i,1) )   = 1;
     VF_Global( V_BC1(i,1),1 )            = V_BC1(i,2);
 end
%---------------------- Solve voltage equations ----------------%
      phi=VK_Global\VF_Global;
```

Appendix B

Computer Implementation of Transient Finite Element Model

All the subroutines will be the same as used in steady state program except "main" program and "matrices" subroutine.

```
%-------------------------------------------------------------------%
%   Gurjinder Singh      'Thesis Work'                                %
%   Program:     Transient heat transfer analysis using FEM          %
%   Requirements:    Six input files (Nodes.txt,Elements.txt,        %
%                    BC1.txt,BC2.txt,Qgen.txt)                       %
%   P.S.     Node numbers should be in order--start from 0->max      %
%-------------------------------------------------------------------%
%   Nomenclature:                                                    %
%   Nodes:       "Node matrix"
%   Elements:    "Element Matrix"
%   BC1:         Boundary condition of first kind
%   BC2:         Boundary Condition of 2nd kind
%   fQgen:   Matrix to store data from heat generation input file
%   Qgen:        Formatted heat generation matrix
%   MatProp:     Material Properties
%   N_Elem:      Total no. of Elements
%   N_Nodes:     Total no. of nodes
%   N_BC1:       Total no. of nodes with BC1
%   N_BC2:       Total no. of elements with BC2
%   N_Qgen:      Total no. of elements with Qgen
%   Beta:        Beta matrix of triangular element
%   Shape_Func:  Shape Function
%   T:           field variable (Temperature)
%   Jacob:       Jacobian matrix for 3node(1quad point)...
%                triangular element
%   Ke,Fe:       Elemental stiffness and force matrices
%   K_Global:    Global stiffness matrix
%   F_Global:    Global Force Matrix
```

```
%   Loop variables: Tvar,iQgen,iRef,iEmf
%-------------------------------------------------------------%
clear all,clc,format long e;
global dt Theta ThermE_Avg
%-------------------------------------------------------------%
Scale=1e6;                              % Parameter to scale mesh size
Theta =2/3;                                     % Transient Method
endtime = 0.08;      maxstep = 100;    dt = endtime/maxstep
Tran_Node = [120];      %Node for which time history data is recorded
T_initial = 30;
ThermE_Avg=0;                %0=Temperature dependent properties
                             %1=Average thermoelectric properties
%-------------------------------------------------------------%
DirPath = 'microT\mesh1';         % Include directory in workspace
addpath(DirPath);
InputData;                           % Reads input from text files
rmpath(DirPath);                  % Remove directory from workspace
%-------------------------------------------------------------%
T=T_initial*ones(N_Nodes,1);
T_old=T_initial*ones(N_Nodes,1);
F_old=zeros(N_Nodes,1);
%-------------------------------------------------------------%
ElemLen = sqrt( (Nodes(1,3)-Nodes(3,3))^2+...
             (Nodes(1,2)-Nodes(3,2))^2 );
FouNo=MatProp(1,1)*dt*(ElemLen^-2)/(MatProp(1,2)*MatProp(1,3))
Tt(1,:) = [0 T(Tran_Node(1,:),1)'];
%-------------------------------------------------------------%
for Tvar=1:maxstep, Tvar
%------------------Internal Joule Heat-------------------------%
    Qgen = JouleHeat(T,1,0);  % Computes Joule  & Thomson heat
%------------------Create FE matrices--------------------------%
    [A_Global,d_Global,F_old] = Matrices(Qgen,F_old,T_old);
%-------------------------------------------------------------%
%     d_Global = Peltier(d_Global,Pel_BC,T);
%------------------Apply Boundary Conditions-------------------%
    [A_Global,d_Global] = BCondition(A_Global,d_Global);
%-------------------------------------------------------------%
    T=A_Global\d_Global;                % Gauss Elimination Method
```

```
%--------------------- Convergence Criteria --------------------%
    Tt(Tvar+1,:) = [dt*Tvar T(Tran_Node(1,:),1)'];
    epsilon     =     abs(     T(Tran_Node,1)     -     T_old(Tran_Node,1)
)/T(Tran_Node,1);
    if abs(epsilon)<1e-10
        display('Solution Converged');
        break
    else
        T_old = T;T(Tran_Node(1,:),1)
    end
%-----------------------------------------------------------------%
end

phi = Voltage(T);
```

"Matrices" Subroutine

```
%-----------------   Transient Analysis ------------------------%
%-----------------------------------------------------------------%
%                % Elemental & Global Matrices %                  %
%-----------------------------------------------------------------%
function[A_Global,d_Global,F_old] =Matrices(Qgen,F_old,T_old)
global Nodes Elements N_Elem N_Nodes Beta Shape_Func MatProp...
    Theta dt

    Ke=zeros(3,3);              K_Global=zeros(N_Nodes,N_Nodes);
      Fe=zeros(3,1);              F_Global=zeros(N_Nodes,1);
    Ce=zeros(3,3);              C_Global=zeros(N_Nodes,N_Nodes);
for i=1:N_Elem

    Jacob=[ Nodes( Elements(i,4),2 )-Nodes( Elements(i,6),2 )...
            Nodes( Elements(i,4),3 )-Nodes( Elements(i,6),3 );...
            Nodes( Elements(i,5),2 )-Nodes( Elements(i,6),2 )...
            Nodes( Elements(i,5),3 )-Nodes( Elements(i,6),3 )];

    Ke =    MatProp(Elements(i,2),1) * Beta * (inv(Jacob))' *...
```

```
            inv(Jacob) * Beta' * det(Jacob) * 0.5;

    Ce =    MatProp(Elements(i,2),2)*MatProp(Elements(i,2),3)*...
            Shape_Func*Shape_Func' * det(Jacob)*0.5;

    Fe=     Shape_Func*det(Jacob)*Qgen(i,1)*0.5;

    for j=1:3
        for k=1:3
            K_Global( Elements(i,j+3),Elements(i,3+k) )=...
            K_Global( Elements(i,j+3),Elements(i,3+k) )+Ke(j,k);

            C_Global( Elements(i,j+3),Elements(i,3+k) )=...
            C_Global( Elements(i,j+3),Elements(i,3+k) )+Ce(j,k);
        end
        F_Global( Elements(i,j+3),1 )=...
        F_Global( Elements(i,j+3),1 )+Fe(j,1);
    end
end

A_Global = (1/dt)*C_Global + Theta*K_Global;
d_Global = ( (1/dt)*C_Global - (1-Theta)*K_Global )*T_old ...
            + (1-Theta)*F_old + Theta*F_Global;
F_old = F_Global;
%-------------------------------------------------------------------%
```